LOAN DOCUMENT

PHOTOGRAPH THIS SHEET

DTIC ACCESSION NUMBER

LEVEL

INVENTORY

AFRL-ML-TY-TR-2000-4522

DOCUMENT IDENTIFICATION

15 May 97

DISTRIBUTION STATEMENT A
Approved for Public Release
Distribution Limited

DISTRIBUTION STATEMENT

DATE ACCESSIONED

DATE RETURNED

H
A
N
D
L
E

W
I
T
H

C
A
R
E

20000523 017

DATE RECEIVED IN DTIC

REGISTERED OR CERTIFIED NUMBER

PHOTOGRAPH THIS SHEET AND RETURN TO DTIC-FDAC

DOCUMENT PROCESSING SHEET

LOAN DOCUMENT

PREVIOUS EDITIONS MAY BE USED UNTIL
STOCK IS EXHAUSTED.

DTIC QUALITY INSPECTED 1

AFRL-ML-TY-TR-2000-4522
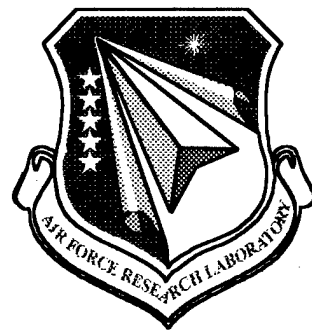
PULSED STREAMER REACTOR CHARACTERIZATION PHASE II

DR. BRUCE R. LOCKE

DEPARTMENT OF CHEMICAL ENGINEERING
FAMU-FSU COLLEGE OF ENGINEERING
FLORIDA STATE UNIVERSITY
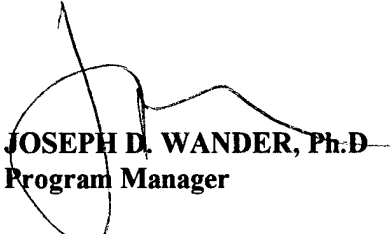2525 POTTSDAMER STREET
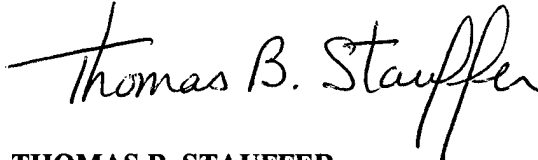TALLAHASSEE FL 32310-6046

NOTICES

USING GOVERNMENT DRAWINGS, SPECIFICATIONS, OR OTHER DATA INCLUDED IN THIS DOCUMENT FOR ANY PURPOSE OTHER THAN GOVERNMENT PROCUREMENT DOES NOT IN ANY WAY OBLIGATE THE US GOVERNMENT. THE FACT THAT THE GOVERNMENT FORMULATED OR SUPPLIED THE DRAWINGS, SPECIFICATIONS, OR OTHER DATA DOES NOT LICENSE THE HOLDER OR ANY OTHER PERSON OR CORPORATION; OR CONVEY ANY RIGHTS OR PERMISSION TO MANUFACTURE, USE, OR SELL ANY PATENTED INVENTION THAT MAY RELATE TO THEM.

THIS TECHNICAL REPORT HAS BEEN REVIEWED AND IS APPROVED FOR PUBLICATION.

JOSEPH D. WANDER, Ph.D
Program Manager

THOMAS B. STAUFFER
Chief, Weapons Systems Logistics Branch

RANDY L. GROSS, Col, USAF, BSC
Chief, Air Expeditionary Forces Technologies Division

REPORT DOCUMENTATION PAGE		Form Approved OMB No. 0704-0188

Public reporting burden for this collection of information is estimated to average 1 hour per response, including the time for reviewing instructions, searching existing data sources, gathering and maintaining the data needed, and completing and reviewing the collection of information. Send comments regarding this burden estimate or any other aspect of this collection of information, including suggestions for reducing this burden, to Washington Headquarters Services, Directorate for Information Operations and Reports, 1215 Jefferson Davis Highway, Suite 1204, Arlington, VA 22202-4302, and to the Office of Management and Budget, Paperwork Reduction Project (0704-0188), Washington, DC 20503.

1. AGENCY USE ONLY *(Leave blank)*	2. REPORT DATE May 15, 1997	3. REPORT TYPE AND DATES COVERED Final Report, Jan 1, 1997 - May 15, 1997	

4. TITLE AND SUBTITLE Pulsed Streamer Reactor Characterization Phase II	5. FUNDING NUMBERS C - F08937-93-C-0020 PE - 0602202F JON - 1900A35B

6. AUTHOR(S)
Locke, Bruce R., PhD

7. PERFORMING ORGANIZATION NAME(S) AND ADDRESS(ES) Department of Chemical Engineering FAMU-FSU College of Engineering 2525 Pottsdamer Street Tallahassee, Florida 32310-6064	8. PERFORMING ORGANIZATION REPORT NUMBER

9. SPONSORING/MONITORING AGENCY NAME(S) AND ADDRESS(ES) Air Force Research Laboratory Air Expeditionary Forces Technologies Division (AFRL/MLQ) 139 Barnes Drive, Suite 2 Tyndall AFB FL 32403-5323	10. SPONSORING/MONITORING AGENCY REPORT NUMBER AFRL-ML-TY-TR-2000-4522

11. SUPPLEMENTARY NOTES

12a. DISTRIBUTION AVAILABILITY STATEMENT Approved for Public Release	12b. DISTRIBUTION CODE A

13. ABSTRACT *(Maximum 200 words)*

Aqueous phase pulsed corona discharge is considered an alternative for wastewater treatment. This report presents an analysis of the physical and chemical aspects of corona discharge in water, in salt solutions, and in solutions containing added particles. The addition of activated carbon to liquid phase corona discharges leads to enhanced streamer production and higher sparkover voltages. Higher sparkover voltages and enhanced streamer production are expected to lead to enhanced production of reactive species that lead to pollutant degradation. A mathematical model describing bulk solution chemical reactions, chemical reactions in the particle phase, and diffusion into the particle phase, has been developed using the methods of spatial averaging. Measurement of phenol degradation and byproduct formation in the liquid phase corona reactor with and without added particles and at various applied voltages was performed. Experiments with corona in the presence of aqueous film-forming foam (AFFF) indicate that corona is able to mechanically disrupt the structure of the foam and that a corona discharge can be created in the presence of a foam. Foamability measurements indicate however, that the pulsed corona may not significantly chemically degrade the AFFF.

14. SUBJECT TERMS Pulsed Corona Discharge, phenol degradation, carbon, aqueous film-forming foam, AFFF	15. NUMBER OF PAGES 119
	16. PRICE CODE

17. SECURITY CLASSIFICATION OF REPORT Unclas	18. SECURITY CLASSIFICATION OF THIS PAGE Unclas	19. SECURITY CLASSIFICATION OF ABSTRACT Unclas	20. LIMITATION OF ABSTRACT UL

Standard Form 298 (Rev. 2-89) (EG)
Prescribed by ANSI Std. 239.18
Designed using Perform Pro, WHS/DIOR, Oct 94

GENERAL INSTRUCTIONS FOR COMPLETING SF 298

The Report Documentation Page (RDP) is used in announcing and cataloging reports. It is important that this information be consistent with the rest of the report, particularly the cover and title page. Instructions for filling in each block of the form follow. It is important to *stay within the lines* to meet *optical scanning requirements.*

Block 1. Agency Use Only *(Leave blank)*.

Block 2. Report Date. Full publication date including day, month, and year, if available (e.g. 1 Jan 88). Must cite at least the year.

Block 3. Type of Report and Dates Covered. State whether report is interim, final, etc. If applicable, enter inclusive report dates (e.g. 10 Jun 87 - 30 Jun 88).

Block 4. Title and Subtitle. A title is taken from the part of the report that provides the most meaningful and complete information. When a report is prepared in more than one volume, repeat the primary title, add volume number, and include subtitle for the specific volume. On classified documents enter the title classification in parentheses.

Block 5. Funding Numbers. To include contract and grant numbers; may include program element number(s), project number(s), task number(s), and work unit number(s). Use the following labels:

C	- Contract	PR	- Project
G	- Grant	TA	- Task
PE	- Program Element	WU	- Work Unit Accession No.

Block 6. Author(s). Name(s) of person(s) responsible for writing the report, performing the research, or credited with the content of the report. If editor or compiler, this should follow the name(s).

Block 7. Performing Organization Name(s) and Address(es). Self-explanatory.

Block 8. Performing Organization Report Number. Enter the unique alphanumeric report number(s) assigned by the organization performing the report.

Block 9. Sponsoring/Monitoring Agency Name(s) and Address(es). Self-explanatory.

Block 10. Sponsoring/Monitoring Agency Report Number. *(If known)*

Block 11. Supplementary Notes. Enter information not included elsewhere such as: Prepared in cooperation with....; Trans. of....; To be published in.... When a report is revised, include a statement whether the new report supersedes or supplements the older report.

Block 12a. Distribution/Availability Statement. Denotes public availability or limitations. Cite any availability to the public. Enter additional limitations or special markings in all capitals (e.g. NOFORN, REL, ITAR).

DOD - See DoDD 5230.24, "Distribution Statements on Technical Documents."
DOE - See authorities.
NASA - See Handbook NHB 2200.2.
NTIS - Leave blank.

Block 12b. Distribution Code.

DOD - Leave blank.
DOE - Enter DOE distribution categories from the Standard Distribution for Unclassified Scientific and Technical Reports.
NASA - Leave blank.
NTIS - Leave blank.

Block 13. Abstract. Include a brief *(Maximum 200 words)* factual summary of the most significant information contained in the report.

Block 14. Subject Terms. Keywords or phrases identifying major subjects in the report.

Block 15. Number of Pages. Enter the total number of pages.

Block 16. Price Code. Enter appropriate price code *(NTIS only)*.

Blocks 17. - 19. Security Classifications. Self-explanatory. Enter U.S. Security Classification in accordance with U.S. Security Regulations (i.e., UNCLASSIFIED). If form contains classified information, stamp classification on the top and bottom of the page.

Block 20. Limitation of Abstract. This block must be completed to assign a limitation to the abstract. Enter either UL (unlimited) or SAR (same as report). An entry in this block is necessary if the abstract is to be limited. If blank, the abstract is assumed to be unlimited.

Standard Form 298 Back (Rev. 2-89)

PREFACE

This report details the work performed during the project "Supplement No 1 to the Subcontract S-5000.42, Phase II, Pulsed Streamer Reactor Characterization," through contract with the United States Air Force and on subcontract with Applied Research Associates, Inc., for the time period January 1, 1997 to May 15, 1997. Some of the work given in this report was performed as part of the master's thesis in chemical engineering of Mr. David Grymonpre' which will be defended in the summer of 1997. Giridhar Saithamoorthy (graduate student in chemical engineering), Steven White (undergraduate student in chemical engineering), Howell Hanson IV (undergraduate student in chemical engineering), Shawn Goldstein (undergraduate student in chemical engineering) and Cadet Dan Lamar (USAFA undergraduate chemistry major) assisted conducting laboratory experiments. Technical assistance from Mr. Wright C. Finney (research associate in chemical engineering) and Dr. Ronald J. Clark (chemistry professor at FSU) was instrumental in performing this work. Work performed from June 26, 1996 to December 1, 1996 was reported in the Interim Report, Pulsed Streamer Corona Reactor Characterization - Phase II, submitted on December 1, 1996. Three papers are under preparation for reporting the results of this work in peer reviewed scientific journals: 1) Chemical Reaction Kinetics and Reactor Modeling of NO_x Removal in a Pulsed Streamer Corona Discharge Reactor (*Industrial and Engineering Chemistry Research*), 2) Pulsed Streamer Corona Discharge Characteristics in Aqueous Solutions Containing Solid Particles (*Applied Physics Letters*), and 3) Chemical Reactions of Phenol Degradation in a Pulsed Corona Reactor with Activated Carbon (*Environmental Science and Technology*). A presentation at the Fourth International Conference on Advanced Oxidation Technologies is also planned.

EXECUTIVE SUMMARY

Aqueous-phase pulsed corona discharge for wastewater treatment is considered in the present work. Analysis of the physical and chemical aspects of corona discharge in water, in salt solutions, and in solutions containing added particles is considered in order to evaluate the potential of this technology for treating water polluted with small aromatic organic compounds. The specific accomplishments of this project include:

1) Activated carbon particles have a unique effect on the streamer characteristics of liquid-phase pulsed corona discharge. The addition of activated carbon to liquid-phase corona discharges leads to enhanced streamer production and higher sparkover voltages. Higher sparkover voltages and enhanced streamer production are expected to lead to enhanced production of reactive species that lead to pollutant degradation. Studies with activated carbon that has been washed to remove salts and other compound residues from the manufacturing process leads to the conclusion that the combination of activated carbon with salts containing potassium cations is responsible for the unique behavior of unwashed activated carbon. Salt solutions containing potassium, sodium, or calcium ions with chlorine anions do not have similar effects on the discharge characteristics. Clean carbon particles alone behave as other particles such as glass spheres or elemental copper. It is only the combination of washed carbon and potassium salts that lead to behavior similar to the unwashed carbon; i.e., they lead to significantly lower power consumption. Electron microscope and x-ray emissions studies indicate surface regions on the activated carbon that are associated with high levels of potassium. The reasons for the enhanced effects of potassium salts are unknown at the present time.

2) A mathematical model describing bulk solution chemical reactions, chemical reactions in the particle phase, and diffusion into the particle phase, has been developed using the methods of spatial averaging. The major parameters in the model include the reaction rate constants, the adsorption constant for adsorption to the activated carbon, and the mass transfer coefficient for transport from the bulk solution to the surface of the particle. Experimental measurement of corona reactions without particles serve to provide information on the bulk solution reaction rate

constants, and measurements of adsorption without corona give the equilibrium and mass transfer coefficients. Through combination of the model and these results, it is expected that the role of surface corona-induced reactions may be elucidated. Further work is needed to fully compare the experiments and model, and to extend the model to include additional byproducts for the reactions.

3) Measurement of phenol degradation and byproduct formation in the liquid-phase corona reactor with and without added particles and at various applied voltages was performed. The major byproducts include hydroquinone, catechol, and resorcinol as measured by HPLC. The formation of different amounts of byproducts in the presence of activated carbon and in its absence lead to the possibility of surface induced reactions; however further work needs to be done before a final conclusion concerning the magnitude of the surface reactions can be made. The rate of decrease of bulk phase phenol concentration in the absence of carbon with corona is much less than the rates of decrease of bulk phase phenol concentration in the presence of corona and carbon. Carbon alone is able to remove phenol from the bulk solution; however, it leads to no degradation since no byproducts are formed. The rate of phenol removal with carbon and no corona is slower than that of corona with carbon indicating that the potential surface reactions may be occurring.

4) Experiments with corona in the presence of aqueous film-forming foam (AFFF) indicate that corona is able to mechanically disrupt the structure of the foam and that a corona discharge can be created in the presence of a foam. Foamability measurements indicate, however, that the pulsed corona may not significantly chemically degrade the AFFF.

TABLE OF CONTENTS

LIST OF FIGURES

LIST OF TABLES

SECTION I
INTRODUCTION

A. RESEARCH OBJECTIVES

The specific emphasis of this project was to determine the effects of powdered activated carbon and other small particles on the removal of small organic compounds from aqueous solutions in the presence of pulsed streamer corona discharges as specified in Tasks 6, 7, and 8 of the contract proposal. In addition, the potential for using pulsed corona discharge to degrade aqueous film-forming foam (AFFF) was investigated.

B. BACKGROUND

The electrical, physical, and chemical characteristics of pulsed streamer corona discharges in air have been extensively studied for applications to nitrogen oxide removal, sulfur dioxide removal, volatile organic contaminant removal, and for the production of ozone (Creyghton, 1994; Masuda and Nakao, 1990; Clements, et al., 1989). Although further work is needed to develop this technology, the fundamental issues of how streamers are formed through the development of Townsend avalanches, electron impact ionization and the formation of ionization waves have been well studied (Nasser, 1971; Loeb, 1965). Recent studies have investigated the application of pulsed streamer corona for the treatment of aqueous-phase pollution (Clements, et al., 1987; Sharma, et al., 1993; Joshi, et al., 1995). Although a number of investigators have studied the fundamental issues involved in dielectric liquid breakdown (Jones and Kunhardt, 1995ab; Klimkin, 1990ab; Kuskova, 1983, 1990; Devins, et al., 1981) little attention has been focused on the effects of solid particles on the liquid-phase breakdown phenomena and, additionally, the effects of additives (solid particles and liquid conductivity) on the sparkover voltage has not been previously reported.

The present study is motivated by earlier work in our group to investigate the potential of aqueous-phase pulsed streamer corona for the degradation of organic contaminants (Sharma, et al., 1993; Joshi, et al., 1995). This work has shown that small aromatics, including phenol, benzene, xylene, and toluene, can be degraded using a point-to-plane electrode geometry with a short-pulse high-voltage electrical discharge. It was also observed that the addition of iron

1

(ferrous sulfate) greatly enhanced the removal of the organic through the Fenton's reaction. Experimental determination of the chemical reaction kinetics and the rates of formation of hydrogen peroxide and hydroxyl radicals has been performed (Joshi, et al., 1995). Activated carbon adsorption is a well known process for physically removing organic contaminants from wastewater and recent work has indicated the existence of oxidation reactions on the surface of the activated carbon in oxidizing environments including oxygen-containing solutions (Abuzald, et al., 1994; Vidac, et al., 1993). The application of aqueous-phase pulsed streamer corona in the presence of solid activated carbon particles may have several advantages over the use of either process alone. One of these advantages is that the addition of activated carbon particles strongly affects the electrical discharge characteristics of the liquid-phase discharge, which may lead to enhanced chemical reactions for pollution degradation.

SECTION II
EXPERIMENTAL APPARATUS AND PROCEDURES

A. POWER SUPPLY AND REACTOR SPECIFICATIONS

The reaction chamber used in this study, shown in Figure 1, consists of a 1000 ml jacketed glass vessel. The region of electrical discharge is located at the tip of a sharp metal rod, which is connected to a high-voltage pulsed power supply. The corona extends from the tip upward toward the stainless steel ground plate in a point-to-plane geometry. The separation distance between the needle tip and ground plate was set at 5 cm for all experimental runs. A magnetic stirrer at the bottom of the vessel provides thorough mixing of the solution. There are four openings on the cover of the vessel; these openings are used for connection of the ground stainless steel plate and for removal of liquid samples for analysis. The high voltage lead is introduced through the side of the reactor in a glass tube specially designed and constructed for this project.

The difference between the present system and other corona discharges such as dc discharge, ac discharge, and long-pulse (μs – ms pulse width) treatments is that the electrical discharge in this reactor has a short pulse width and a fast rise time. Pulsed power is produced by a rotating spark gap high-voltage pulsed power supply, capable of supplying the reactor discharge electrode with high voltage (10 – 80 kV), short duration, (200 – 1000 ns), fast rise time (20 – 50 ns), repetitive (60 Hz), electrical pulses. The source input is a high-voltage transformer supplying rectified AC power to the pulse-forming circuit. This high voltage goes through a series of current-limiting resistors and a set of diodes that remove the negative part of the sine wave. The half-wave rectified voltage then charges an array of ceramic "doorknob" capacitors, which discharge into the reactor load whenever the rotating spark gap closes. Further details are given in Sharma, et al. (1993), Joshi, et al. (1995), and Clements, et al. (1987).

B. ANALYTICAL INSTRUMENTATION

Experimental work on this project focused on two aspects; physical characterization of the effects of added particles on the pulsed corona discharge, and chemical analysis of the effects of added particles on the degradation of model compounds in the corona discharge. The physical
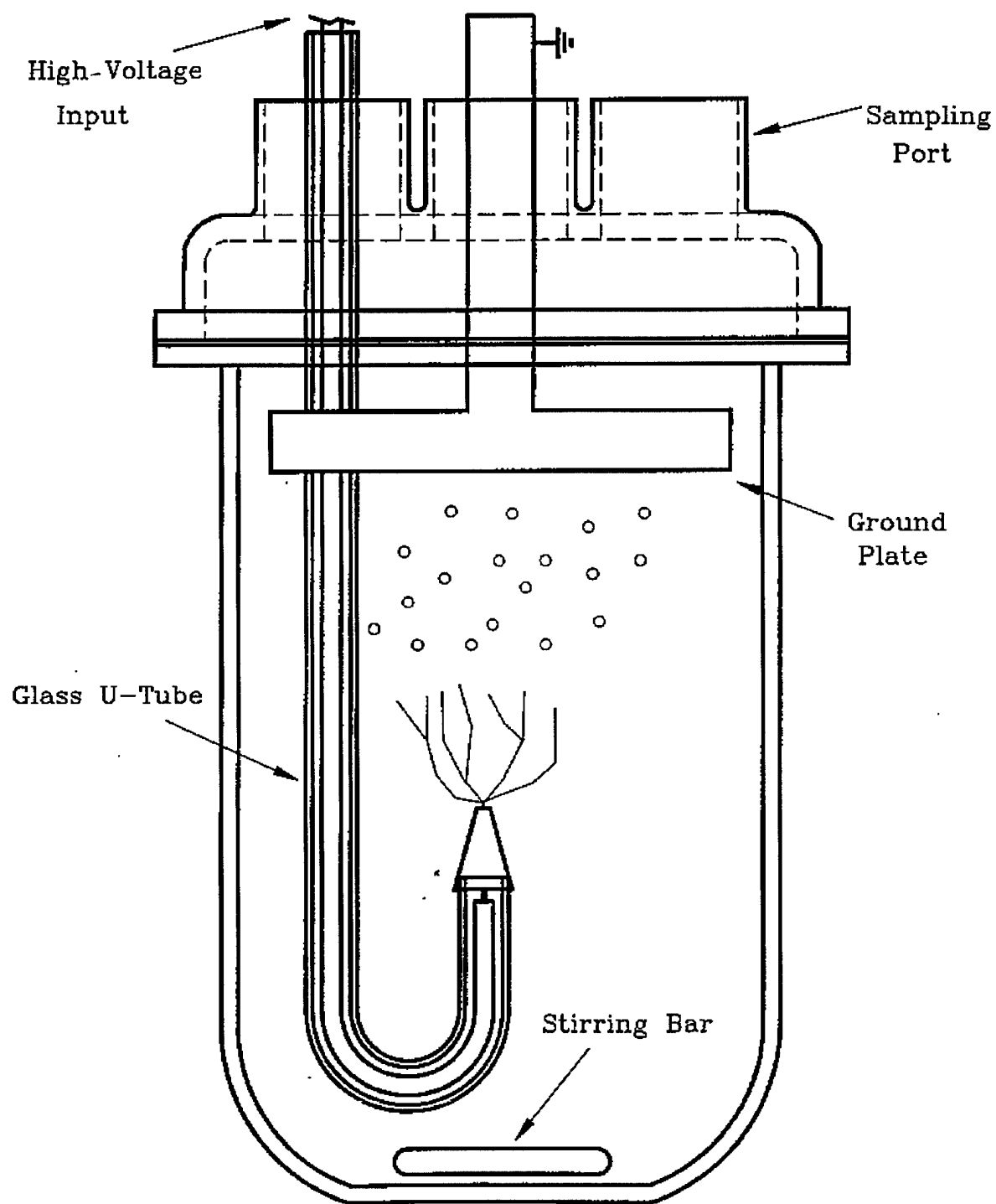
Figure 1. Schematic of liquid-phase reactor

characterization of the effects of particles on the discharge, including measurement of pulse voltage, current and power, utilized a Tektronix TDX 460 four-channel digitizing oscilloscope with a P6015A 1000x 3.0-pF, 1000-MΩ voltage probe and a current probe (P6016). In addition, a series of electron microscope studies, Proton Induced X-ray Emission (PIXIE) scans, and x-ray emissions measurements were performed on samples of activated carbon in order to determine the chemical composition and physical structure of these particles. These measurements were made using facilities located in the Department of Biological Sciences at Florida State University. Chemical analysis of the byproducts from the degradation of phenols in the pulsed corona reactor was made using a Perkin-Elmer HPLC located in the Department of Chemical Engineering and using a C-18 column.

SECTION III
REACTION MODELING (Task 8)

In order to describe the effects of added particles on the removal of small organic species from aqueous solution in the presence of pulsed corona discharge a reaction/diffusion model has been developed. The model includes chemical reaction within the pore space of the activated carbon particles as well as chemical reaction in the bulk solution. Adsorption and mass transfer effects are also included. Several cases of reaction/diffusion are developed below and example calculations given.

Case I

Consider a single porous particle suspended in a well-mixed batch reactor containing one reactive species with concentration c. The species continuity equation for the bulk phase is

$$V\frac{dc_b}{dt} = -AD\frac{\partial c}{\partial r}\Big|_R - k_b c_b V \tag{1}$$

where V is the volume of the bulk phase, D is the effective diffusion coefficient within the particle, A is the total external surface area of all particles (note that all particles are assumed to be identical spheres with radius R), k_b is the reaction rate constant in the bulk phase, and c_b is the bulk concentration of the reacting species. The particle-phase species balance is given by

$$\frac{\partial c}{\partial t} = D\frac{\partial^2 c}{\partial r^2} - k_p c \tag{2}$$

where c is the concentration in the particle, k_p is the reaction rate constant in the particle, and, for simplicity, particle curvature has been neglected (this will affect the final results only through a constant term).

The boundary and initial conditions are as follows,

$$c\Big|_{r=R} = Kc_b\Big|_{r=R} \tag{3}$$

$$\frac{\partial c}{\partial r}\Big|_{r=0} = 0 \tag{4}$$

$$c_b(t=0) = c_{b0} \tag{5}$$

$$c(t=0) = 0 \tag{6}$$

where K is the adsorption constant. The first step in solving equations (1) and (2) is to non-dimensionalize both of these equations by defining

$$S = \frac{r}{R} \tag{7}$$

$$\tau = \frac{tD}{R^2} \tag{8}$$

Substituting equations (7) and (8) into (1) and (2) gives

$$\frac{dc_b}{d\tau} = -\gamma \left.\frac{\partial c}{\partial s}\right|_1 - \phi_b c_b \tag{9}$$

$$\frac{\partial c}{\partial \tau} = \frac{\partial^2 c}{\partial s^2} - \phi_p c \tag{10}$$

Where the following definitions have been used,

$$\phi_b = \frac{k_b R^2}{D} \tag{11}$$

$$\phi_p = \frac{k_p R^2}{D} \tag{12}$$

$$\gamma = \frac{AR}{V} \tag{13}$$

The initial conditions (5) and (6) remain the same and the boundary conditions are now

$$\left.c\right|_1 = \left.Kc_b\right|_1 \tag{14}$$

$$\left.\frac{\partial c}{\partial s}\right|_0 = 0 \tag{15}$$

The solution of equation (10) will give the time and space variation of the concentration of the reactive species surrounding the particle. An averaging technique can be applied to simplify the analysis. An average concentration can be defined by

$$\langle c \rangle = \int_0^1 c\, ds \tag{16}$$

Applying the average to equation (10) gives

$$\frac{\partial \langle c \rangle}{\partial \tau} = \left.\frac{\partial c}{\partial s}\right|_1 - \phi_p \langle c \rangle \tag{17}$$

7

Equation (17) can be solved using a closure technique, which will lead to the following set of ordinary differential equations describing the average particle concentration and the bulk concentration as functions of time

$$\frac{d<c>}{d\tau} = (\psi - \phi_p)<c> -\psi K c_b \tag{18}$$

$$\frac{dc_b}{d\tau} = -\gamma\psi <c> +(\gamma K \psi - \phi_b)c_b \tag{19}$$

Defining the following groups

$$W = \psi - \phi_p \tag{20}$$

$$V = -K\psi \tag{21}$$

$$X = -\gamma\psi \tag{22}$$

$$Z = -(K\gamma\psi - \phi_b) \tag{23}$$

$$Q = 1/2(W - Z) \tag{24}$$

$$T = \frac{1}{2}\sqrt{(Z+W)^2 + 4XV} \tag{25}$$

where

$$\psi = \frac{\phi_p \tanh\sqrt{\phi_p}}{\tanh\sqrt{\phi_p} - \sqrt{\phi_p}}$$

and

$$\gamma = \frac{AR}{V}$$

leads to the final solution

$$c_b(\tau) = \left[\frac{c_{b0}}{2T}(T-Q-Z)\right]\left\{e^{(Q+T)\tau} - e^{(Q-T)\tau}\right\} + c_{bo}e^{(Q-T)\tau} \tag{26}$$

$$<c>(\tau) = \frac{Vc_{b0}}{2T}\left(e^{(Q+T)\tau} - e^{(Q-T)\tau}\right) \tag{27}$$

Case II

In this case the reaction rate is assumed to be negligible in the closure problem and all remaining aspects are the same as in case I. This approach leads to

$$\frac{d<c>}{d\tau} = (-3-\phi_p)<c> +3Kc_b \tag{28}$$

$$\frac{dc_b}{d\tau} = 3\gamma<c> -(3\gamma K+\phi_b)c_b \tag{29}$$

For these differential equations, the coefficients can be defined as

$$W = (-3-\phi_p) \tag{30}$$

$$V = 3K \tag{31}$$

$$X = 3\gamma \tag{32}$$

$$Z = (3\gamma K+\phi_b) \tag{33}$$

Case III

The previous two cases solved the problem without mass transfer resistance of the reactive species from the bulk solution to the carbon particle. This case will include the effects of mass transfer resistance for the case of a single-component system and, as in Case II, the reaction term will be left out of the closure problem. The species continuity equations for the bulk phase is, and the particle phase are, the same as before; however, the boundary condition for the particle phase changes to

$$- AD\frac{dc}{dr}\Big|_{r=R} = AK_{mt}(cR - Kc_b) \tag{34}$$

where K_{mt} is the mass transfer coefficient. Use of this boundary condition, following the same averaging procedure as outlined above, leads to

$$\frac{d<c>}{d\tau} = \left(\frac{-3RK_{mt}}{RK_{mt}+3D} - \phi_p\right)<c> +\left(\frac{3KK_{mt}R}{K_{mt}R+3D}\right)c_b \tag{35}$$

$$\frac{dc_b}{d\tau} = \left(\frac{AR^2 3K_{mt}}{VRK_{mt}+3VD}\right)<c> -\left(\frac{3AR^2 KK_{mt}}{VRK_{mt}+3VD}+\phi_b\right)c_b \tag{36}$$

Defining the groups

$$W = \left(\frac{-3RK_{mt}}{RK_{mt}+3D} - \phi_p\right) \tag{37}$$

9

$$V = \left(\frac{3KK_{mt}R}{K_{mt}R + 3D} \right) \qquad (38)$$

$$X = \left(\frac{AR^2 3K_{mt}}{VRK_{mt} + 3VD} \right) \qquad (39)$$

$$Z = \left(\frac{3AR^2 KK_{mt}}{VRK_{mt} + 3VD} + \phi_b \right) \qquad (40)$$

$$Q = 1/2(W\text{-}Z) \qquad (41)$$

$$T = \frac{1}{2}\sqrt{(Z+W)^2 + 4VX} \qquad (42)$$

The same general solution as in the two previous cases applies.

Figure 2 shows sample calculations of the bulk and particle concentrations as a function of time determined by the model. The bulk concentration decreases monotonically and the average particle concentration initially increases as solute is adsorbed and gradually drops as surface particle reactions begin to take place. Increasing the reaction rate constant in the particle, as shown in Figure 3, leads to a more rapid drop in solute concentration in the particle, as is to be expected. Figure 4 shows the effect of decreasing γ, which reflects a decrease in area of particle divided by volume of solution, leads to a slower decay in the average particle concentration. This model has been extended to account for a system of multi-component interacting species. Further work is necessary to couple this model of the chemical reactions to physical descriptions of the nature of streamer propagation in the liquid phase. Currently, there is no well-developed or accepted treatment for the description of streamer formation and propagation in liquid phase, although of the two competing models, the model that involves thermal bubble formation (Jones and Kundhardt, 1995) is perhaps more applicable to the longer pulses used in the present study. Joshi, et al. (1995), considered the effect of the electrical field on the reaction rate constants and found the initiation reactions to depend upon the field in a manner described by Kuskova (1990). Further experimental data at various electrical fields in the presence of particles is necessary to test this model for the conditions reported in the present study.
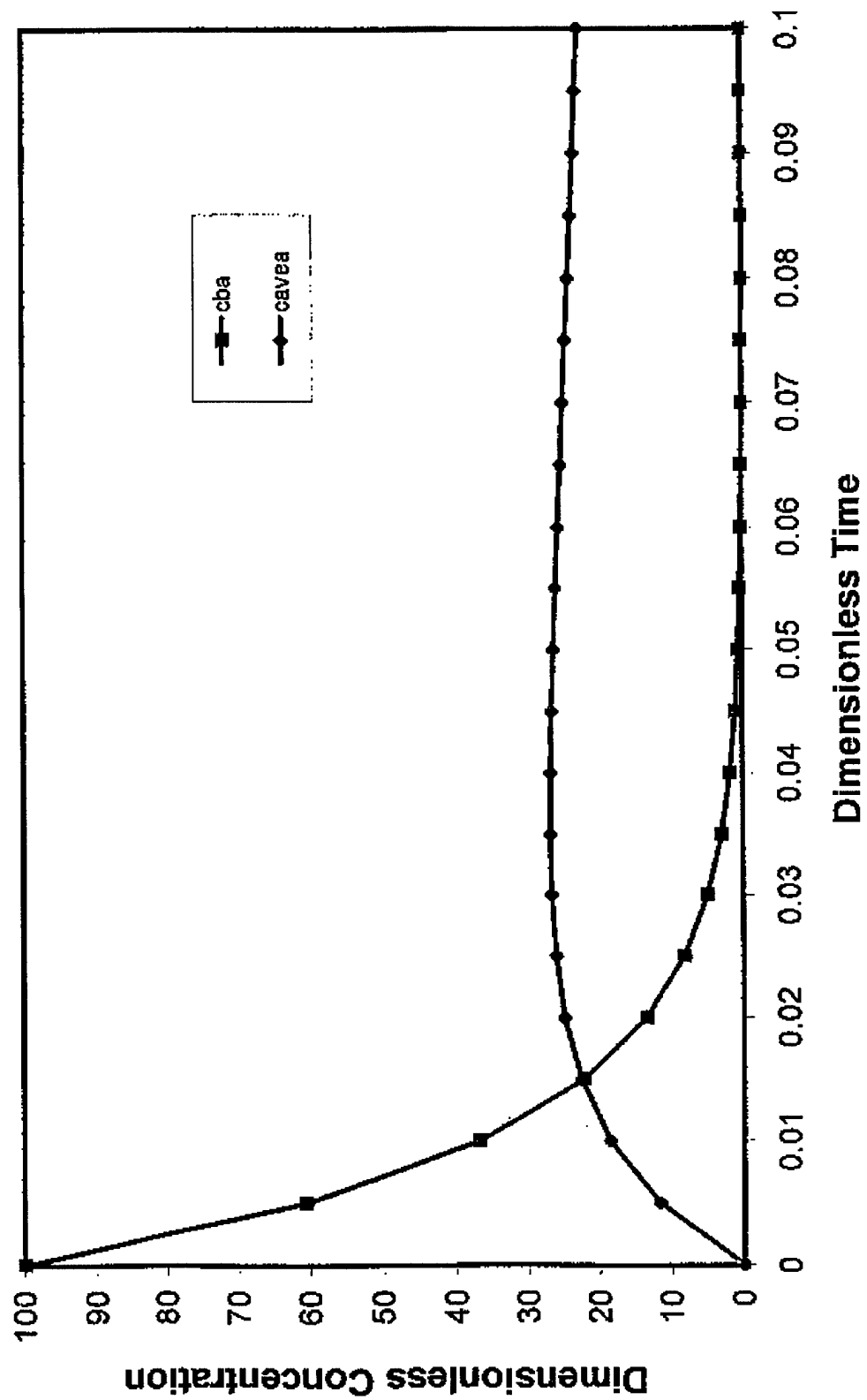
Figure 2. Concentrations of bulk and particle with time as calculated by the model. Monocomponent Model $\phi_b=10^2$, $\phi_p=10^{-1}$, $\gamma=10^{-4}$, $K=10^{-1}$
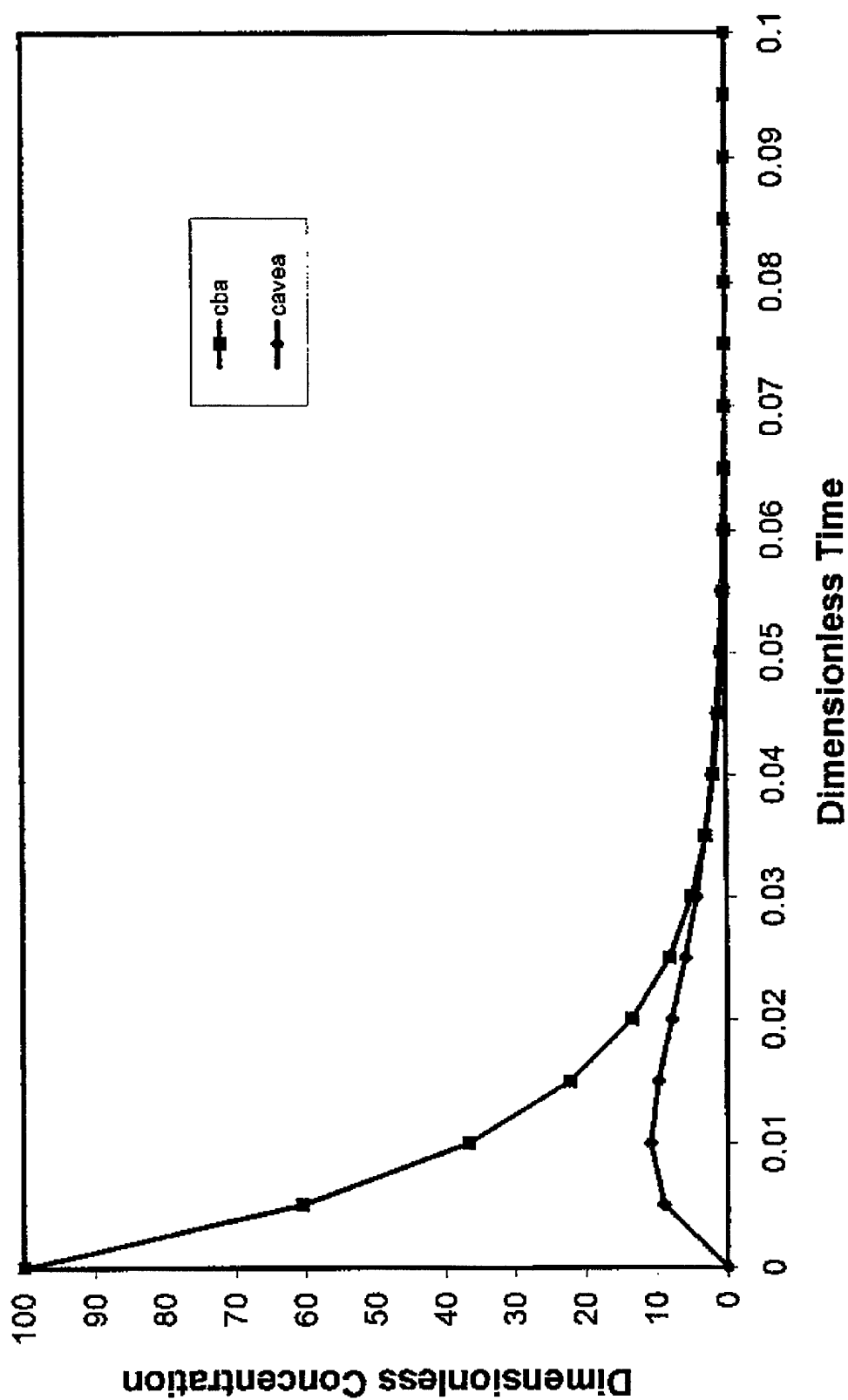
Figure 3. Model calculations for large particle reaction rates. Monocomponent Model $\phi_b=10^2$, $\phi_p=10^2$, $\gamma=10^{-4}$, $K=10^1$
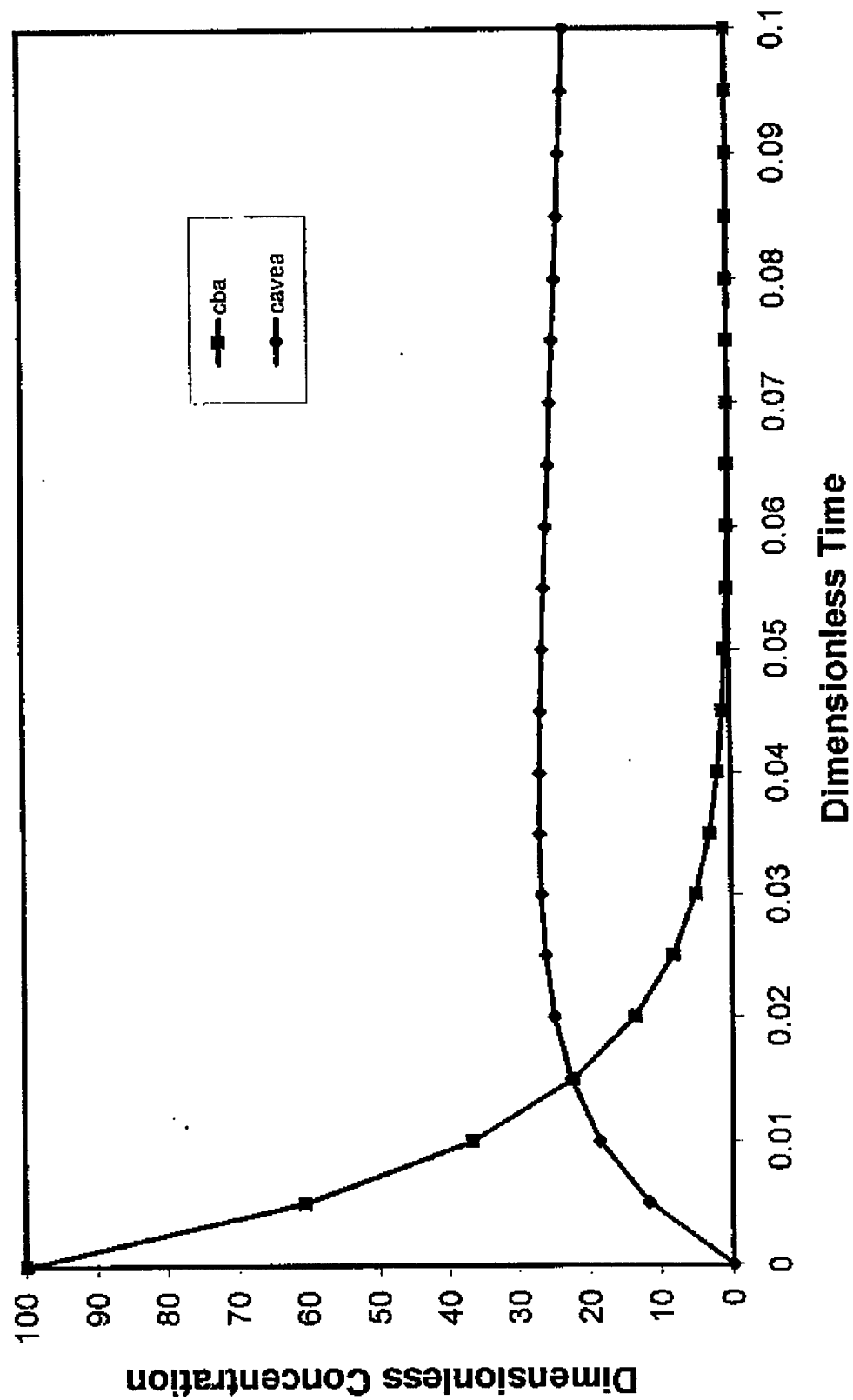
Figure 4. Effect of decreasing Υ on bulk and particle concentrations.
Monocomponent Model $\phi_b=10^2$, $\phi_p=10^{-1}$, $\gamma=10^{-6}$, $K=10^1$

SECTION IV
EXPERIMENTAL RESULTS & DISCUSSION

A. PHYSICAL DISCHARGE CHARACTERISTICS (Task 6)

Analysis of the effects of the added particles in combination with various types and concentrations of salts is very important in assessing the utility of aqueous phase pulsed corona. An extensive series of runs with activated carbon, washed activated carbon, glass spheres, washed glass spheres, and copper particles was conducted. Measurement of power, voltage, current, and sparkover voltage was made with various concentrations of salts and particles.

Figure 5 summarizes the effects of the added particles on the sparkover characteristics of the corona discharge. From these experiments and earlier results it is clear that powdered activated carbon has a substantially different effect on the corona reactor performance than any other additive that we have considered. In addition to an increase in the sparkover voltage, visual observations also show enhanced streamer length, width, and intensity. The addition of salts, such as KI and others, also leads to increased sparkover voltages, however they do not enhance streamer production and propagation.

To determine what was unique about activated carbon, elemental analysis of the carbon was performed. Proton Induced X-ray Emission (PIXIE) of activated carbon powder, aqueous solutions leached from the activated carbon, and aqueous solutions leached from the glass beads gave the elemental composition of these samples as shown in Table 1. The commonest element observed by PIXIE in the activated carbon was potassium (9210 ppm). This was followed by 1040 ppm of sulfur, 397 ppm calcium, 247 ppm phosphorus, and 129 ppm chlorine; the remaining elements as shown in the table were below 100 ppm. The leached solution also contained high levels of potassium, i.e., 157 ppm, and the various amounts of all the other remaining elements were below 5 ppm. For comparison the solution leached from the glass beads contained 39 ppm sodium, 9.4 ppm silicon, 9.9 ppm sulfur, 6.4 ppm calcium, 5.07 ppm chlorine, no potassium, and very low levels of several other elements.
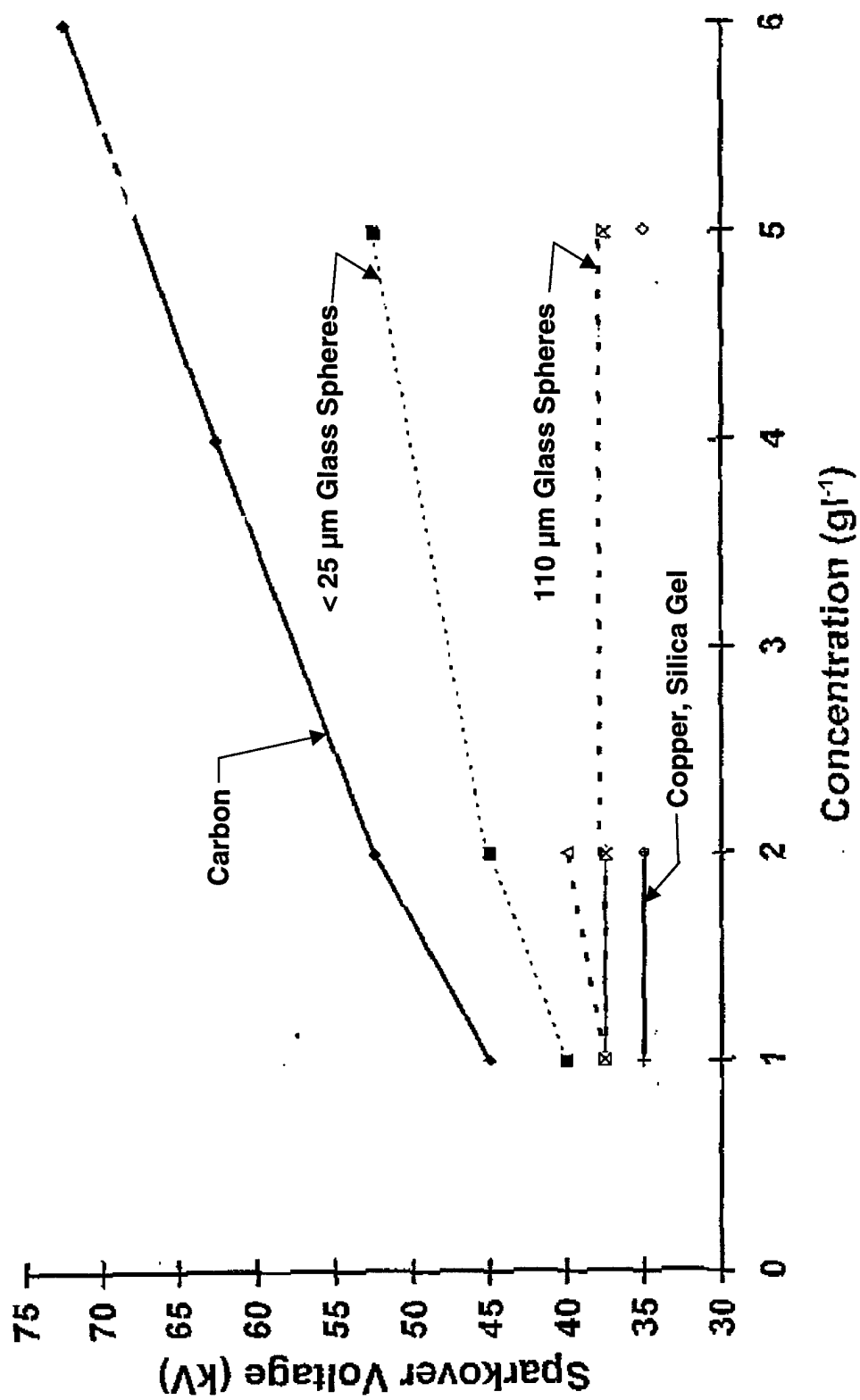
14

Figure 5. Summary of effects of additives on sparkover voltages

TABLE 1. Elemental Composition from PIXIE analysis of carbon particles and wash solutions.

element	carbon	carbon leachate	glass bead leachate
sodium	bdl	12 ppm	39 ppm
silicon	86 ppm	4.90 ppm	9.39 ppm
phosphorous	247 ppm	4.20 ppm	bdl
sulfur	1040 ppm	bdl	9.89 ppm
chlorine	129 ppm	2.63 ppm	5.07 ppm
potassium	9210 ppm	157 ppm	bdl
calcium	397 ppm	3.07 ppm	6.39 ppm
chromium	2.6 ppm	bdl	0.188 ppm
manganese	4.7 ppm	bdl	bdl
nickel	bdl	bdl	0.016
iron	94 ppm	0.069 ppm	0.061 ppm
copper	19 ppm	0.05p ppm	0.030 ppm
zinc	1.56 ppm	0.122 ppm	0.100 ppm
rubidium	17 ppm	0.294 ppm	bdl
molybdenum	6.66 ppm	bdl	bdl
selenium	bdl	bdl	0.022
strontium	13 ppm	bdl	bdl

(bdl = 1 ppb)

A series of experiments using cleaned activated carbon with various added salts was performed in order to determine if the chemical composition of the salts affected the electrical discharge. Figure 6 shows the power, in mJ/pulse, versus the applied voltage for samples of 1 and 2 g/l cleaned activated carbon with potassium chloride solutions of the same conductivity. It is clear that the combination of potassium chloride and activated carbon results in significantly lower power consumption in the reactor. Figure 7 shows the effects of carbon in combination with sodium chloride and calcium chloride solutions of the same conductivity. Clearly these two solutions behave as the potassium chloride solution without the addition of carbon. The
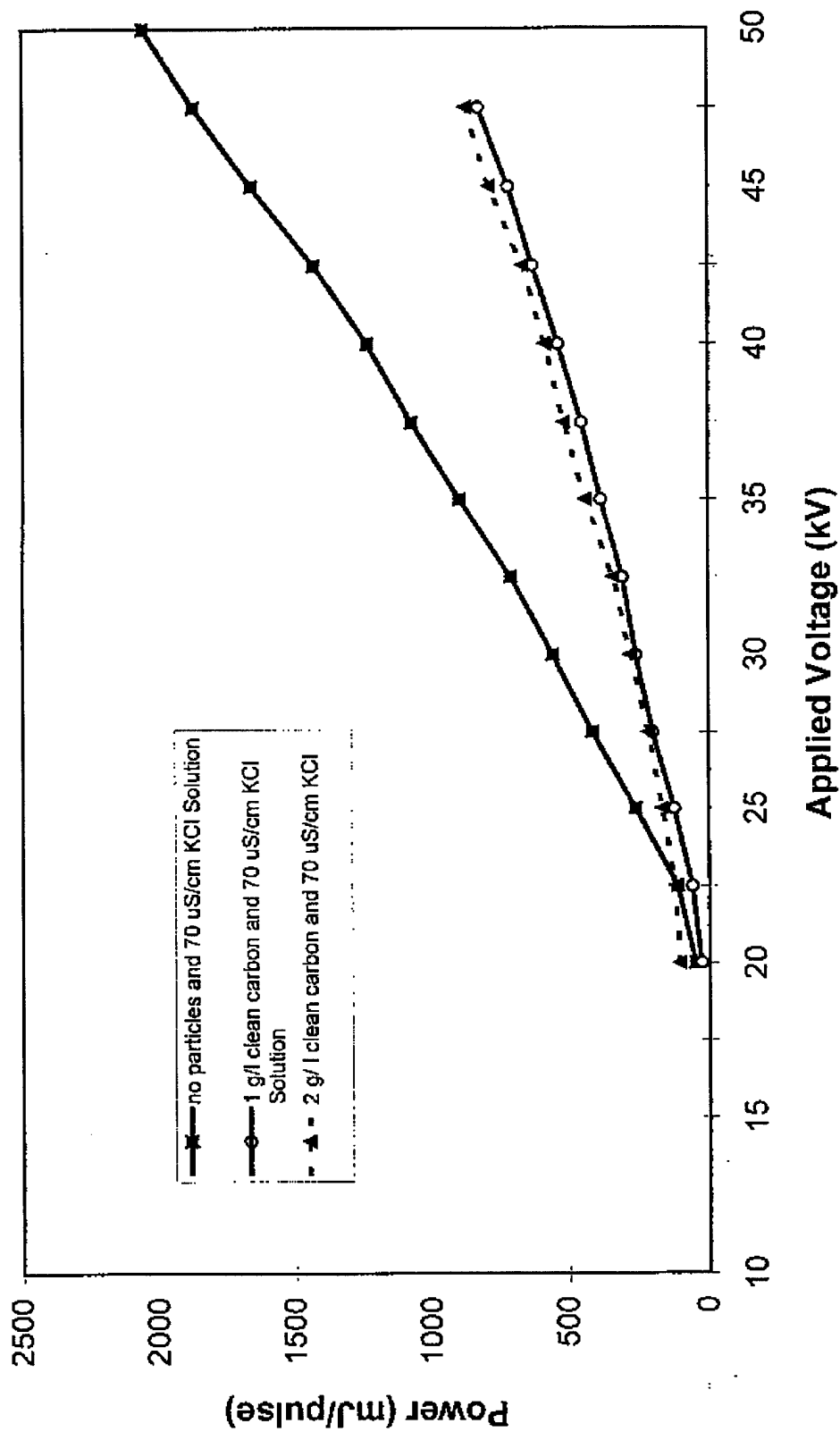
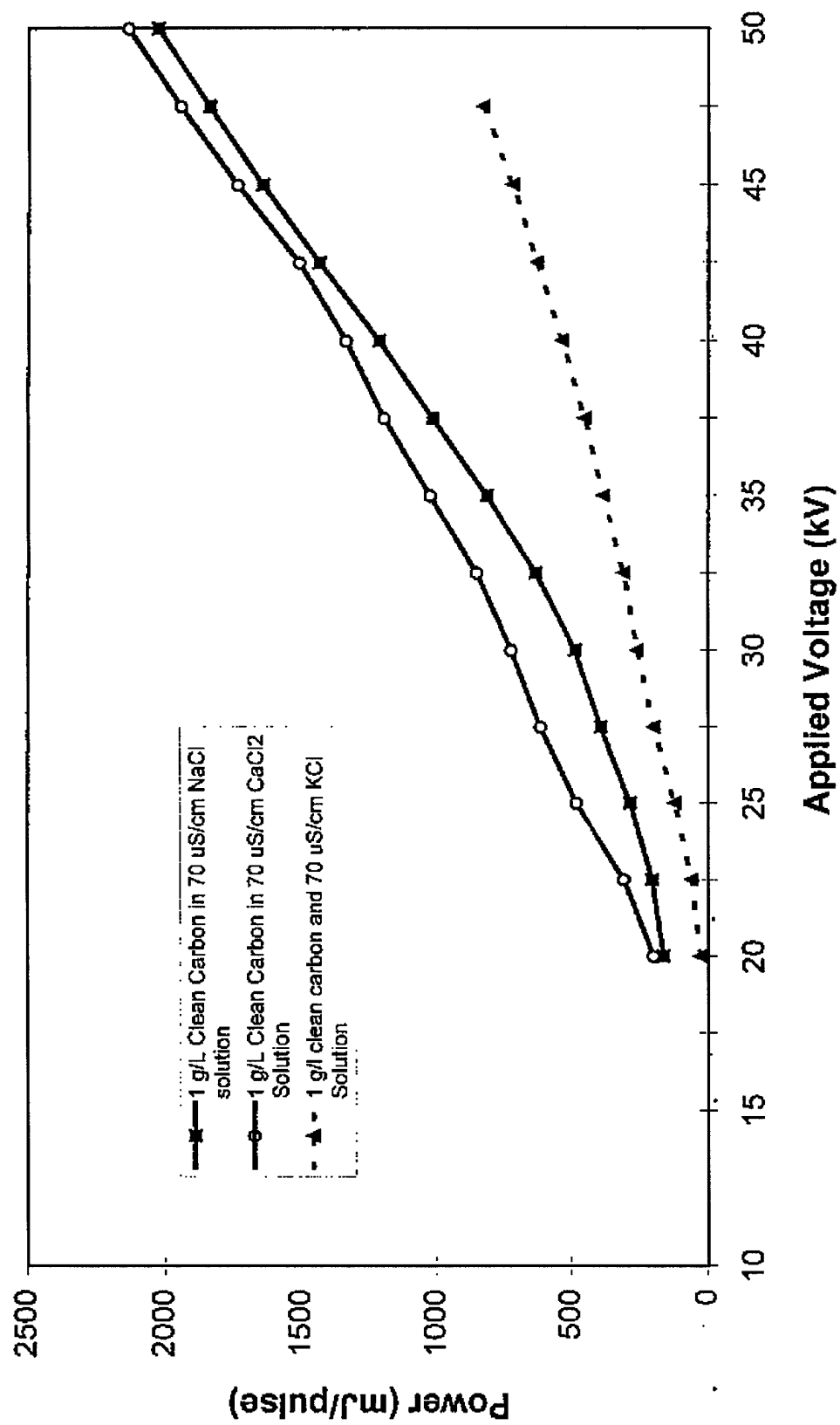Figure 6. Power consumption of carbon solutions with and without potassium chloride.

Figure 7. Power consumption of carbon with various salt solutions.

combination of potassium and cleaned carbon clearly results in lower power consumption than any of the other solutions considered. Glass beads in all salt solutions also resulted in behavior very similar to the case of sodium chloride and calcium chloride with and without added carbon particles.

Electron microscope studies of dirty and clean carbon were also performed and showed a large variety of basic surface and pore features of the carbon and distinct "spots" associated with the dirty carbon. These spots appeared to be removed when the carbon was washed with de-ionized water. The general pore structure was not changed with washing, as expected, and the macropores were generally of about 1 micron size. X-ray emissions scans of dirty and clean carbon also showed high levels of potassium and some sulfur, silicon, and chlorine associated with distinct spots on the surface of the carbon. The potassium, as well as these spots, disappeared after the carbon was washed with de-ionized water. Scans of dirty and clean carbon treated with pulsed corona discharge were also performed. The dirty carbon showed both silicon and potassium on both the overall surface and the surface deposits. The washed carbon, after corona treatment, showed no potassium, but had high levels of chlorine and silicon.

B. PHENOL DEGRADATION EXPERIMENTS (Tasks 6 and 7)

Figure 8 shows the concentration of phenol and several byproducts as a function of time for solutions containing 1 g/l of clean activated carbon at 45 kV. The overall concentration of phenol decreased from about 100 ppm to about 10 ppm in 15 minutes and at the same time the byproduct with the largest concentration was catechol. Figure 9 compares the corona and no carbon case with the corona and carbon case and the no corona and carbon case. Clearly corona alone has the slowest decrease of phenol with time, although about 40 ppm of phenol is removed in 15 minutes. The rate of decrease without corona and with carbon alone reflects the adsorptive capacity of the activated carbon, however, no degradation reactions occur for this case. The corona with carbon showed the highest removal of phenol and, as reflected in Figure 8, the phenol is not just removed from solution; it is chemically degraded into byproducts. Figures 10 and 11 show the concentrations of catechol and hydroquinone for 45-kV corona discharge with and without carbon. Figure 10 shows a higher bulk solution concentration of catechol for the
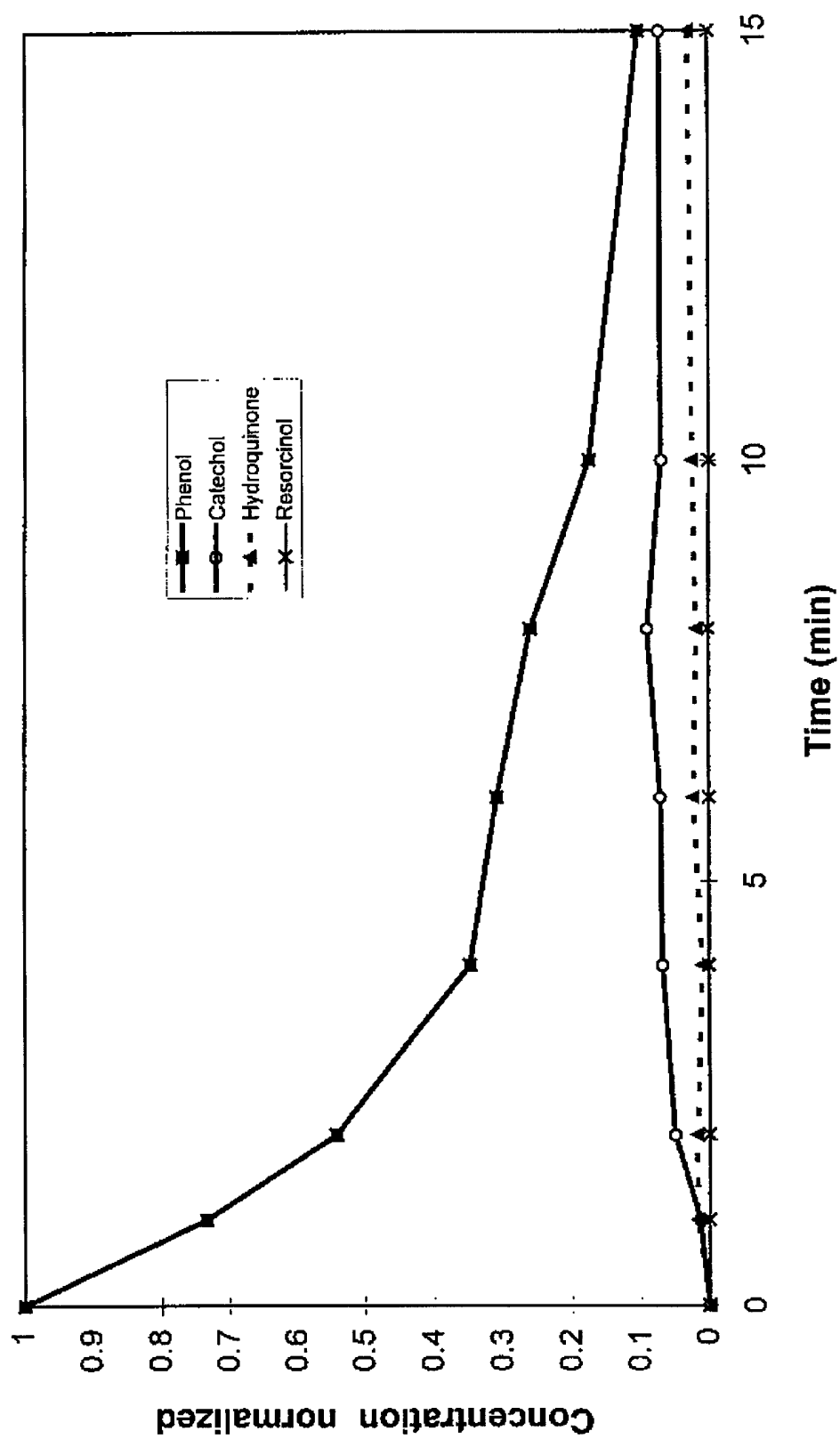
19

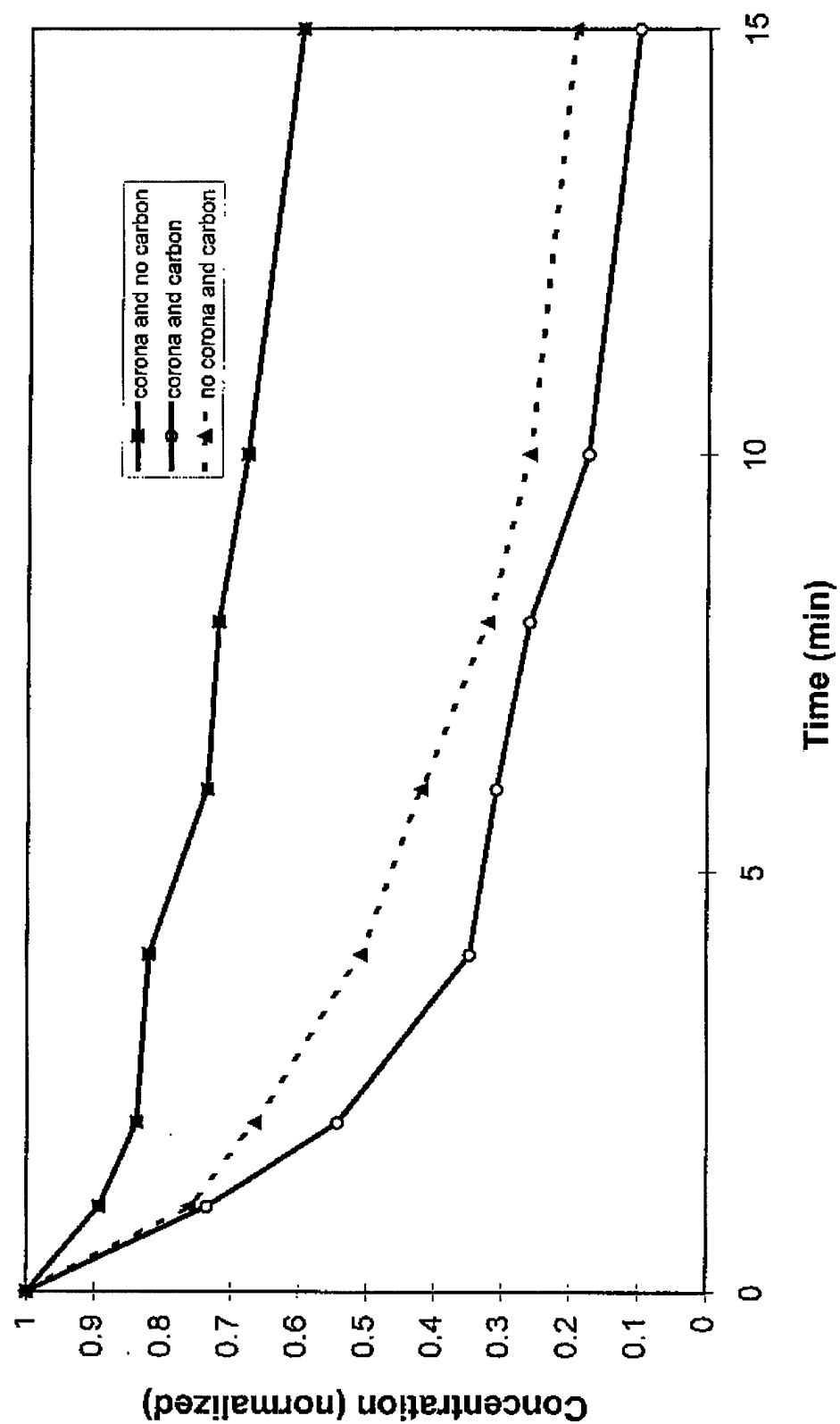Figure 8. Phenol and byproducts for 1 g/l clean carbon at 45 kV

Figure 9. Comparison of corona without carbon to corona with carbon and to carbon without corona
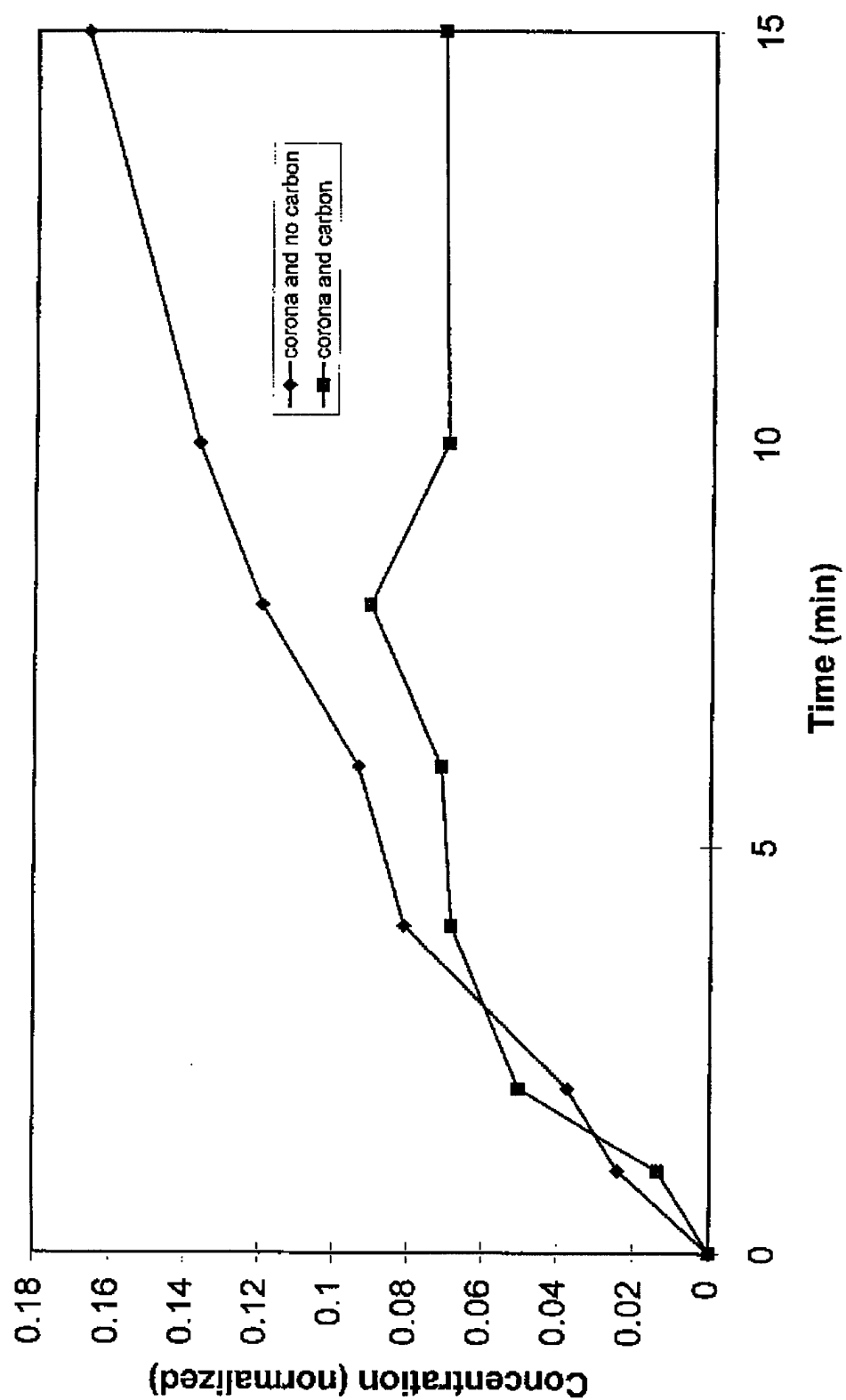
21

Figure 10. Catechol concentration for cases with and without activated carbon with 45 kV
pulsed corona.

corona without carbon, however, clearly the catechol also adsorbs onto the carbon. Figure 11 shows a higher concentration of hydroquinone in the bulk solution for the case of carbon and corona than for corona without carbon. Therefore, the presence of carbon dramatically affects the product distribution, which indicates the possibility of surface-induced or at least carbon-corona-induced chemical reactions that do not occur with corona alone or certainly with carbon alone.

C. EXPERIMENTS ON CORONA WITH FOAM

Aqueous Film-Forming Foam (AFFF) is a popular fire fighting material used in extinguishing fires of flammable liquids or on vertical surfaces. AFFF is a very stable foam that is not readily degraded by biological or chemical methods. Experiments performed with pulsed corona discharge and AFFF have focused on qualitative analysis of the physical changes in the foam structure during a pulsed corona discharge and quantitative analysis of the pulse characteristics of the corona discharge in the foam (Lamar, 1996).

A series of runs with various amounts of surfactant in the reactor were performed. It was found that the properties of the waveform varied with the amount of surfactant present and with the location of the discharge needle. The rise time was greater and the pulse width and maximum voltages were smaller when the concentration of foam was larger. There was no change in foamability of the solution or stability of the resulting foam after treatment with pulsed corona for 15 minutes. In addition, no significant changes in the conductivity or pH of the solution could be observed. When foam filled the gap between the electrodes, it was found that approximately 700 ml of foam was broken down in about 10 minutes. Since the resulting solution could be refoamed and the stability and structure of the foam was not different from the original, it was concluded that the foam was not chemically degraded by the corona and that mechanical shock waves created by the foam led to rupture of the films in the foam (Lamar, 1996).
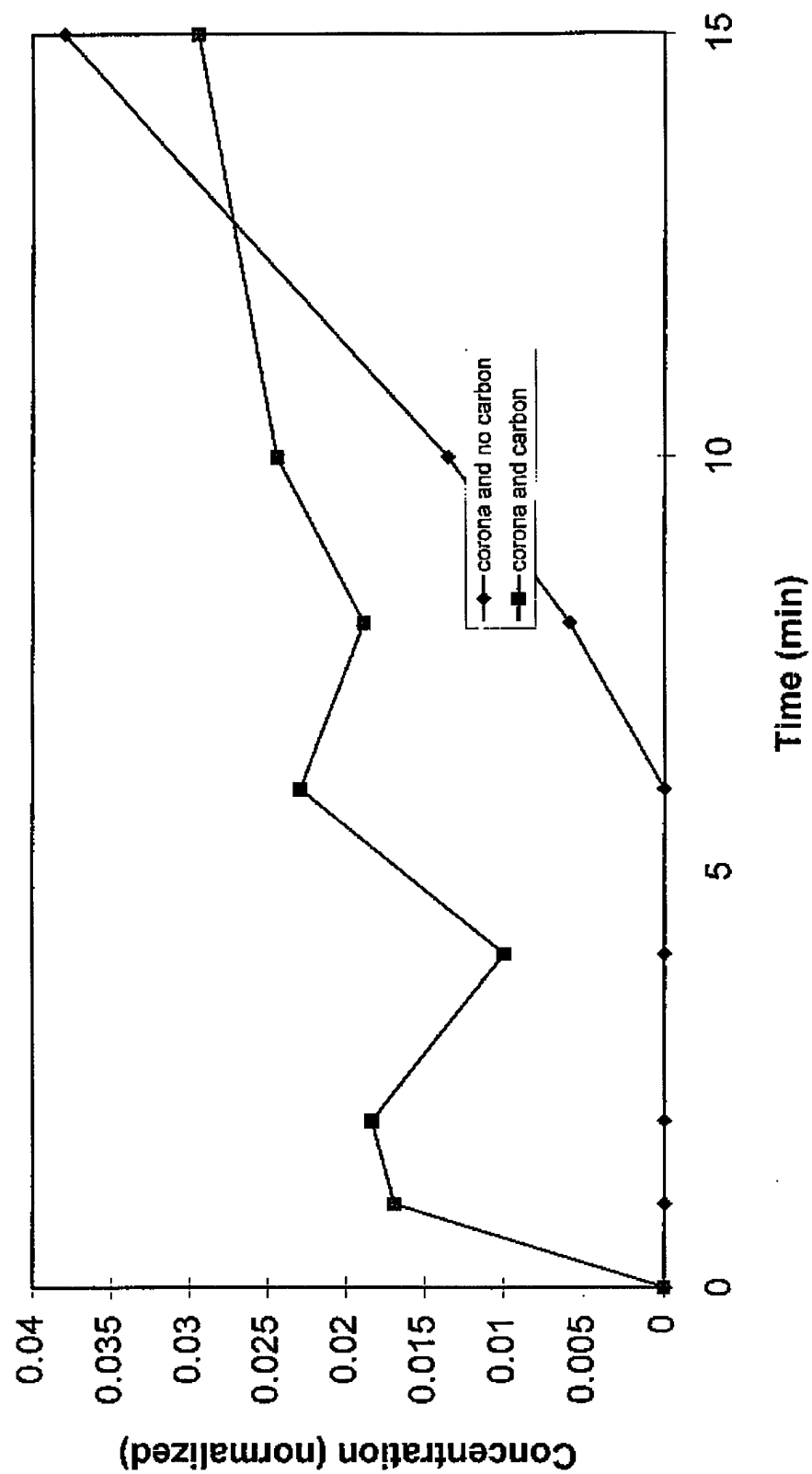
Figure 11. Hydroquinone concentration for cases with and without activated carbon with 45 kV pulsed corona

SECTION V

CONCLUSIONS

Pulsed corona discharge in aqueous solutions is a potential method to treat contaminated water containing small aromatic compounds. The addition of activated carbon has been found to dramatically affect the power characteristics and the streamer properties of liquid phase discharges. The addition of potassium in combination with cleaned carbon caused the power consumption of the reactor to decrease and also led to enhanced streamer production and streamer intensity. A mathematical model using concepts from reaction/diffusion analysis describes the general effects of combined bulk chemical reaction, particle surface reaction, adsorption, and mass transfer on reactant depletion in the corona reactor. The major byproducts observed for phenol degradation include hydroquinone, catechol, and resorcinol. Analysis of the rates of change of bulk solution concentration with time indicate that corona combined with activated carbon leads to enhanced phenol degradation in comparison to corona alone and to simple adsorption that occurs with carbon alone.

SECTION VI
RECOMMENDATIONS

The present study has focused on the application of pulsed corona discharge in the presence of activated carbon particles and leads to the possibility of surface-induced chemical reactions. In order to consider more fully surface-induced chemical reaction by corona discharge, it is recommended that further work on the modification of the corona electrodes be conducted. Specific recommendations include:

1) Modify liquid-phase reactor for use with reticulated vitreous carbon electrodes. Perform electrical field studies by connecting carbon electrodes to high-voltage power supply source. Measure current, voltage, and power waveforms using high-voltage oscilloscope. Perform electrical tests by connecting various carbon electrodes to the ground side of the electrical circuit. Measure current, voltage, and power waveforms using high-voltage oscilloscope.

2) Measure effects of carbon electrodes on the production of hydrogen peroxide and hydroxyl radicals in de-ionized water and water containing various salt compositions and concentrations following methods given in Joshi, et al. (1995).

3) Measure effect of electrodes on ozone production when air or oxygen gas is bubbled into the corona reactor.

4) Determine the effect of the above electrode modifications on model test compound destruction through measurement of reaction products and rate of decomposition. Measure products and reactants with HPLC following methods used by Grymonpre' (1997) and compare with experiments conducted for a non-modified corona reactor.

5) Modify electrodes through coating with transition metal catalysts and other catalysts and determine if these modifications lead to enhanced chemical degradation of target pollutants or enhanced production of reactive species.

SECTION VII

REFERENCES

Abuzald, N. S. and G. F. Nakhla, 1994 : Dissolved Oxygen Effects on Equilibrium and Kinetics of Phenolics Adsorption by Activated Carbon. *Environmental Science & Technology*, 216.

Clements, J.C., M. Sato, and R.H. Davis, 1987 : Preliminary Investigation of Prebreakdown Phenomena and Chemical Reactions Using a Pulsed High-Voltage Discharge in Water, *IEEE Transactions on Industrial Applications* IA-23(2), 224.

Clements, J.S., A. Mizuno, W. C. Finney, and R. H. Davis, 1989 : Combined Removal of SO_2, NO_x, and Fly Ash from Simulated Flue Gas Using Pulsed Streamer Corona, *IEEE Transactions on Industrial Applications*, 25, 62–69.

Creyghton, Y. L. M., 1994 : *Pulsed Positive Corona Discharges, Fundamental Study and Application to Flue Gas Treatment*, CIP-DATA, Koninkijke Biblitheck, Den Haag, Netherlands.

Devins, J.C., S.J. Rzad, and R.J. Schwabe, 1981 : Breakdown and Prebreakdown Phenomena in Liquids, *Journal of Applied Physics*, 52 (7), 4531.

Jones, H. M. and E. E. Kundhardt, 1995a : Development of Pulsed Dielectric Breakdown in Liquids, *Journal of Physics Design: Applied Physics*, 28, 178–188.

Jones, H. M. and E. E. Kunhardt, 1995b : Pulsed Dielectric Breakdown of Pressurized Water and Salt Solutions, *Journal of Applied Physics*, 77(2), 795.

Joshi, A. A., B. R. Locke, P. Arce, and W.C. Finney, 1995 : Formation of Hydroxyl Radicals, Hydrogen Peroxide and Aqueous Electron by Pulsed Streamer Corona Discharge in Aqueous Solution, *Journal of Hazardous Materials*, 41(1), 3.

Klimkin, V. F., 1986 : Development of Electrical Breakdown in *n*-Hexane in Microsecond to Nanosecond Range, *Sov. Phys. Tech. Phys.* 31(190), 1223.

Klimkin, V. F., 1990 : Mechanisms of Electric Breakdown of Water from Pointed Anode in the Nanosecond Range, *Sov. Tech. Phys. Lett.* 16(2), 146.

Kuskova, N. I., 1990 : Mechanism of Electrical Breakdown in Water, *Sov. Tech. Phys. Lett.*, 15(12), 936.

LaMar, D., 1996 Exploratory Experimental Studies of Foam Breakdown and Electrical Characteristics in a Pulsed Corona Reactor, Summer Research Report for Cadet Summer Research Program, United States Air Force Academy Department of Chemistry, performed at Florida State University, Department of Chemical Engineering. (Appendix)

Loeb, L. B., 1965, *Electrical Coronas*, University of California Press.

Masuda, S. and H. Nakao, 1990 : Control of NO_x by Positive and Negative Pulsed Corona Discharges, *IEEE Transactions on Industrial Applications*, 26, 374–383.

Nasser, E., 1971 : *Fundamentals of Gaseous Ionization and Plasma Electronics*, Wiley-Interscience, New York.

Sharma, A. K., B. R. Locke, P. Arce, and W.C. Finney, 1993 : A Preliminary Study of Pulsed Streamer Corona Discharge for the Degradation of Phenol in Aqueous Solutions, *Hazardous Waste & Hazardous Materials*, 10(2), 209.

Vidic, R. D., M. T. Suldan, and R. T. Brenner, 1993 : Oxidative Coupling of Phenols on Activated Carbon : Impact on Adsorption Equilibrium, *Environmental Science & Technology*, 27, 2085.

APPENDIX

EXPLORATORY EXPERIMENTAL STUDIES OF FOAM BREAKDOWN AND

ELECTRICAL CHARACTERISTICS IN A PULSED CORONA REACTOR

by

Daniel LaMar

Cadet Daniel LaMar

Department of Chemistry
United States Air Force Academy
Colorado Springs, CO 80841

Submitted in partial fulfillment of the requirements for the
Cadet Summer Research Program

14 June 1996

Bruce R. Locke

Dr. Bruce R. Locke
Department of Chemical Engineering
FAMU-FSU College of Engineering
Tallahassee, FL 32310-6046
Associate Professor and Directing Advisor

PREFACE

This report was prepared by Cadet Daniel LaMar from the United States Air Force Academy while working on the Cadet Summer Research Program (CSRP). The research was conducted at the FAMU-FSU College of Engineering under the supervision of Dr. Bruce R. Locke.

This final report describes the physical and electrical characteristics observed for the pulsed corona reactor with different electrode configurations in the presence of foam and surfactant solutions. It also describes the effects of different gases in the spark gap during the trial runs and provides recommendations for future studies with the foam in the pulsed corona reactor.

The author would like to thank Mr. David Grymonpré and Mr. Steven White for their help in this project.

The work was performed between May 24 and June 14, 1996 at the Department of Chemical Engineering at the FAMU-FSU College of Engineering. The Air Force Academy CSRP Officer was Capt. Steve Thompson. The Tyndall AFB point of contact was Mr. Alan Canfield.

INTRODUCTION

1. STATEMENT OF PROBLEM

Controlling fire has been a problem for an extremely long time. Fire is very destructive and is fairly difficult to control. For this reason, there has been much emphasis placed on the capability to fight fires effectively. There are several methods that are currently used; the most common of which is the addition of water. However, water has some major problems when used against certain types of fires. The first type of fire that cannot be controlled with water is the Class B fire, or the normal flammable liquid fire, where the fuel has a specific gravity of less than 1. This makes the fuel less dense than water. When the fire fighters add water to put these fires out, the fuels tend to float on the water and continue to burn. The other kind of fire that water does not work well on is the Class A fire made from ordinary combustibles with vertical surfaces. When there is a vertical surface that is on fire, the water tends to run off this surface, and it does not stay in the heat zone long enough to get maximum benefit from its heat absorbing capabilities (Mellot 1992). Due to these important problems with water as a fire fighting material, there has been work performed to develop other fire fighting technologies.

The main fire fighting material that is used in extinguishing fires of flammable liquids or vertical surfaces is a foam. A foam is "an agglomeration of gas bubbles separated from each other by thin liquid films (Bikerman 1973)". One type of foam that is used in this work is AFFF (Aqueous Film Forming Foam). This foam is popular enough that it dominates the American market in fire fighting foams (Wilson 1989). Although AFFF has good fire fighting characteristics, there is one major problem that

arises each time the foam is used. AFFF is a very stable foam that does not break down easily. It is stable enough that the foam does not go away for a long period of time after its use. Because of this, Tyndall AFB is facilitating research at Florida State University in order to determine whether a pulsed streamer corona can be used to break down this foam.

2. STRUCTURE OF A FOAM

The structure of a foam is important in understanding why some foams are stable and others are not. It is therefore important to distinguish the difference between good stability and good foamability. In general, a foam that has good foamability has "the capacity for rapid adsorption and unfolding at the interface." According to Wilson, "Foam stability on the other hand, is dependent on the ability...to form a strong, flexible, cohesive film, so as to reduce gas permeability and inhibit bubble coalescence." (Wilson 1989). Thus, a foam that is very foamable can easily form foam, while a foam with good stability does not necessarily form a lot of foam, but it does not break down easily. There are many foams that are foamable but not stable, or vice versa.

In order for a foam to exist, it must have two characteristics. The liquid must exhibit surface tension (Aubert 1986). There is nearly always an attraction to like molecules due to van der Waals forces. All purely polar or purely non-polar liquids have surface tension, however the molecules that are both polar and non-polar such as isopropyl alcohol tend to have very little surface tension. The molecules of any pure liquid like to be close to molecules of the same molecular structure. When these

molecules are in the bulk liquid they feel an isotropic attraction from all directions. However, when any of these molecules start getting close to the liquid-air interface, they are more strongly attracted to the bulk liquid than to the surface. This makes the energy higher at the surface than in the bulk liquid, and demonstrates the phenomenon of surface tension. Also, there can not be a single substance by itself; there must be an impurity added (Aubert 1986). In the example of AFFF, there are four main ingredients: 2-(2-butoxyethoxy) ethanol, water, flouroalkyl surfactants, and synthetic detergents. One of these ingredients by itself could not create a foam. However, the combination of these compounds creates an extremely good foam. In this paper, the only type of foam that will be referred to are aqueous foams which are foams that must be mixed with water in order to form a "good" foam.

The foaming agent that is added to water must have a particular chemical structure in order to be a suitable surfactant. This agent must have an end that is hydrophilic and an end that is hydrophobic. In order to form a foam the surface tension of the overall liquid must be lowered as mentioned above. When this happens, the difference in energy between the bulk liquid and the surface is not as great. Thus, the molecules have a greater affinity for the surface than they did before the surfactant was added. The reason for this lowering of the surface tension is due to the hydrophobic end being attracted to the surface while the hydrophilic end is attracted to the bulk liquid. This causes the energy inside the liquid to be raised, and the energy on the surface to be lowered. With this liquid having a lower energy differential between the surface and the bulk liquid it is possible to make a foam. The typical surface tension of water is approximately 73 mN/m,

while the surface tension of water with a surfactant will generally be 35 mN/m or less (Wilson 1989).

Once a film has been formed, the Gibbs and the Marangoni effects can be used to explain the stability of the foam cells. The Gibbs effect states that as a foam cell increases in size, the surface tension also increases, thus making the bubble contract and become smaller (Aubert 76). This effect is caused by the concentration of surfactant molecules at the surface. There are a finite number of these surfactant molecules in each bubble, and when the bubble gets stretched, the proportions of surfactant molecules at the surface decrease. As shown earlier, a decrease in surfactant concentration gives an increase in surface tension. This causes a decrease in the size of the bubble. The Marangoni effect is a temporary effect that states that as a bubble gets larger it takes a certain amount of time for the surfactant molecules to diffuse to the surface of the bubble (Aubert 1986). This makes it where the surface tension slowly decreases to the Gibbs value. This slow transition causes the bubbles to stay virtually the same size without small fluctuations in thickness.

The final factor that is interesting about foams is the shape of their bubbles. When a foam is wet (just after it has been foamed), the bubbles are perfectly spherical (Aubert 1986). If there is a lot of water in the foam, the water stays in between each bubble and causes it to be perfectly spherical. However, when a bubble has become dry as liquid drains off, it no longer has the spherical shape. The bubbles take on an irregular polyhedral shape caused by the lack of water in the boundaries. Without water to fill up the boundaries between the bubbles, there is nothing to keep them perfectly spherical, and

they instead become irregular in shape with straight lines, and up to 120° corners between the bubbles.

3. PULSED STREAMER CORONA - LIQUID PHASE

The pulsed streamer corona is a technology that has been in use for more than fifteen years. However, the first use of a pulsed streamer corona in a liquid came in 1985 (Clements 1985). This technology uses a high voltage power supply to produce a pulse across a gap sometimes filled with air, water, or other liquids. When the voltage becomes high enough a corona discharge is formed. This corona forms what are considered streamers. These streamers are actually "region(s) of highly ionized gas (a non-thermal plasma) where a wide range of highly reactive radicals and species are formed through collisions among electrons, molecules, and ions (Chang 1992)." The variables that can be changed in these experiments range from the rate of pulsing to the voltage of the charge, though the pulse rate is rarely changed.

This technology is important in the field of pollution research because it has been found that a pulsed corona can chemically break down various molecules. It was found that water could lead to formation of hydrogen peroxide and hydroxyl radicals by putting it into a pulsed streamer corona, and that a catalyst of iron could facilitate the subsequent breakdown of phenol (Joshi 1994). These findings are important because they show the magnitude of some of the work that can be done with the pulsed streamer corona.

4. OBJECTIVES FOR CURRENT STUDY

This study will have a qualitative analysis of the physical changes in foams that have been subjected to the pulsed streamer corona. There will also be a quantitative study of the waveforms made by the foam. The first thing needed in order to understand the results that were obtained is to understand the electrical characteristics of a foam. The conductance of a foam is directly proportional to the amount of liquid in the foam (Bikerman 1973). This is important because it shows that it will be much more difficult for a current to travel through an aqueous foam that has become virtually dry, while it will travel much better through a wet foam. The other electrical characteristic of importance is that the current will travel through the path of least resistance. Therefore, if the current is traveling vertically from the anode to the cathode, the current will not travel along horizontal walls of the foam bubbles (Bikerman 1973). An interesting result of the present study was the observation that the current does not seem to affect the chemical structure or characteristics of the surfactant. This study is a preliminary investigation to determine whether a pulse corona can break down AFFF. This is important because at Tyndall Air Force Base, as well as many other locations, the foams used for fire fighting are not easy to dispose of. The pulsed streamer corona is a possible solution to this problem, and this study will be the first of many to determine the usefulness of this method for foam breakdown and degradation.

This study will examine both the visual characteristics of the foam and the electrical characteristics of the waveform, the pulse width, rise time, and maximum voltage. This study will provide good examples of each of these waveforms. A physical

description of what happened under each condition tested will also be given. Due to the nature of these tests, there are many non-quantifiable results that will be recorded. However, future studies can be recommended to find more quantifiable results to each of the problems that will be posed in this paper. These experiments will be extremely important in determining what should be pursued in the future.

MATERIALS AND EXPERIMENTAL METHODS

The experimental setup for the pulsed corona is shown below in Figure 1.
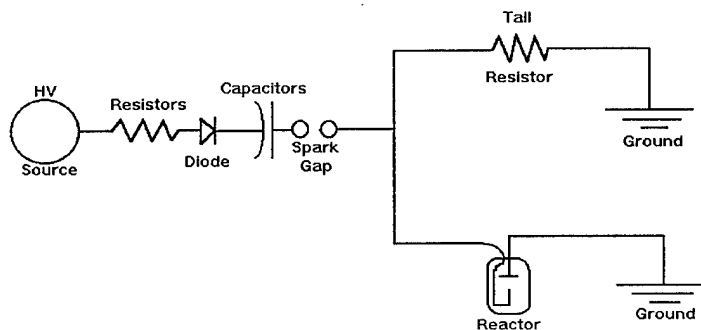
Figure 1

In this figure, the high voltage power supply is a high voltage transformer

providing alternating current at 60 Hz and voltage up to 100 kV. The current then travels

into a series of resistors totaling 3000 kΩ, which are used to lower the current. The signal

then passes into four diodes used to remove the lower half of the signal. This signal is

then sent into four 2000 pF capacitors. These capacitors are used to hold the charge until

the spark gap completes the circuit. The spark gap is a cylindrical rod that rotates at 3600

rpm between two metal spheres. The sphere on the left side is connected to the capacitors

and the sphere on the right side is connected to the anode in the reactor. Thus, as the rod

rotates, it completes the circuit twice per revolution. After the current leaves the spark

gap, there are two options. One option is for the current to go directly into the reactor,

and from there into the ground wire. The second option is for the tail resistors to be

connected to the system. If they are connected, the current leaves the spark gap, and goes

throughout the tail resistors and the reactor with these two devices being connected in

parallel. The purpose for the tail resistors is to make sure that the current goes across the spark gap when using a gas in the reactor. When considering the system, if the reactor has air in it, then it also has an extremely high resistance. This resistance might be high enough to prevent the voltage pulse from traveling across the gap between the anode and the cathode. However, if there is another path for the current to travel across, then it will take that path. When the tail resistors are attached the current will travel through them, and the current will travel across the spark gap every time the circuit is completed.

A diagram of the liquid phase reactor is shown in Figure 2.

Reactor Setup
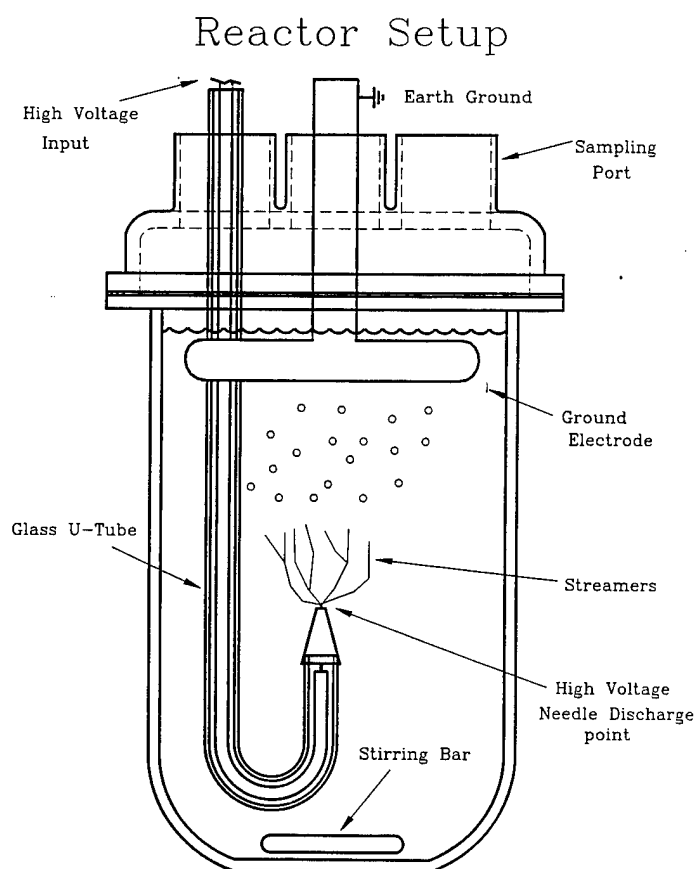
Figure 2

This diagram shows how the current will travel while it is in the reactor. The current first travels into the reactor in the wire along the side. This wire is insulated by a piece of plastic shrink wrap. It is also encased in a glass tube to further insulate it. This wire is connected to a hypodermic needle. This needle provides a "point" for the current to travel from. Then, the current travels across the gap to the ground plate. This plate provides the "point to plane" geometry that was used in each of the trials accomplished in this series of experiments. A sparger was placed in the reactor in order to make the foam.

Connected to the input wire of the reactor, there was a Tektronix P6015 voltage probe. This voltage probe was connected to a Tektronix TDS 460 oscilloscope which was used to determine the pulse width, rise time, and voltage maximum of the waves going into the reactor. Connected to the output wire, between the ground plate and the ground wire, was a Tektronix P6021 current probe. This was used to determine the maximum current that traveled through the reactor. These waveforms were saved on the oscilloscope and afterwards they were plotted on a Tektronix HC100 Color Plotter and attached in Appendix A.

There were several experiments that were run in order to characterize the waveforms that were created. First, there were four runs that were performed in order to determine the effects of adding different gases into the spark gap. The reason for this was oxidation. There was a lot of residue that was building up on the metal spheres and the cylindrical rod in the spark gap due to oxygen reacting with the metal to oxidize the metal surface. After the oxidation built up for 15-20 minutes, the sparks became very intermittent. Because of this, it was determined to see if it would be possible to change

the atmosphere in the spark gap to another gas which could in turn lower the amount of oxidation. The gases that were tried were helium, nitrogen, compressed air, and standing room air. The helium and nitrogen were used to determine whether these different gases could lower the oxidation, and if they had any effect on the waveform. In order to perform this series of experiments there was a trickle of each gas run into the spark gap, and the waveforms were saved at 0 minutes and again at 10 minutes with the input voltage set at 35 kV.

There was an additional series of experiments that was done in order to provide a standard to compare with the results from the foam runs. First there was a run with just air in the reactor. This was done to compare to the results when the reactor was full of foam. This case was run with and without the tail resistors attached, and it was performed with input voltages of 30 kV, 35 kV, and 40 kV. Another run was made with water covering the anode but not reaching the ground plate. This was performed in order to compare with the results when the foam solution liquid was over the anode and foam covered the ground plate. Again, this was done with and without tail resistors at 30 kV, 35 kV, and 40 kV. The final run that was performed as a standard was a run with the reactor full of water. This was completed without the tail resistors at 30 kV and 35 kV input voltage.

After these standards were completed, the runs with foam were started. There were several experiments that were completed and each was run for 30 minutes with an input voltage of 35 kV. Readings of rise time, pulse width, and maximum voltage were taken at the beginning, and then again every five minutes throughout the thirty minutes.

There were five runs that were performed with a concentration of approximately 0.1% foam solution with 99.9% de-ionized water. One run was performed with the surfactant liquid filling the reactor from the anode to the cathode without the tail resistors. The second and third runs were completed with the liquid over the anode and the foam over the cathode with and without the tail resistors. These runs gave an approximate volume of 800 mL of liquid and 200 mL of foam. The fourth and the fifth runs were completed with foam covering both the anode and the cathode with and without the tail resistors. After these runs were completed these same experiments were performed with a 0.01% foam solution. The only difference was that the fourth and fifth runs were omitted due to the foamability of the solution. The solution was not foamable enough at 0.01% concentration to fill the reactor to the top with foam, thus it necessitated the omission of these runs. Before and after each run the pH, temperature, and conductivity of the solution were measured in each solution.

The final experiment that was performed was an analysis of the refoamability of each solution after being treated by the corona. In order to do this, a beaker with 100 mL of the untreated liquid was placed in one 500 mL beaker, and 100 mL of the treated liquid was placed in another 500 mL beaker. A sparger was placed in each one, and they were bubbled until they were full. It was then watched for 30 minutes to determined if there was any apparent difference in the stability of the foam.

RESULTS AND DISCUSSION

The initial experiment performed was to determine the effects that the atmosphere in the spark gap had on the resulting waveform and the oxidation on the spark gap. Table 1 summarizes these results.

Waveform data with different atmospheres in the spark gap

Gas	Pulse Width	Rise Time	Max Voltage
Helium	470 µs	70 ns	35 V
Nitrogen	820 µs	16 ns	54.8 V
Compressed Air	880 µs	16 ns	54.4 V
Air	890 µs	17 ns	56.0 V

Table 1

This table shows that with helium in the spark gap it changes virtually every measurable characteristic of the waveform. It was also noticed that the initiation time for each spark was irregular with helium in the spark gap. This was because the spark could travel through the helium easily enough that the spark was not traveling across the gap at the same point in the rod's rotation. Each rotation of the spark gap caused the spark to initiate at different times. Therefore, the pulse was irregular even though the rod in the spark gap was rotating at the same speed. It was noticed that the nitrogen, the compressed air, and the still air gave almost the same results for the waveform characteristics. However, the nitrogen did not decrease the amount of oxidation that built up on the electrode. This may be due to insufficient purging of the spark gap atmosphere.

After these experiments were run, the standards with air, water, and a combination of both were performed. The results are shown in Table 2.

Waveform Characteristics for Standard Solutions

Sample	Input Voltage	Tail Resistors	Rise Time	Peak Voltage	Pulse Width
Air	30 kV	Yes	23 ns	45.0 V	1.25 μs
Air	35 kV	Yes	27 ns	55.4 V	1.25 μs
Air	40 kV	Yes	28 ns	61.2 V	1.5 μs
Air	30 kV	No	15 ns	50.0 V	10 ms
Air	35 kV	No	15 ns	39.0 V	12 ms
Air	40 kV	No	22 ns	55.0 V	12 ms
½ Air, ½ Water	30 kV	Yes	26 ns	46.0 V	1.1 μs
½ Air, ½ Water	35 kV	Yes	28 ns	51.4 V	1.1 μs
½ Air, ½ Water	40 kV	Yes	37 ns	57.4 V	1.25 μs
½ Air, ½ Water	35 kV	No	14 ns	53.0 V	6 ms
Water	30 kV	No	21 ns	44.4 V	>4 ms
Water	35 kV	No	19 ns	52.2 V	>4 ms

Table 2

This table shows that the tail resistors have a huge effect on the pulse width. The pulse width is much less with the tail resistors on the system. The pulse width is greater than one millisecond for each of the trials without the tail resistors, however, the trials

with the tail resistors gave pulse widths of between one and two microseconds. In general, the input voltage had a direct correlation with the maximum voltage. The tail resistors also had a big impact on the rise times for the different waveforms. When the tail resistors were on the system, the rise time ranged from 23-37 ns, however, when the tail resistors were removed, the rise time was only 15-22 ns. Thus, the rise time was generally higher without the tail resistors on the system.

During these runs, the physical characteristics of the corona and the streamers were very noticeable. For the runs with just air, and the tail resistors on, there was not much that was visually apparent. However, when the tail resistors were removed, the streamers were apparent with the lights turned out. They were short streamers (approximately 1-2 cm) and they were pink. They were nearly all in the upward direction towards the ground plate. As the voltage was increased, the streamers got a little bit more noticeable, however, it was still necessary to have the lights turned off in order to see them. When there was water filling the entire reactor, the streamers were much longer. They would reach lengths of 3-4 cm. They were much brighter as well. It was possible to see all of the streamers with all of the lights in the room on. These streamers were again nearly all going straight toward the ground plate.

The most interesting case was the case where there was approximately 800 mL water and 200 mL air in the reactor. In this case, the anode was approximately 2.2 cm below the surface of the liquid, and the surface was approximately 2.8 cm below the ground plate. During these runs there were intermittent streamers coming off of the anode. At the times when there were streamers coming off the anode, there was an

electrical discharge propagating from the cathode that appeared to be confined to the walls or surfaces of the reactor. These discharges will be referred to as cathode initiated streamers. These cathode initiated streamers would travel from the ground plate to the wall of the reactor. Then, they would travel down the wall in a straight line to the water. Once this cathode initiated streamer would reach the surface of the water, it would branch out into several branches and go across the top of the water in several directions. Sometimes the cathode initiated streamers would last for 1-2 seconds. The cathode initiated streamers were a lot more frequent where the glass tube was touching the side of the reactor. This is probably due to a conductive pathway from the water. There was probably water that was forming a path that went from the water to the area near the ground tube. Although all of the sparks did not travel down this tube, there were definitely more of them there than other areas of the reactor wall. Another change that was apparent in some of the runs was the ringing that was present in the waveforms. When the reactor had air in it, both all air and 200 mL air - 800 mL water, there was a significantly greater amount of ringing that was present in the voltage waveform. An example of these waveforms is shown in Figure 3.
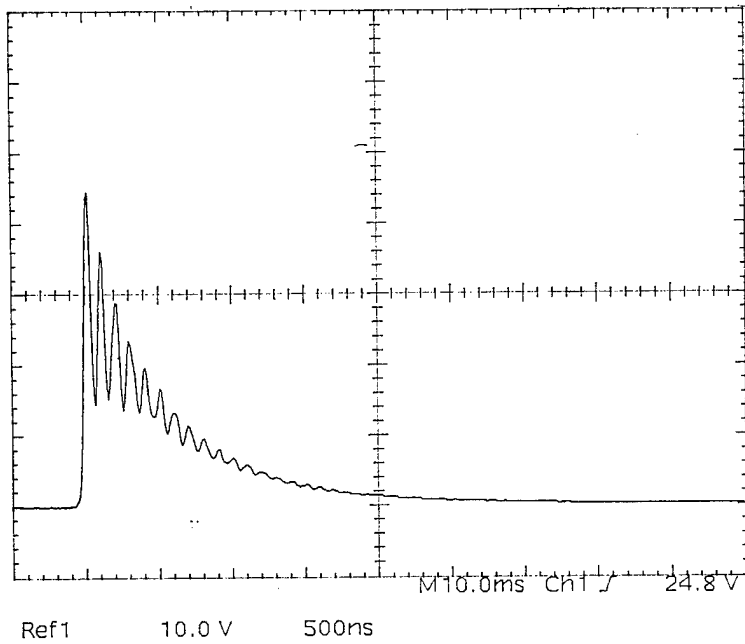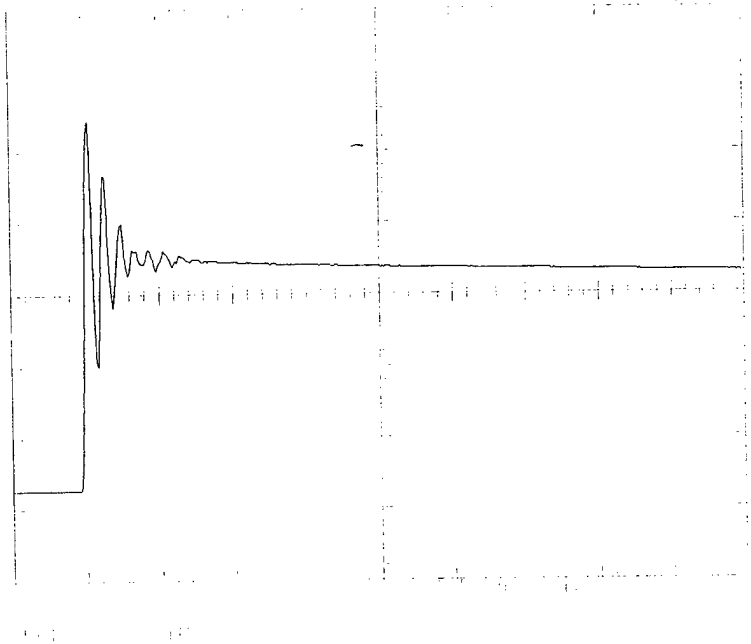
Figure 3

The results from the experiments of the foam are given in Table 3.

Waveform Characteristics for Foam Solutions

Concentration	Tail Resistors	Configuration	Rise Time	Peak Voltage	Pulse Width
.1%	No	All Liquid	26 ns	50.0 V	11.7 μs
.1%	No	½ foam, ½ liquid	76 ns	57.4 V	160 μs
.1%	No	All Foam	15 ns	57.2 V	108 μs
.1%	Yes	½ foam, ½ liquid	28 ns	52.8 V	500 ns
.01%	No	All Liquid	17 ns	56.2 V	76 μs
.01%	No	½ foam, ½ liquid	15 ns	57.6 V	1.04 ms
.01%	Yes	½ foam, ½ liquid	27-19 ns	53.6-61.4 V	500 ns

Table 3

The results in Table 3 show that for the most part, the properties of the waveform are different for each of the different configurations and concentrations. The rise time was greater and the pulse width and maximum voltage were smaller when the concentration was higher. In this table, there does not seem to be anything in particular that changed the maximum voltage, however, the rise time was definitely smaller with the tail resistors on the system than without them. The pulse width was significantly smaller with the tail resistors on than without them.

The visible characteristics are most interesting to watch during these runs. For the runs that were all liquid, there was very little change that could be seen. Many microbubbles were formed in the solution during the time that the corona was running. These microbubbles rose to the top of the solution as soon as the corona was turned off. However, there was very little change in the conductivity or pH of the solution. In general, the pH went down slightly and the conductivity went up slightly. These results are shown below in Table 4. After running the corona, the solution was bubbled to form a foam. There was no change in the foamability or the stability of the foam before or after the experiment. With the lack of significant change in the conductivity or pH of the solution, and the lack of change of the foam, there is no evidence to support a chemical degradation of the surfactant.

Characteristics of the Foam Solutions Before and After Corona Treatment

Concentration	Tail Resistors	Configuration	Before pH	After pH	Before Cond. (μs/cm)	After Cond. (μs/cm)	Before Temp. (°C)	After Temp. (°C)
0.1%	No	All Liquid	5.0	3.9	11.5	23	21.1	33.4
0.1%	No	200 ml Foam, 800 ml Liquid	4.9	3.4	11.5	75	22.0	30.1
0.1%	Yes	200 ml Foam, 800 ml Liquid	5.09	5.17	11.8	12.4	21.5	28.6
0.01%	No	All Liquid	4.8	4.5	1.55	2.2	21.5	29.8
0.01%	Yes	200 ml Foam, 800 ml Liquid	4.8	5.0	1.8	1.55	21.7	30.1

Table 4

For the runs with foam filling the gap between the electrodes, the physical

breakdown of the foam depended on whether the tail resistors were being used or not.

When the tail resistors were not used, there was no change in the foam, and there was no

visible corona. Because of this, it is extremely unlikely that there was very much current

that was going through the reactor, instead it was going through the tail resistors. When

the tail resistors were not used, there were definite streamers that went through the foam

toward the ground plate. As the streamers were going through the foam they broke the

foam down visibly. This experiment also caused the same cathode initiated streamers

that moved along the side of the reactor that occurred in the water when it was half full.

As soon as these sparks touched the foam it would break down. This experiment caused

the foam (approximately 700 mL) to break down within 10 minutes. There is not a

known reason for this physical breakdown, but one hypothesis is that there is a shock

wave that moves through the foam that is strong enough to break the foam. It could also

be related to the Gibbs and Marangoni effects. It is possible that the streamers moving through the foam cause a change in concentration of the surfactant in the bubbles. This change in concentration could cause an increase in the surface tension and cause the foam to break down.

When the reactor had 800 mL liquid and 200 mL foam, the foam was broken down the quickest. During these runs, about 200 mL of foam were totally broken down in 5 minutes. There was very little change for the first 2.5-3 minutes, but all of the foam broke down in the last 2-2.5 minutes. This experiment caused the same cathode initiated streamers as the runs with 800 mL water and 200 mL air. These sparks ran down the side of the reactor generally along the same path as the glass tube holding the wire, and the sparger. These sparks are what break down the foam. Again, with the little change in pH and conductivity, it is very unlikely that there is a significant change in the chemical structure of the surfactant, and it appears to be only a change in the physical structure of the bubbles.

CONCLUSION

During these experiments there was a definite breakdown of the foam that was observed. However, the problem that was found is that the cause of the breakdown is unknown. It is unknown whether it was the anode initiated streamer or the cathode initiated streamer traveling down the side of the reactor. This is important because the results should be very easy to duplicate in the field if it is the anode initiated streamers, while it will be much more difficult to reproduce if it is the cathode initiated streamers that are causing the foam to break down. We also found that there was a physical breakdown of the foam, but no appreciable chemical breakdown of the foam. The best way to operate the reactor in order to break down the foam appeared to be when there was only foam, or 200 mL foam and 800 mL water without tail resistors. Although the runs where there was 200 mL foam and 800 mL liquid appeared to work the best, there is a problem with the feasibility of the application in the field. It would be very difficult to actually use a pulsed corona with the setup similar to what was used in the previous experiments with liquid covering the anode and foam covering the cathode. When there were tail resistors, there was no change in the structure of the foam.

RECOMMENDATIONS

There are several experiments that need to be considered in the future in order to more fully understand the mechanism of what is happening in the reactor. First, it is apparent that there are generally several conductive pathways from the ground plate down to the surface of the liquid. This is a big problem because it would be difficult to employ this technique in the field to break down the AFFF because there would not always be any conductive pathways from the anode to the cathode. There are a couple of solutions for this. One would be to use a larger reactor, this would make the ground plate farther from the side of the reactor. The other solution to this problem would be to use a smaller ground plate, this would alleviate the problem in the same manner.

Another experiment that could be conducted is to determine if the corona will break down the foam if there is a continuous feed of foam. If there is an optimal amount of foam that can be in the reactor, and if it will break down foam as it is being added when there is this optimal amount in the solution, it could be useful for understanding the mechanism of the foam breakdown. This is an important question in order to know the rate at which the foam can be broken down. Another question is how fast the foam can be broken down. This rate can possibly be increased by increasing the voltage. In the cases considered in the present experiments, all of the runs were performed with the input voltage at 35 kV. It is possible that the foam will break down faster at higher voltages.

Another question is whether the surfactant is actually being broken down. The best way to test this would be to collect samples of the liquid before and after running

pulsed corona experiments. They could then be tested to determine what is in them, and compared analytically to determine if there are any differences. In addition to this, if there is a chemical breakdown of the surfactant, it is possible that there could be a catalyst added to the solution to facilitate the chemical breakdown of this compound. In previous studies it was found that the addition of iron salts "was found to significantly enhance phenol degradation (Sharma 1993)". This same technique might possibly be useful in breaking down the surfactant. Another possibility to increase chemical degradation would be to add O_2 through the needle electrode. Oxygen addition through the needle electrode is known to lead to ozone production (Clements 1985). This might also lead to the chemical breakdown of the surfactant.

Other experiments that would be of interest in order to get a better fundamental understanding of the mechanism that takes place during corona discharge in foams would be to test what happens with different surfactants with known chemical structures, such as single hydrocarbons, alkyl chains, and other structures that might be easier to chemically degrade. If it is known how each of these break down, it would also help in understanding at least the rate of breakdown of AFFF or other foams.

REFERENCES

1. Adamson, Arthur W. Physical Chemistry of Surfaces, Fourth Ed. John Wiley & Sons: 1982.

2. Aubert, James H., Andrew M. Kraynik, and Peter B. Rand. "Aqueous Foams". Scientific American, May 1986 p. 74-128.

3. Bikerman, J. J. Foams. Springer-Verlag Inc. New York: 1973.

4. Boon, Charles. "Choosing the Right Foam for the Military". Military Firefighter, November 1991, p. 55-58.

5. Chang, M. B., M. J. Kushner and M. J. Rood, "Gas Phase Removal of NO from Gas Streams via Dielectric Barrier Discharges", Envir. Sci. Technol., **26** (1992), 777-781.

6. Clements, J. S., Sato, M., and Davis, R. H., 1985: Preliminary Investigation of Prebreakdown in Liquids. Journal of Physics D: Applies Physics V. 28, p. 178-188.

7. Joshi, A. A., 1994: Formation of Hydroxyl Radicals, Hydrogen Peroxide, and Aqueous Electrons by Pulsed Streamer Corona Discharge in Aqueous Solutions, M.S. Thesis FAMU-FSU College of Engineering, Tallahassee, FL.

8. Mellot, Kevin. "Foam Proportioning and Deliver Systems". Military Firefighter, November 1992, p. 30-33.

9. Olson, Keith and Jim Cox. "High-Expansion Foam Systems Minimize Risk of Contaminated Water Run-Off". Fire Protection Contractor, April 1994, Vol. 17, p. 24-26.

10. Sharma, A. K., Locke, B. R., Arce, P., Finney, W. C., 1993, A Preliminary Study of Pulsed Streamer Corona Discharge for the Degradation of Phenol in Aqueous Solutions. Hazardous waste & Hazardous Materials, 10 (2), p. 209.

11. Wilson, A. J. Ed. Foams: Physics, Chemistry and Structure. Springer-Verlag Inc. London: 1989.

Appendix A

Tek Run: 5.00kS/s   Sample Air @ 30 kV w/ tail resistors. 30 May 96
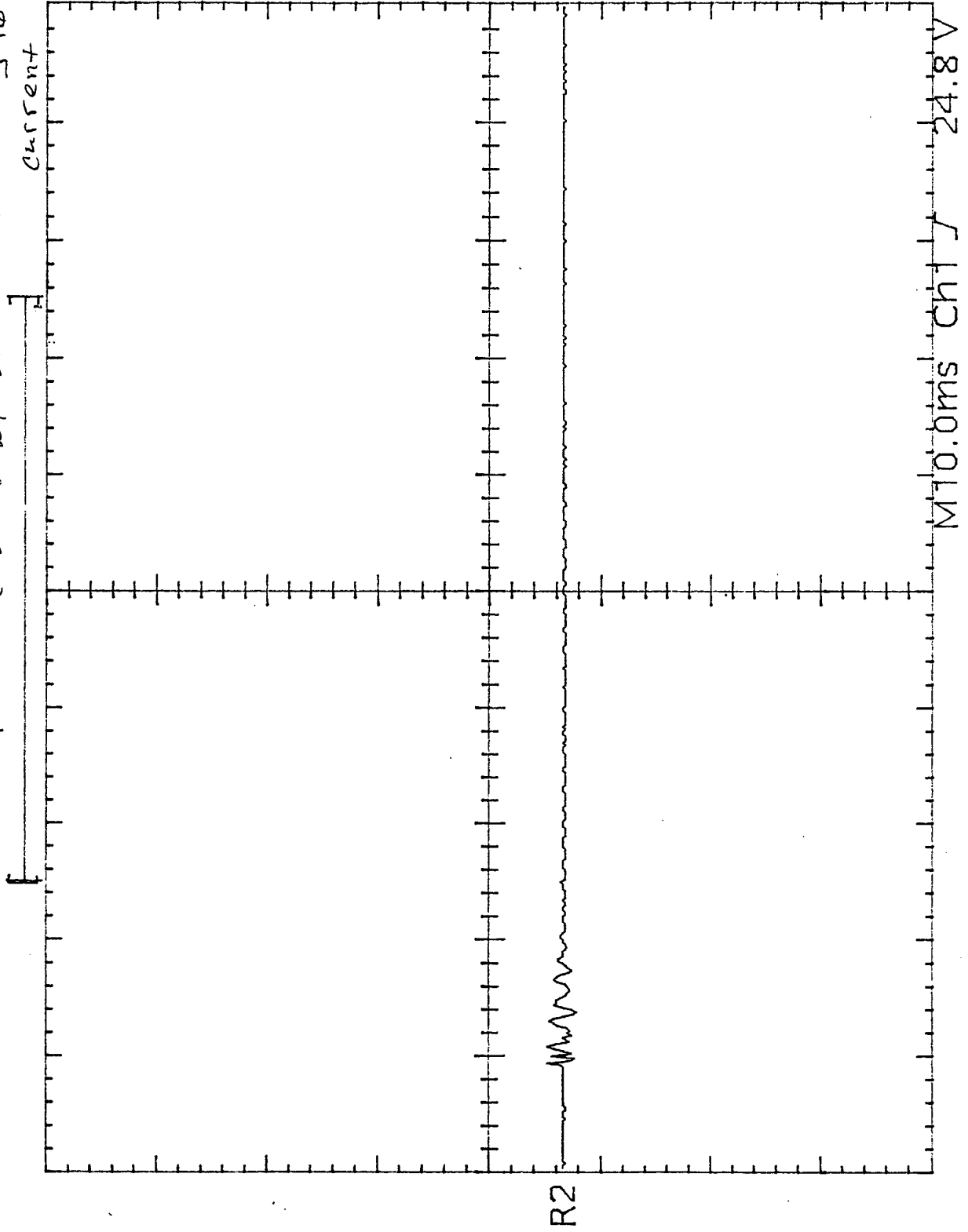
Current

Ref2 Max
1.2 V

R2 ~~~~~~

Ref2   10.0 V   500ns   M 10.0ms Ch1 ⌐ 24.8 V

Tek Run: 100MS/s   Average Air @ 35 kV w/ tail resistors 30 May 96

Voltage
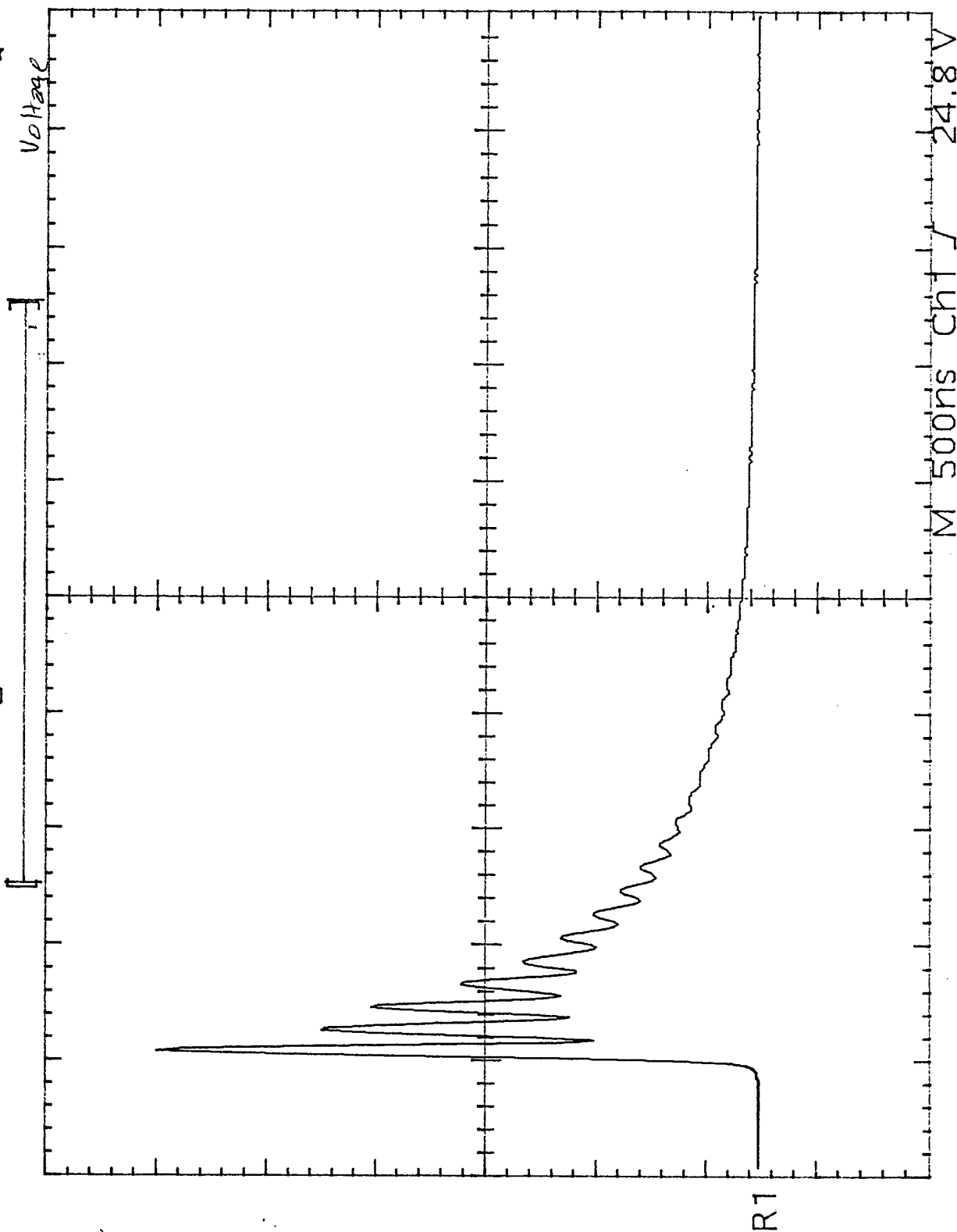
Ref1 Max
55.2 V

Ref1 Rise
26ns
Unstable
histogram

R1

M 500ns Ch1 ⌐ 24.8 V

Ref1   10.0 V   500ns

Ref2 Max
1.4 V

Average Air @ 35kV w/tail resistors   30 May 96
current

R2

M 500ns   Ch1 ∫   24.8 V

Ref2   10.0 V   500ns

A-3

Tek Run: 200MS/s ET Average Air @ 40 kV w/tail resistors 30 May 96

Voltage
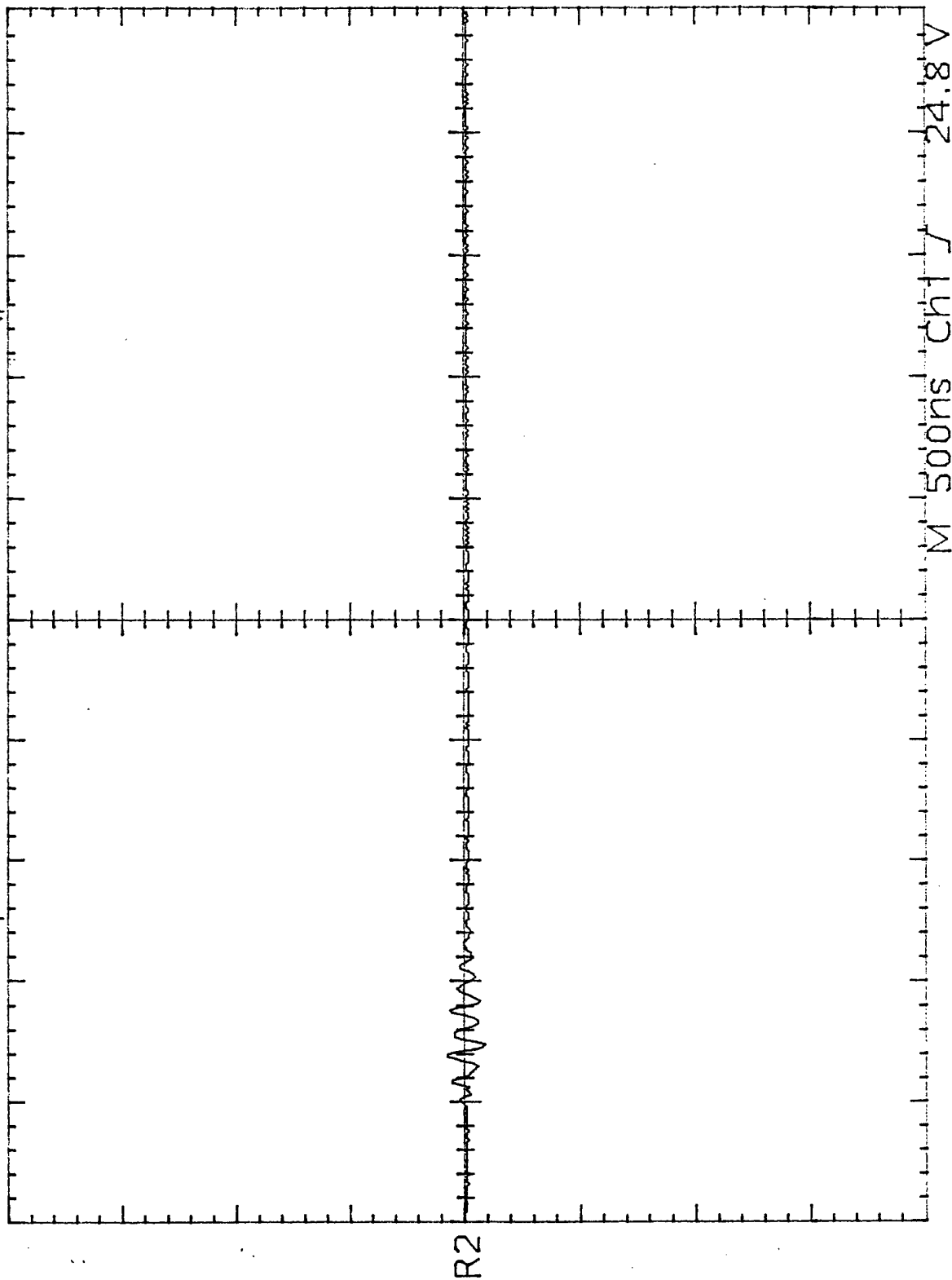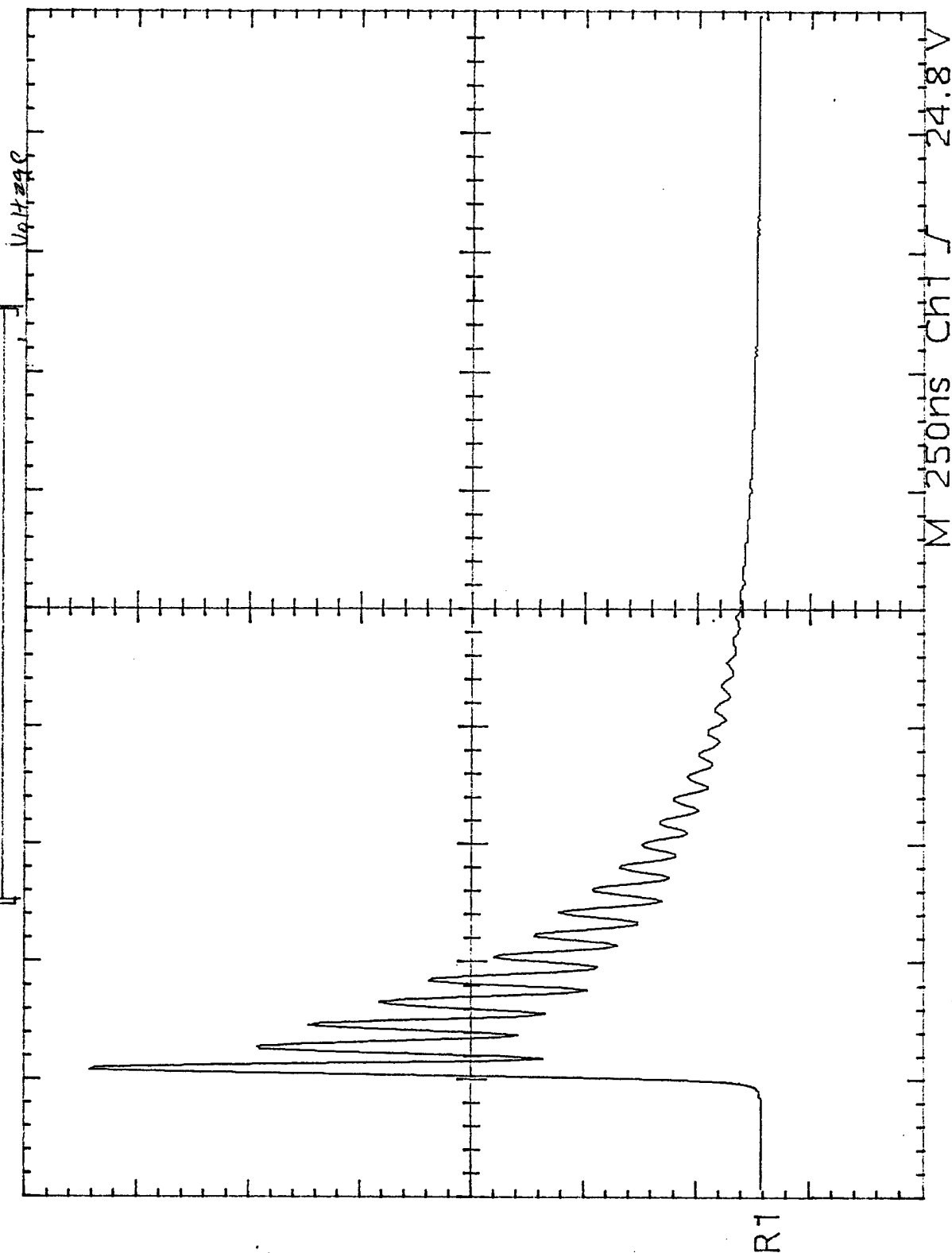
Ref1 Max
60.4 V

Ref1 Rise
31ns
Unstable
histogram

R1

M 250ns Ch1 24.8 V

Ref1   10.0 V   500ns

A-4

Tek Run: 200MS/s ET Average Air @ 40 kV w/ tail resistors 30 May 96

Ref2 Max
2.8mV

Current

R2

Ref2   10.0mV   250ns   M 250ns Ch1 ⌐ 24.8 V

A-5
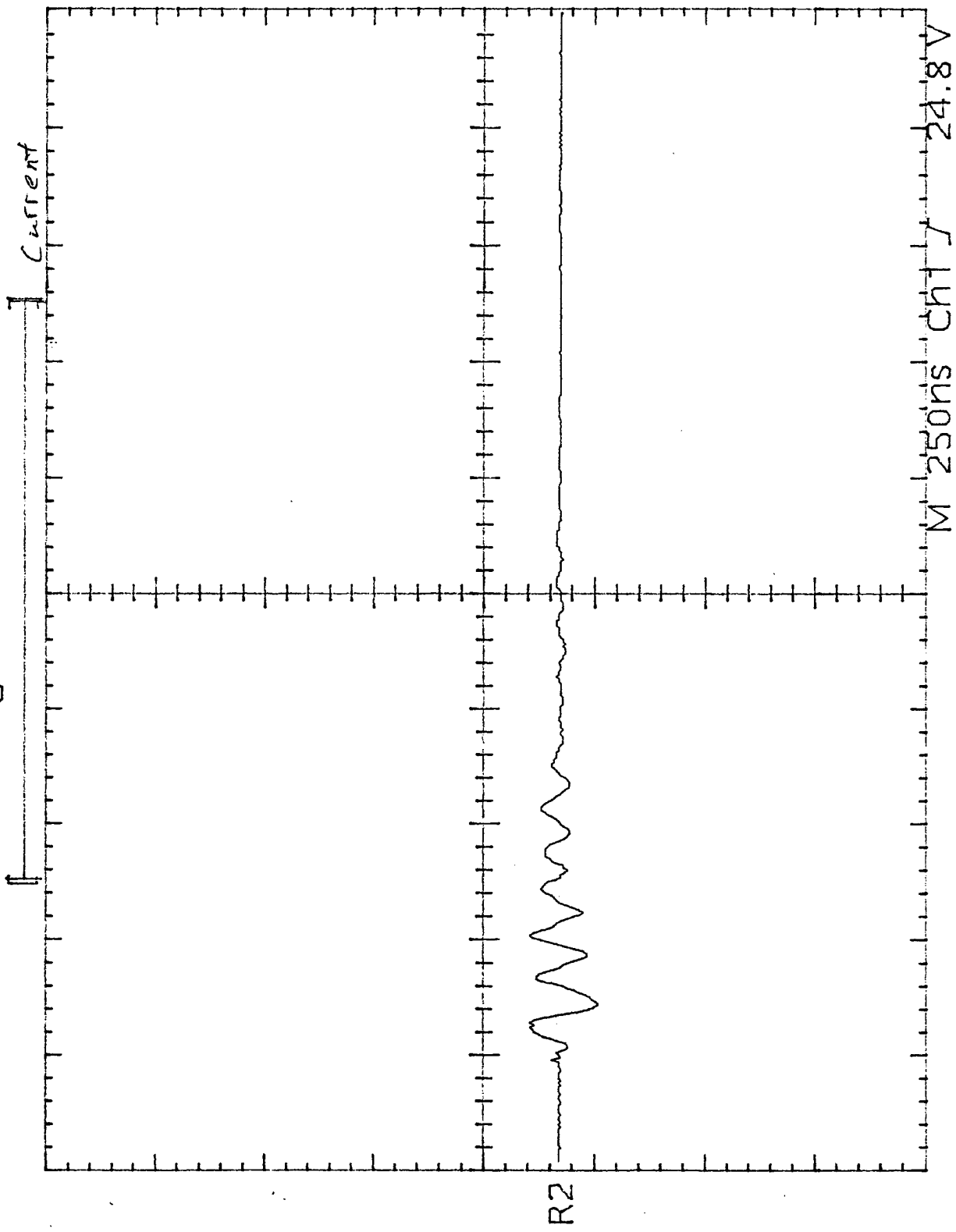
Tek Run: 100MS/s   Average   Air @ 30kV w/o rail resistors 30 Meg 96

Voltage
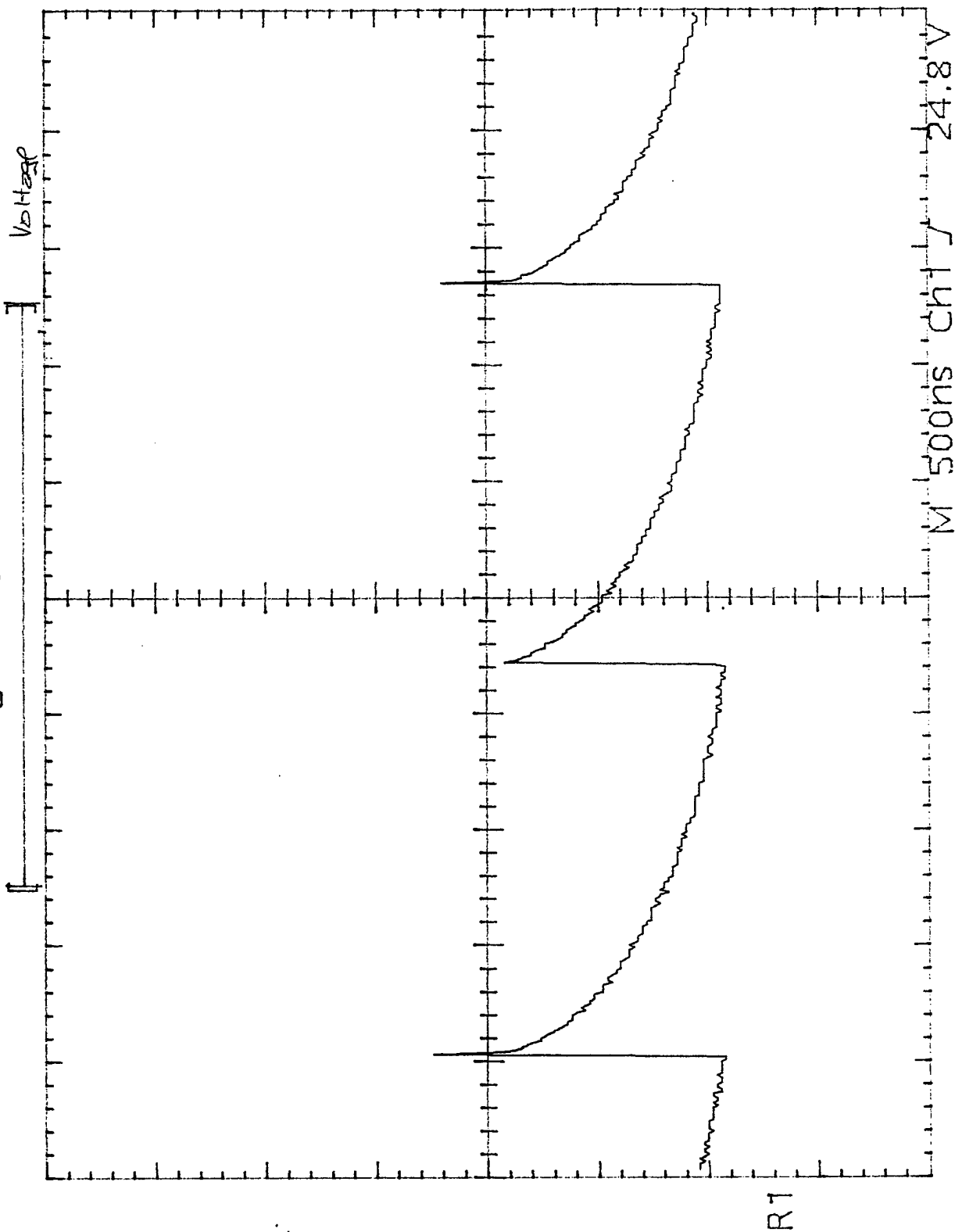
Ref1 Max
31.0 V

Ref1 Rise
40μs
Low signal
amplitude

R1

M 500ns Ch1 ╱ 24.8 V

Ref1   10.0 V   5.00ms

A-6

Tek Run: 100MS/s   Average Air @ 30 kV w/o resistors 30 May 96

Voltage
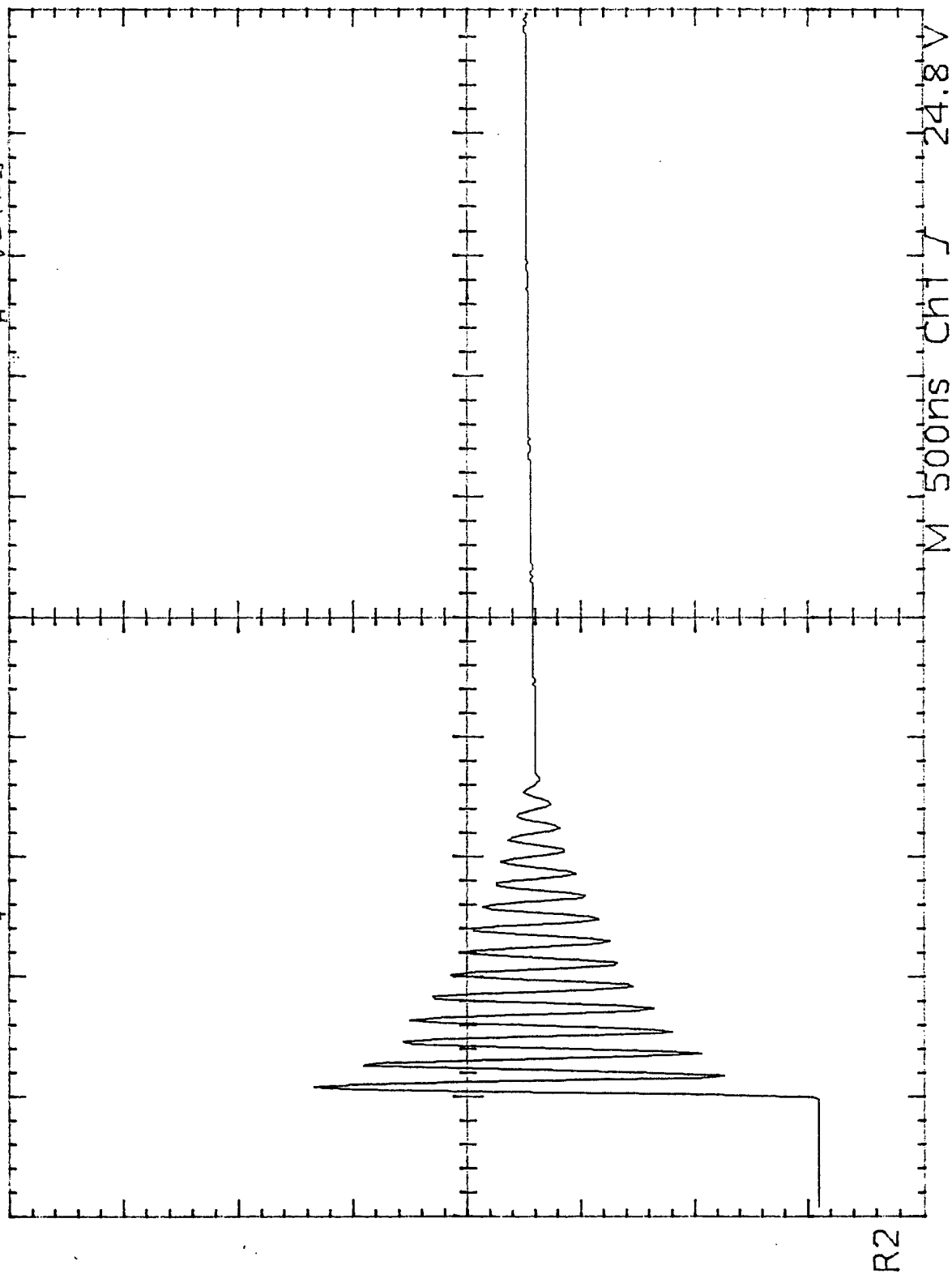
Ref2 Rise
15ns
Low
resolution

Ref2 Max
50.0 V

M 500ns Ch1 ⌐ 24.8 V

Ref2   10.0 V   500ns

R2

Tek Run: 100MS/s   Average

Ref3 Max
2.2 V

A_r @ 30 kV w/o tail resistors 30 May 96

Current

R3

M 500ns Ch1 ↗ 24.8 V

Ref3   10.0 V   500ns

A-8
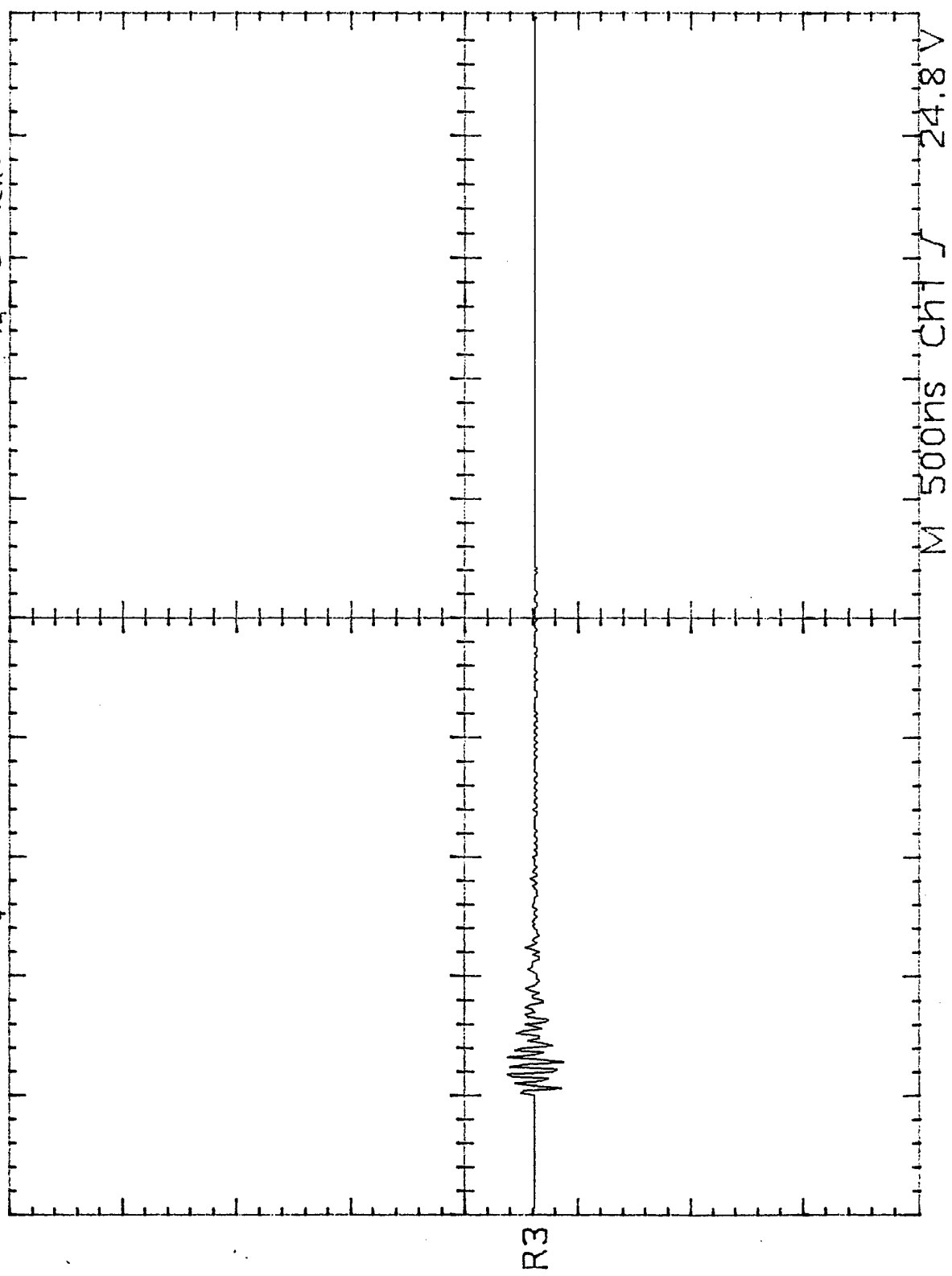
Tek Run: 100MS/s   Average   Air @ 35 kV w/o tail resistors 30 May 96
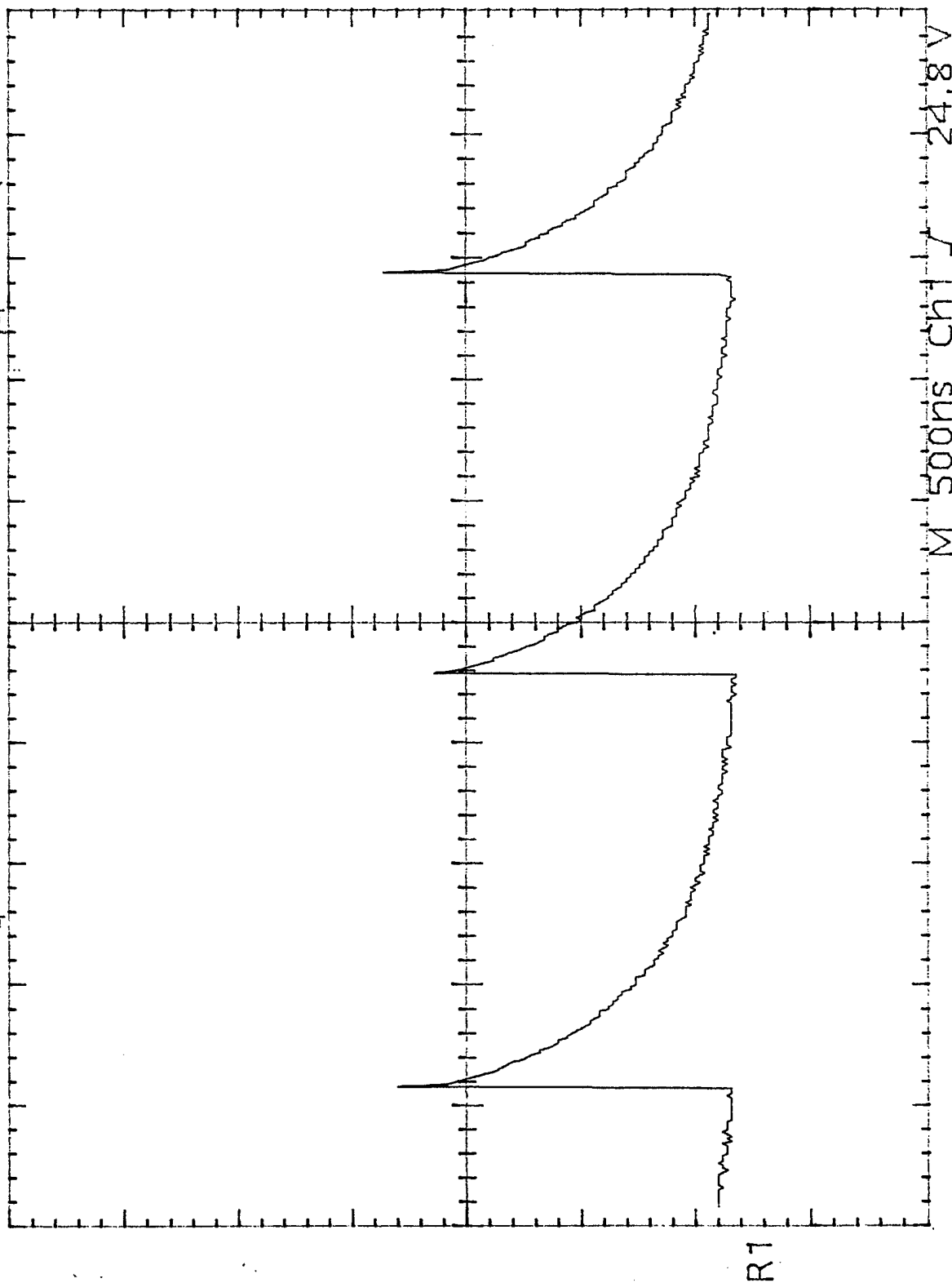
Ref1 Rise
50µs
Low signal
amplitude

Ref1 Max
32.6 V

Vo Hage

M 500ns Ch1 ↗ 24.8 V

Ref1   10.0 V   5.00ms

R1

A-9

Tek Run: 100MS/s   Average   Air @ 35 kV w/o tail resistors 30 Mez, 96

Voltage
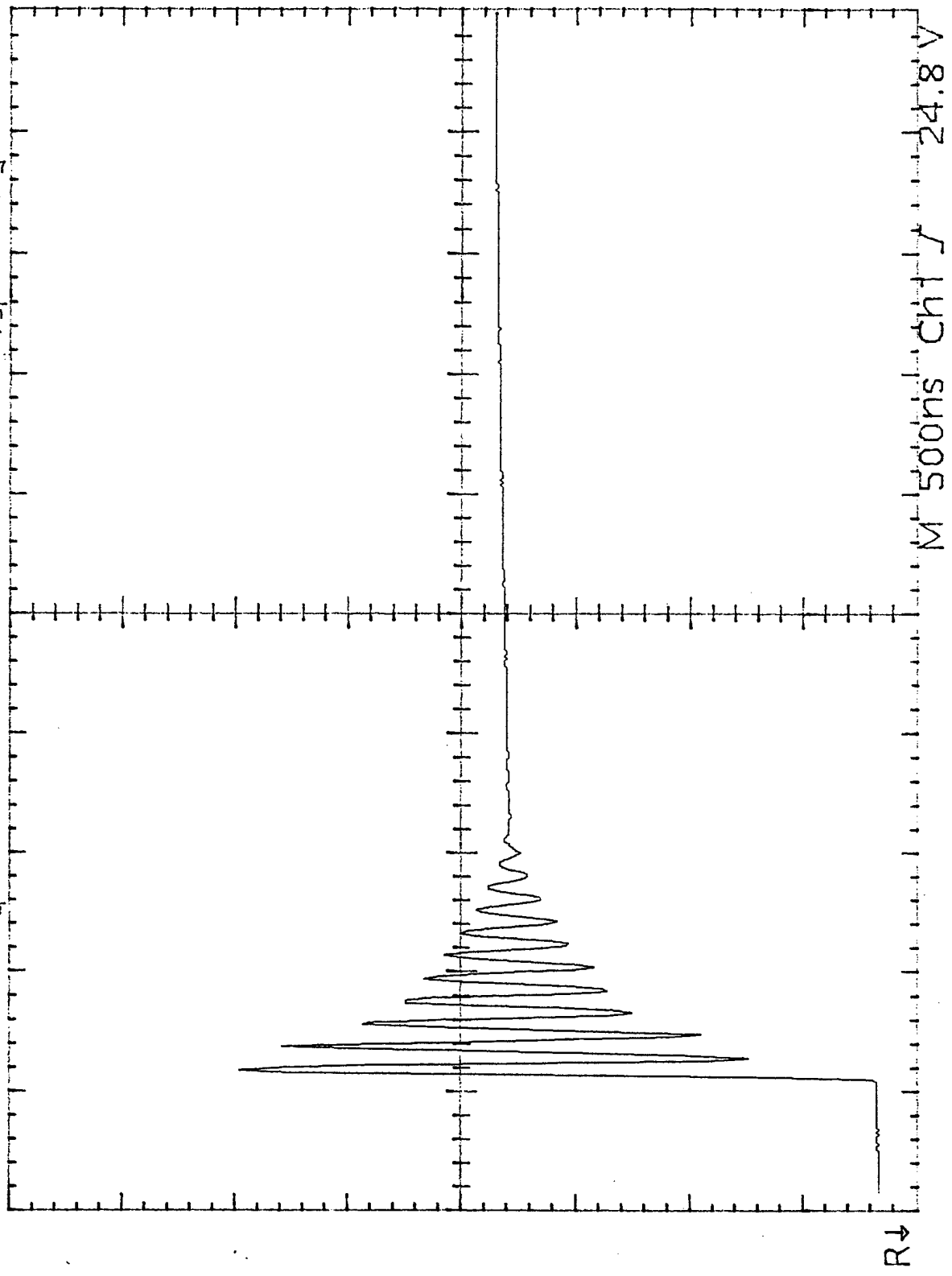
Ref3 Max
59.2 V

Ref3 Rise
15ns
Low
resolution

M 500ns Ch1 ⌐ 24.8 V

Ref3   10.0 V   500ns

Tek Run: 100MS/s   Average   Air @ 35 kV w/o tail resistors 30 MΩ 9½

Ref2 Max
3.2 V

Current

R2

M 500ns   Ch1 ⌐ 24.8 V

Ref2   10.0 V   500ns

A-11
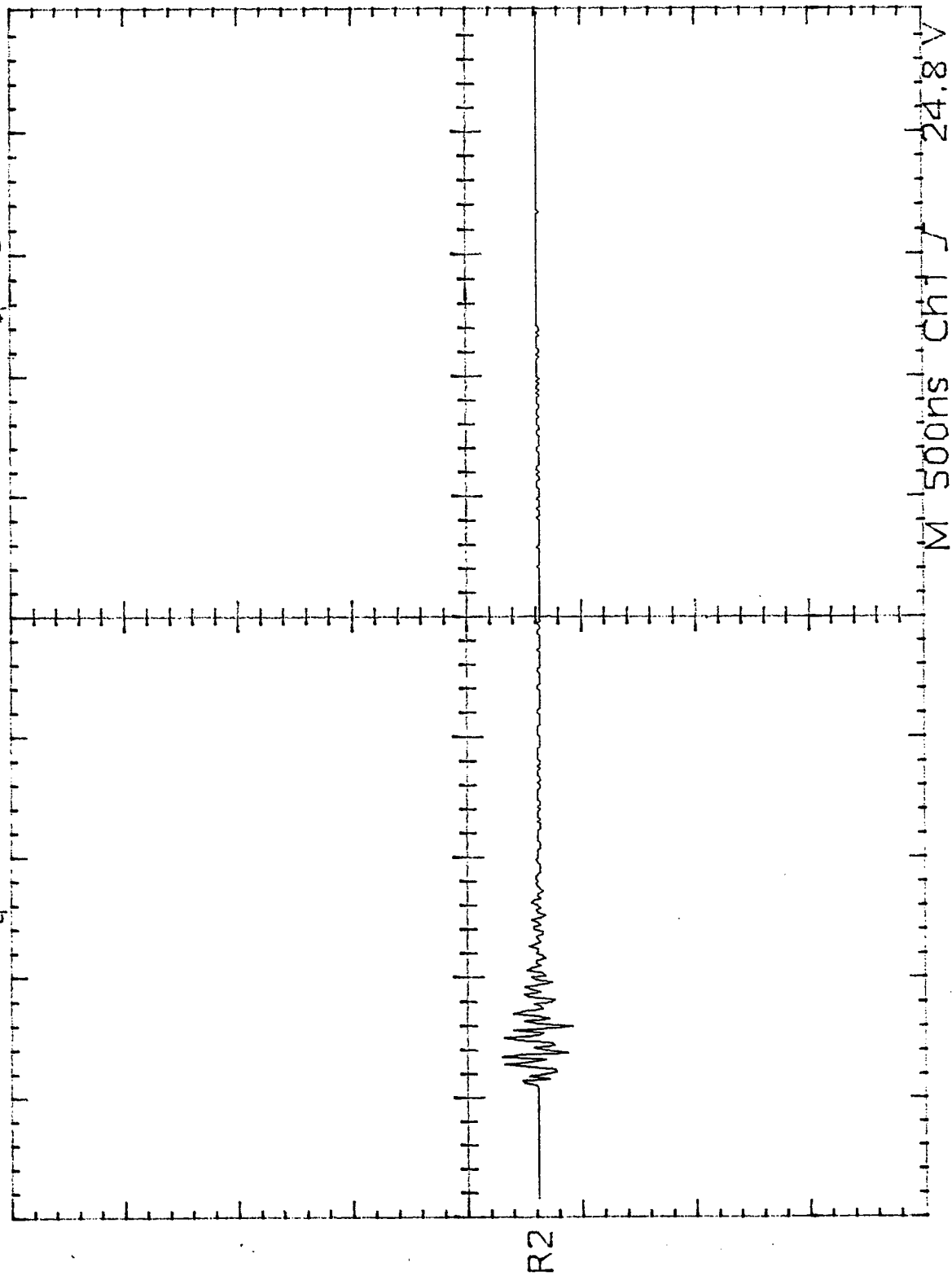
Tek Run: 100MS/s   Average   Air @ 40 kV w/o tail resistors   30 Meg %
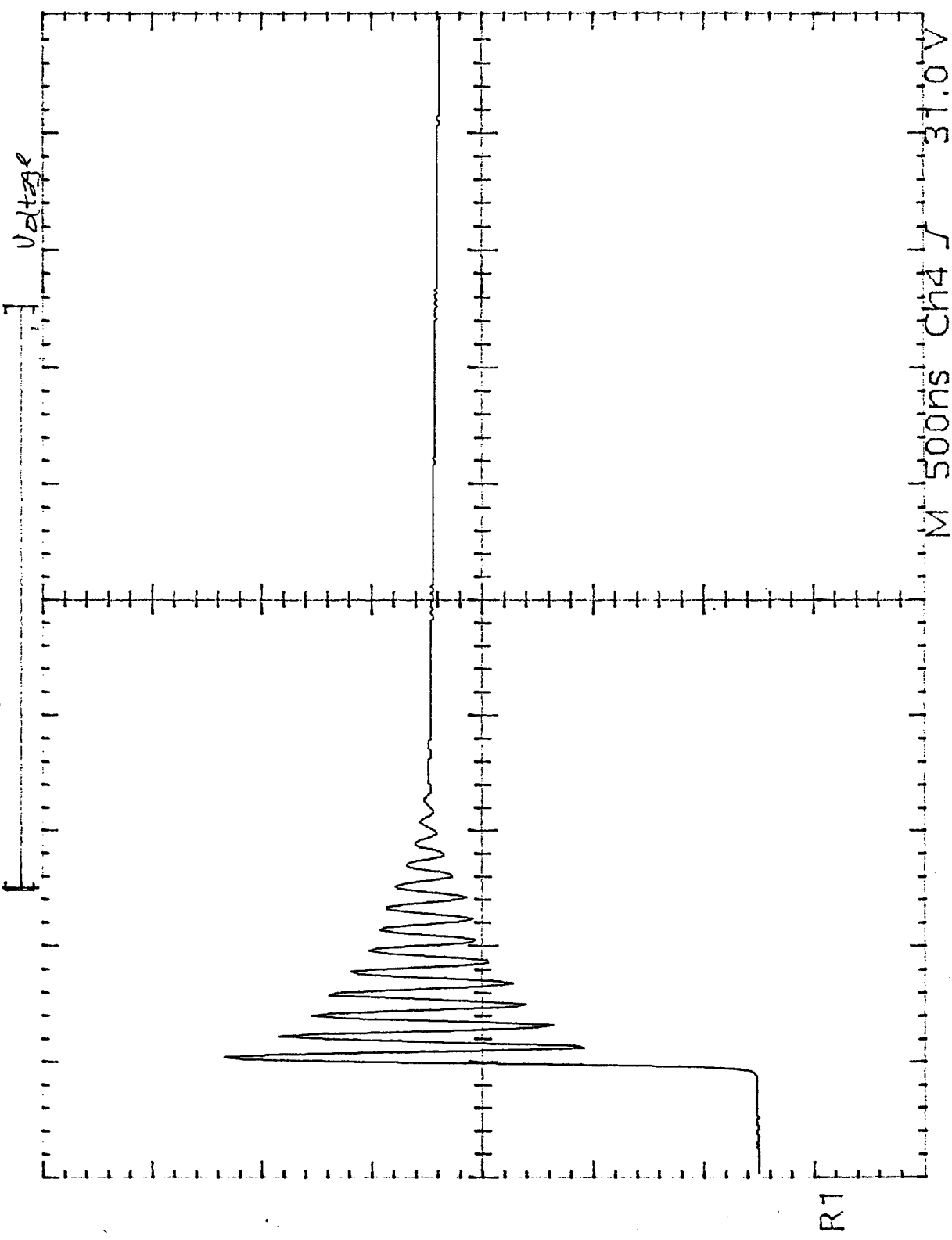
Ref1 Max
54.8 V

Ref1 Rise
22ns

Voltage

M 500ns Ch4 ∫ 31.0 V

Ref1   10.0 V   500ns

R1

A-12

Tek Run: 100MS/s   Average Air @ 4b kV w/o tail resistors 30 May 96

                                                        current

Ref2 Max
800mV

R2

Ref2   10.0 V   500ns   M 500ns Ch4 ╱ 31.0 V

A-13
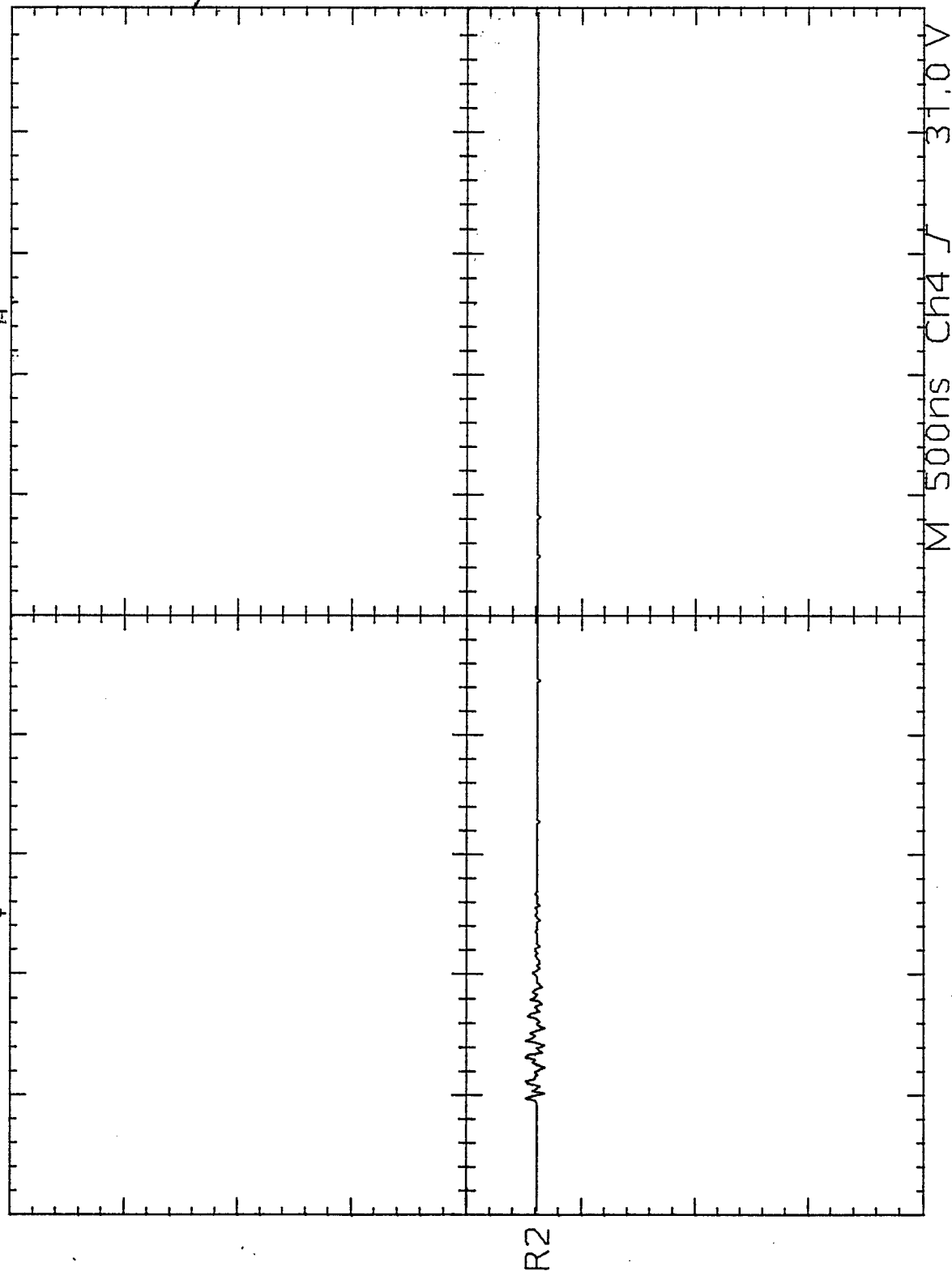
Tek Run: 100MS/s   Average Air & H₂O @ 30 kV w/ Tail resistors   1 June 96
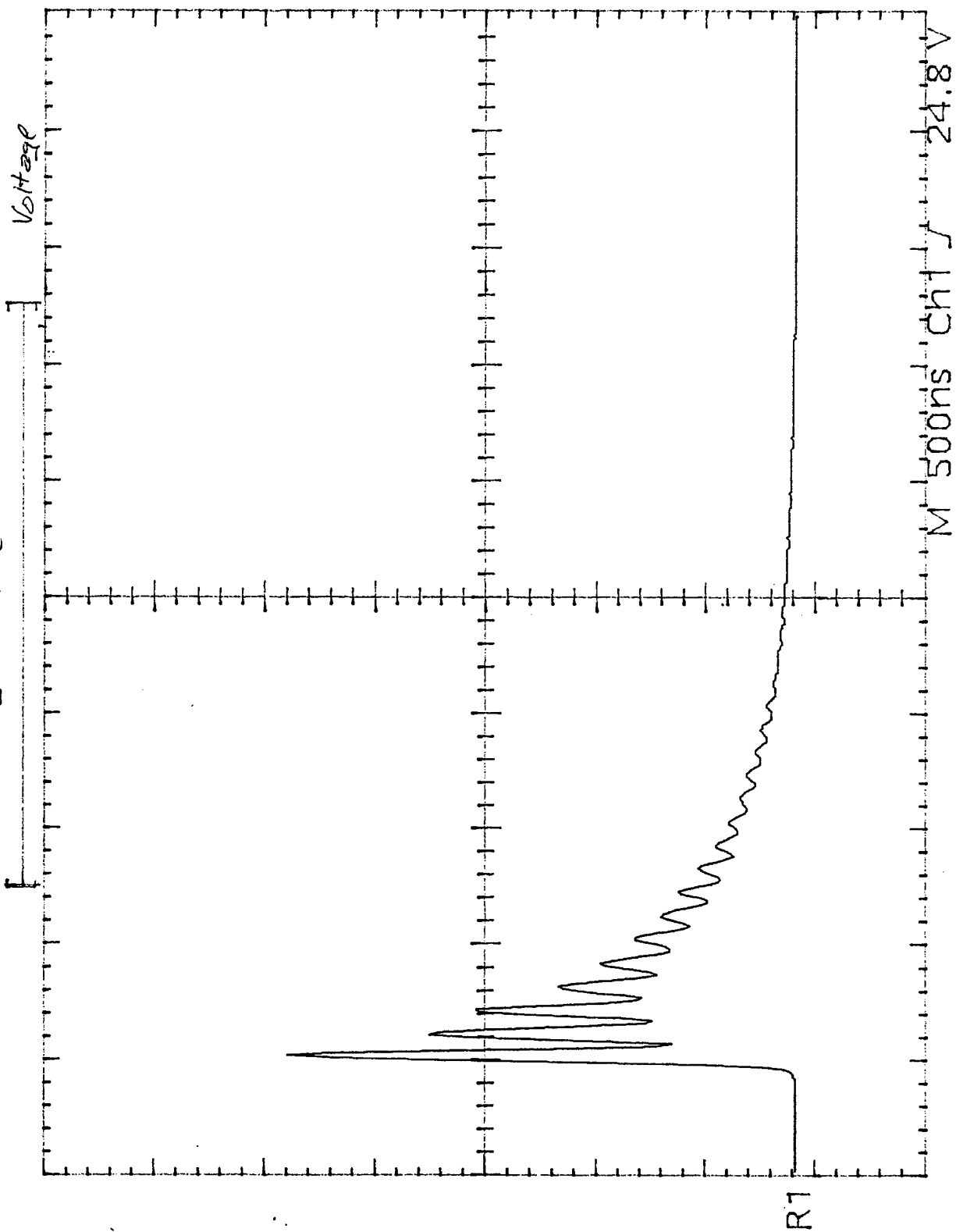
Voltage

Ref1 Max
46.4 V

Ref1 Rise
26ns
Unstable
histogram

M 500ns Ch1 ∫ 24.8 V

Ref1   10.0 V   500ns

R1

A-14

Tek Run: 100MS/s   Average Air & H$_2$O w/ Tail resistors @ 30 kV 1June 96

Current

Ref2 Max
1.8 V

R2

M 500ns Ch1 ʃ 24.8 V
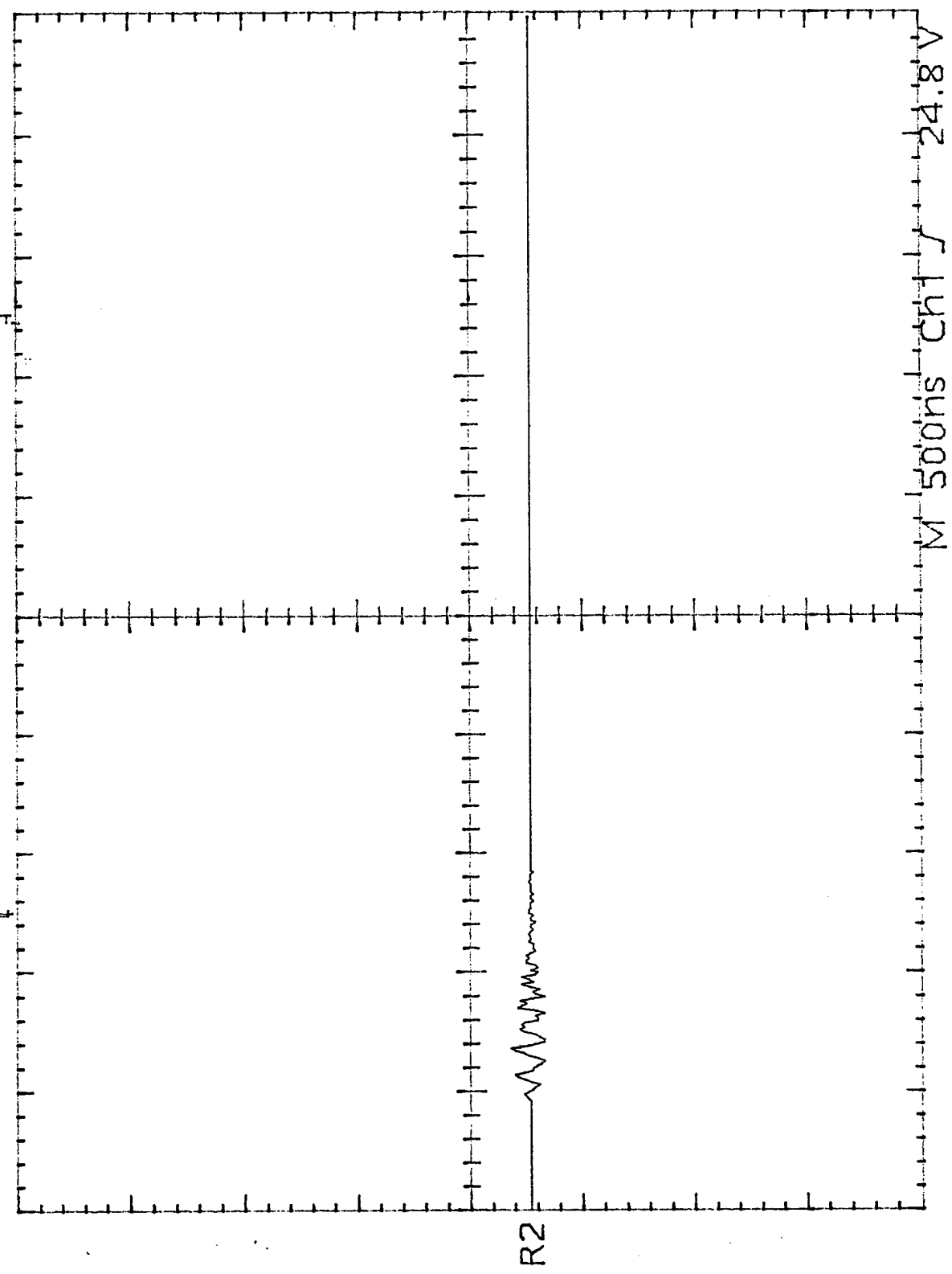
Ref2   10.0 V   500ns

Tek Run: 100MS/s   Average Air & H_2O @ 35kV w/ tail Resistors 11Jun96
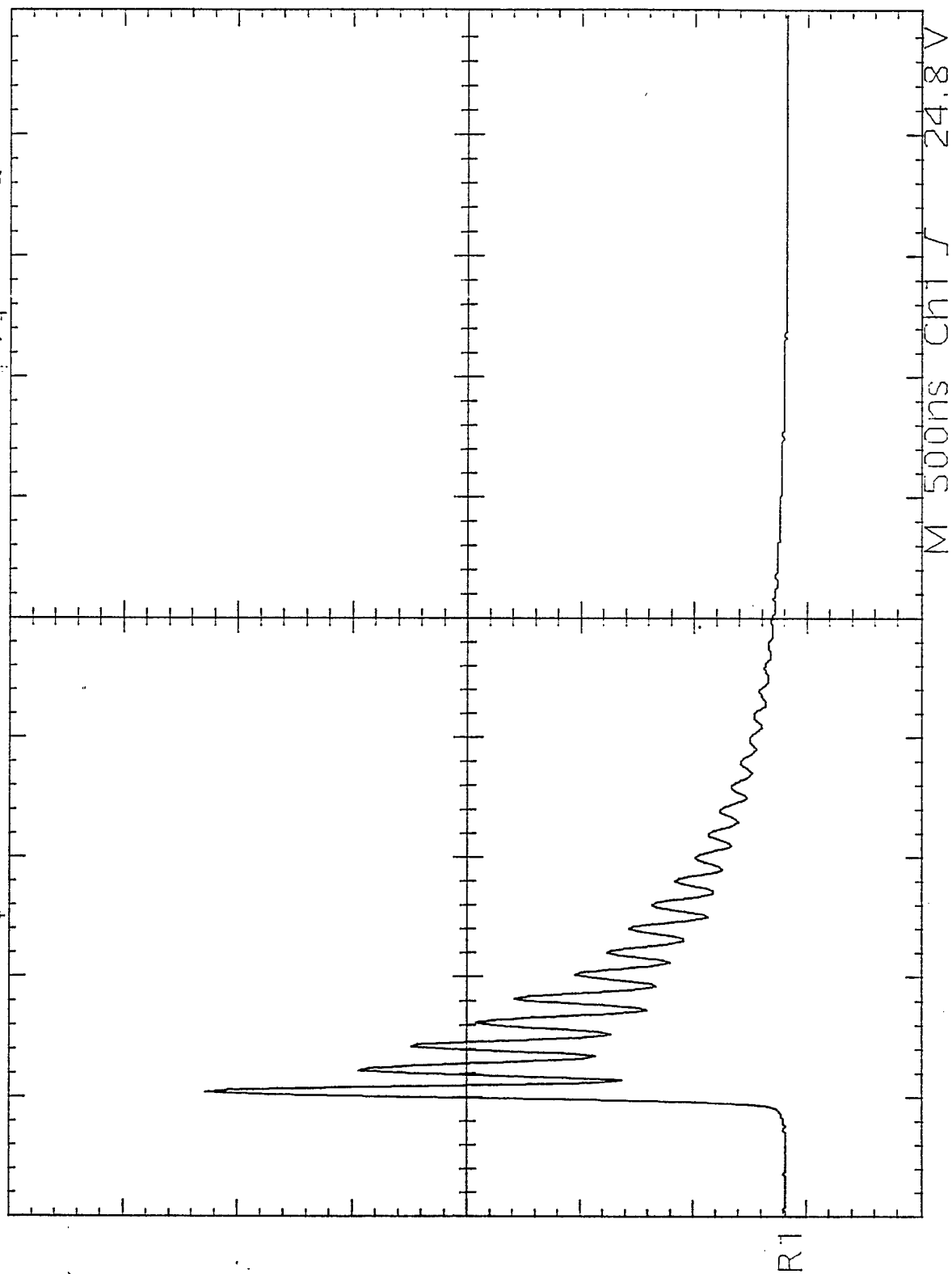
Voltage

Ref1 Max
51.2 V

Ref1 Rise
27ns
Unstable
histogram

R1

M 500ns Ch1 ∫ 24.8 V

Ref1   10.0 V   500ns

Tek Run: 100MS/s   Average thr 2 HD @35kV w/ to resistors   1 June 96

Ref2 Max
1.4 V

Current

M 500ns   Ch1 ∫   24.8 V
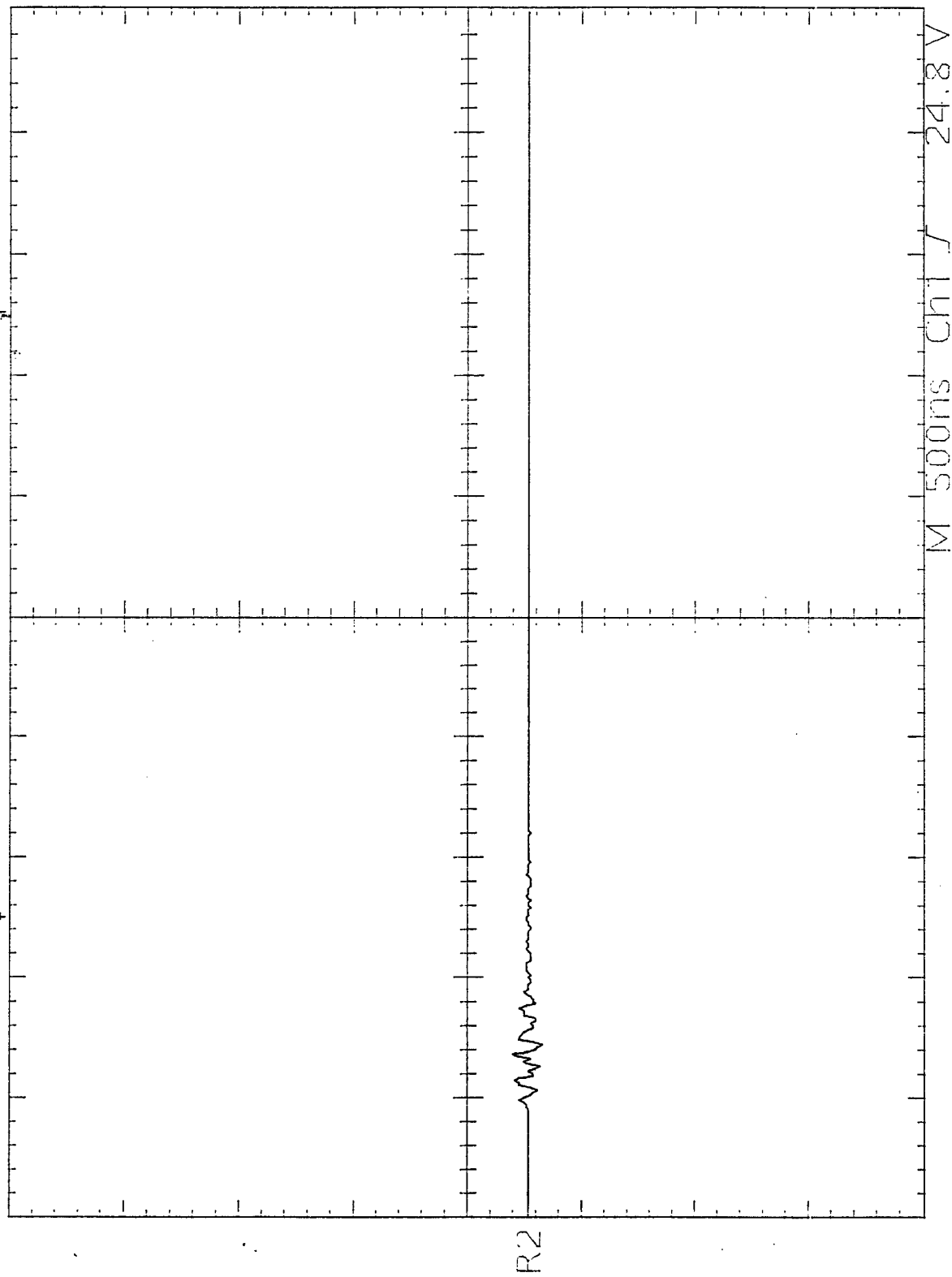
Ref2   10.0 V   500ns

Tek Run: 100MS/s   Average Air & H$_2$O @ 40kV w/ Tail Resistors 1 Jun 96

Voltage
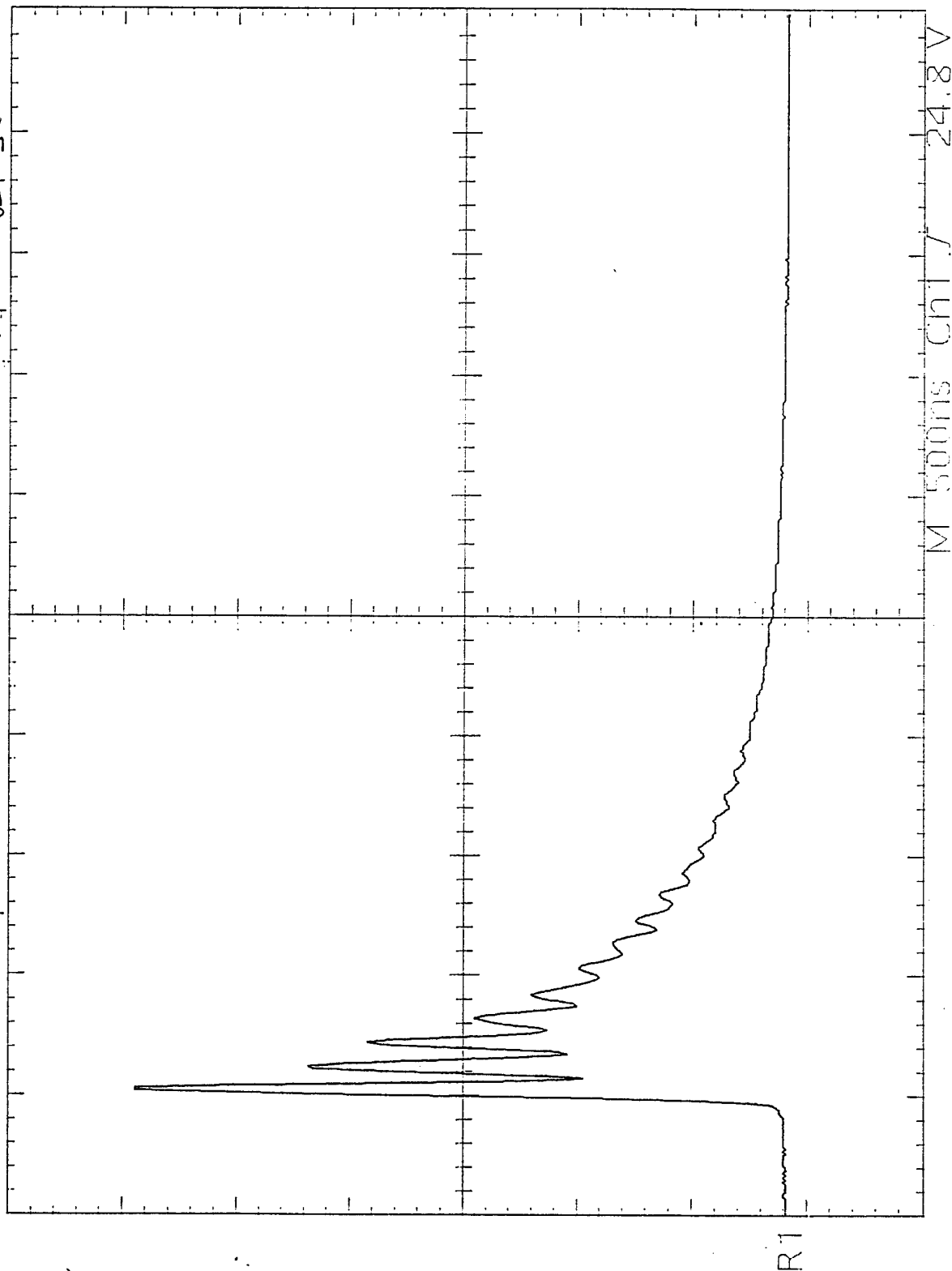
Ref1 Rise
37ns
Unstable
histogram

Ref1 Max
57.4 V

R1

M 500ns Cn1 / 24.8 V

500ns

Ref1   10.0 V

Tek Run: 100MS/s   Average Air & H₂O @ 840 kV w/ Tail Resistors / Jim 96

Current

Ref2 Max
1.8 V

R2

M 500ns Ch1 ∫ 24.8 V
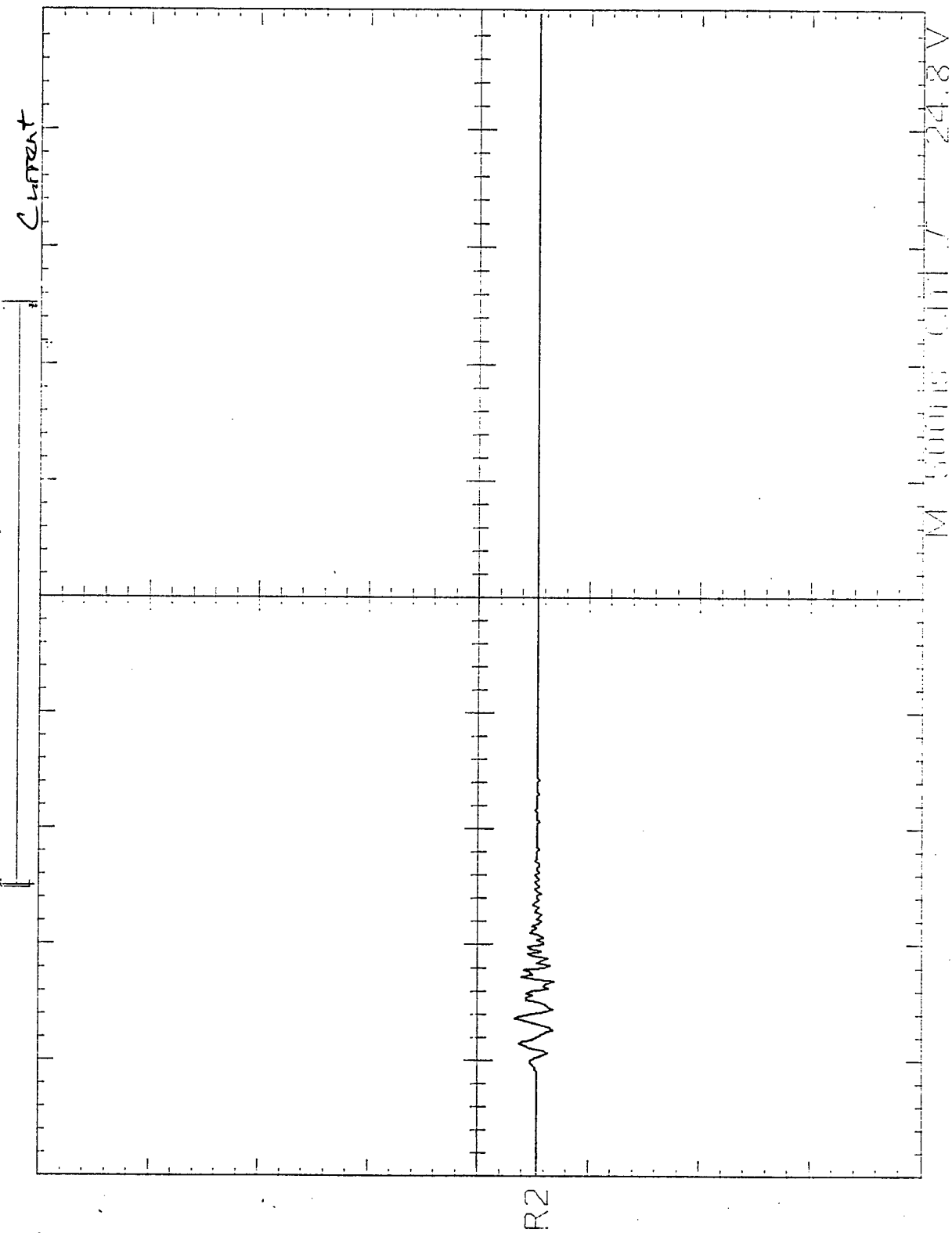
Ref2   10.0 V   500ns

Tek Run: 5.00MS/s   Average

Air & H₂O @ 20 kV w/o tail resistors   30 May 96

Vb (tagge
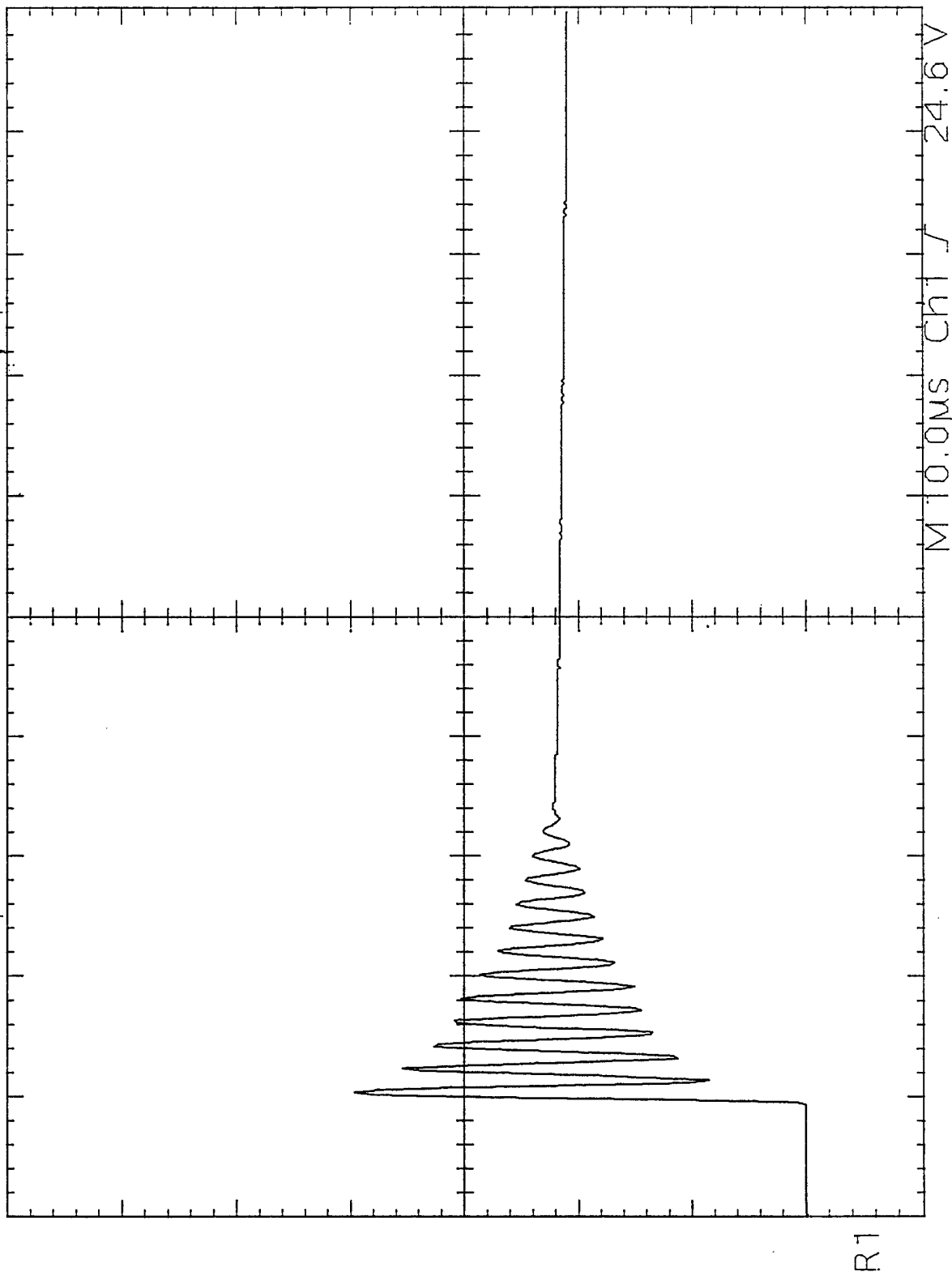
Ref1 Rise
13ns
Low
resolution

Ref1 Max
44.8 V

R1

M 10.0ms Ch1 ∫ 24.6 V

Ref1   10.0 V   500ns

Tek Run: 100MS/s   Average Air & H₂O w/o Tail Resistors @ 35 kV 1 Jun 96
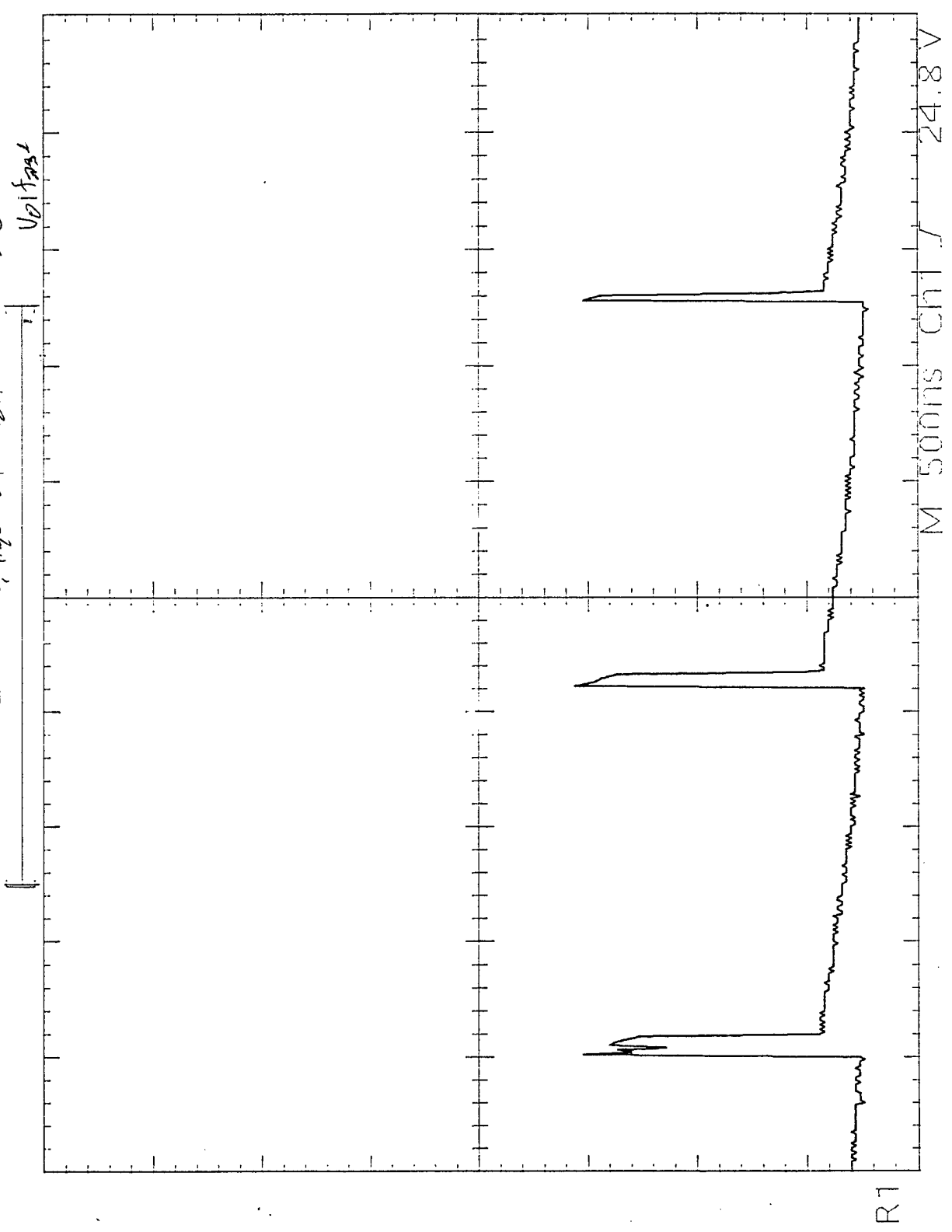
Ref1 +Width
890µs
Low
resolution

Ref1 Rise
80µs
Low
resolution

Ref1 Max
28.2 V

Voltage

M 500ns Ch1 /   24.8 V

Ref1   10.0 V   5.00ms

R1

A-21

Tek Run: 100MS/s   Average
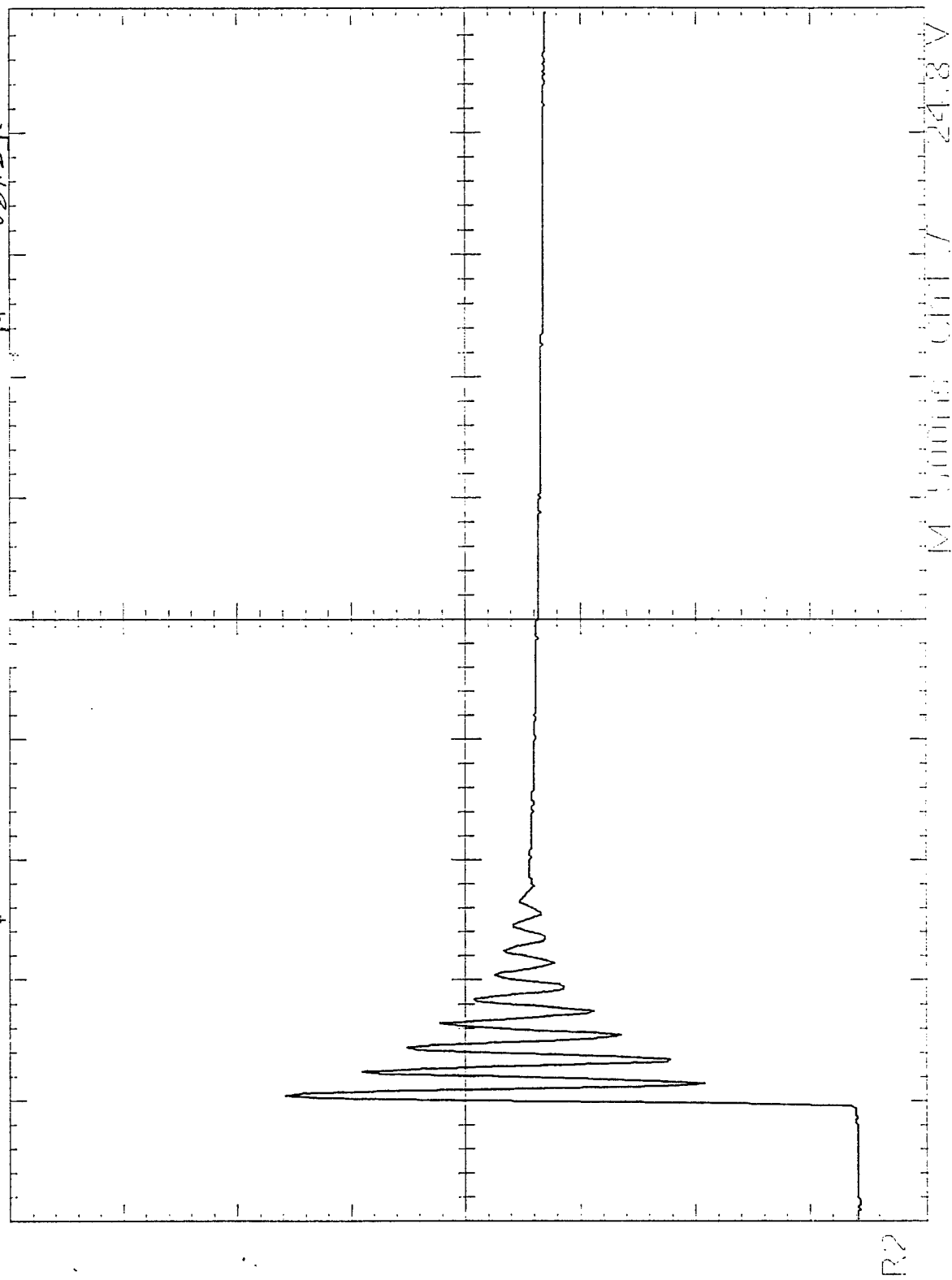
Ref2 Max
53.0 V

Ref2 Rise
14ns
LOW
resolution

M 500ns Ch1 / -24.8 V

Ref2   10.0 V   500ns

R2

Tek Run: 100MS/s   Average Air & H₂O @ 35 kV w/o Tail Resistors   1 Jun 96

Ref3 Max
2.4 V

Current

R3

M 500ns   A 24.8 V
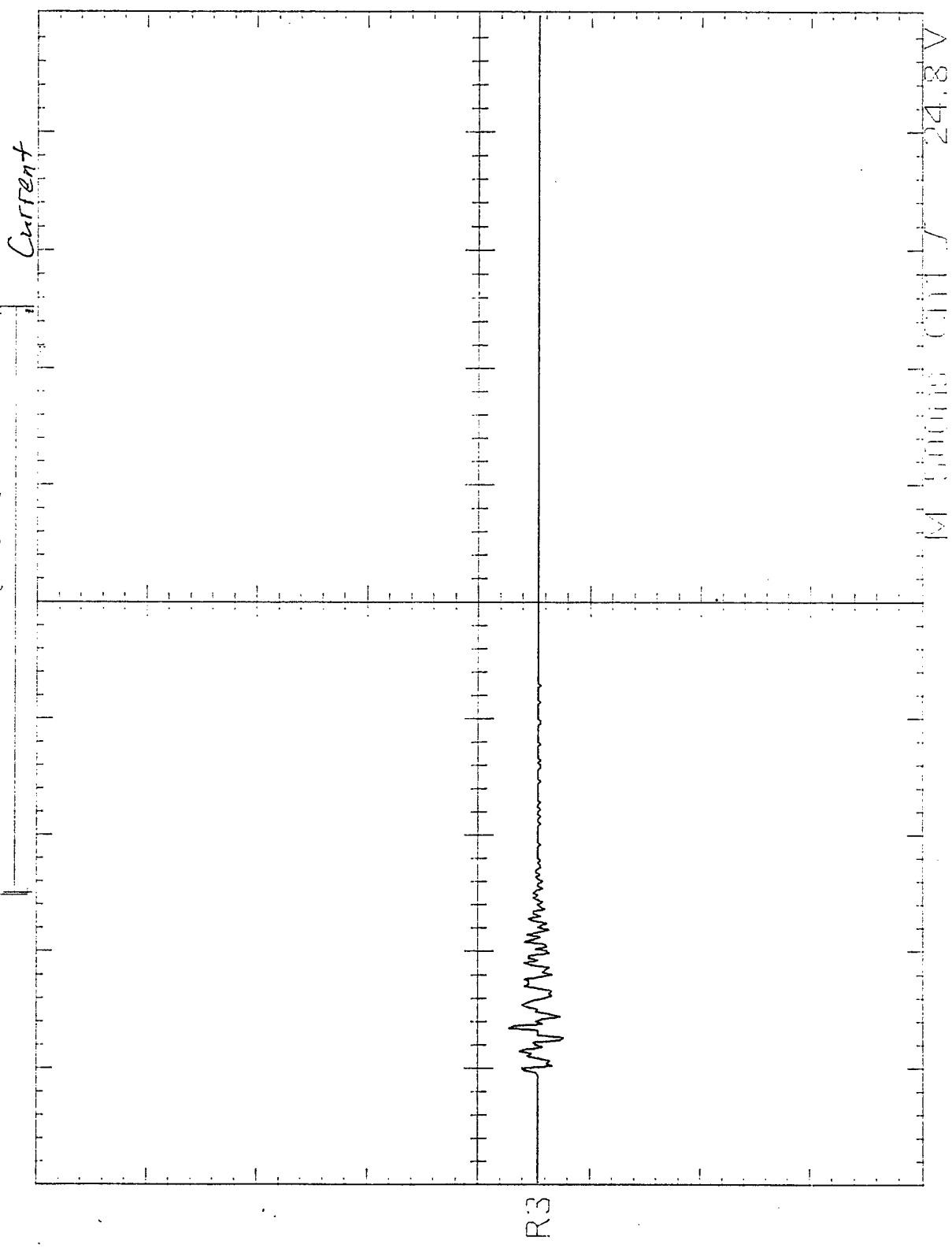
Ref3   10.0 V   500ns

Tek Run: 100MS/s   Average   DI H₂O @ 35kV w/o Tail Resistors   15 Jun 96

Voltage
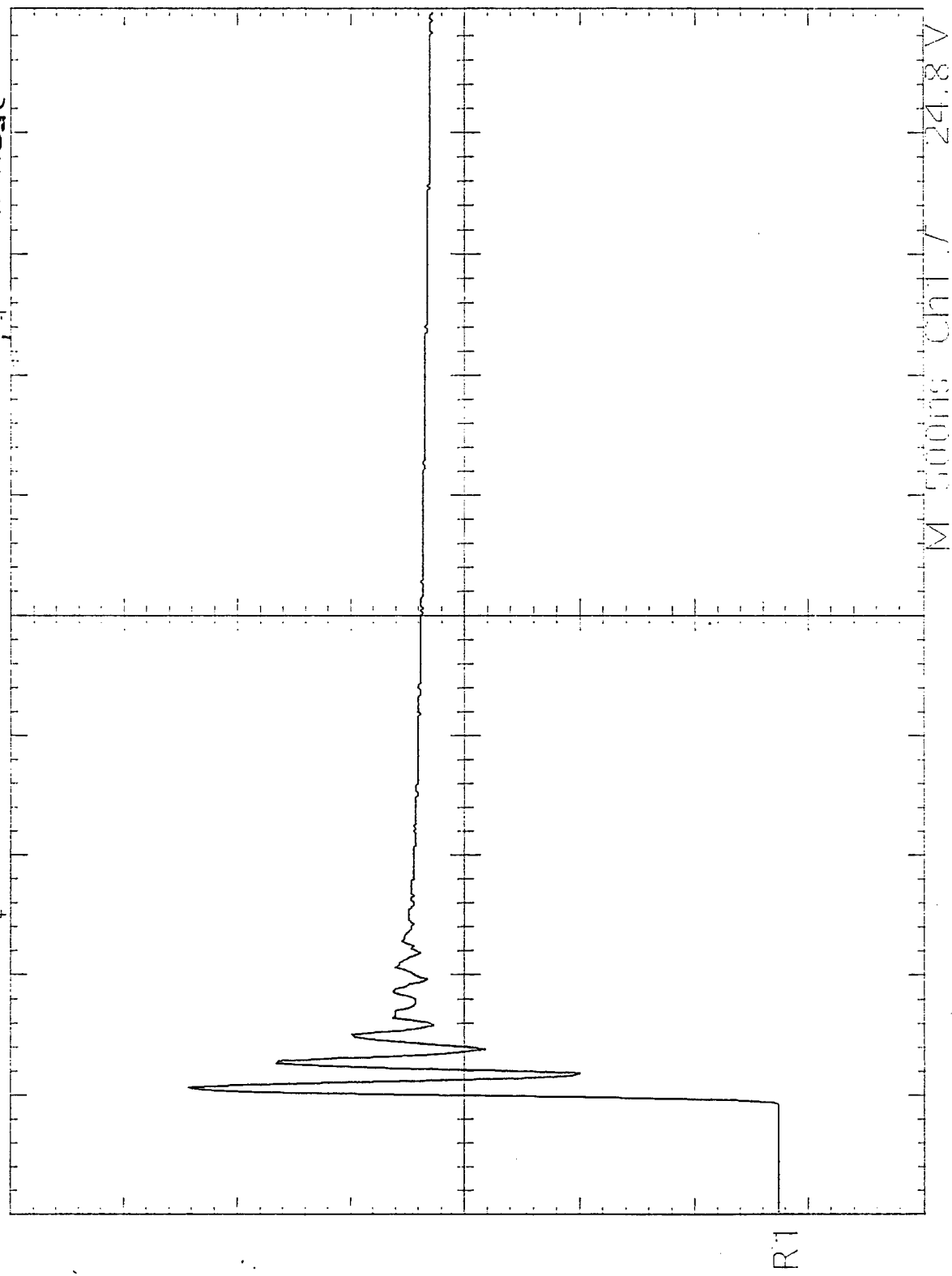
Ref1 Max
52.0 V

Ref1 Rise
20ns

M 500ns Ch1 √ 24.8 V

Ref1   10.0 V   500ns

R1

Tek Run: 100MS/s   Average DI H₂O w/o Tail Resistors @ 35kV 1 Jun 96

Current
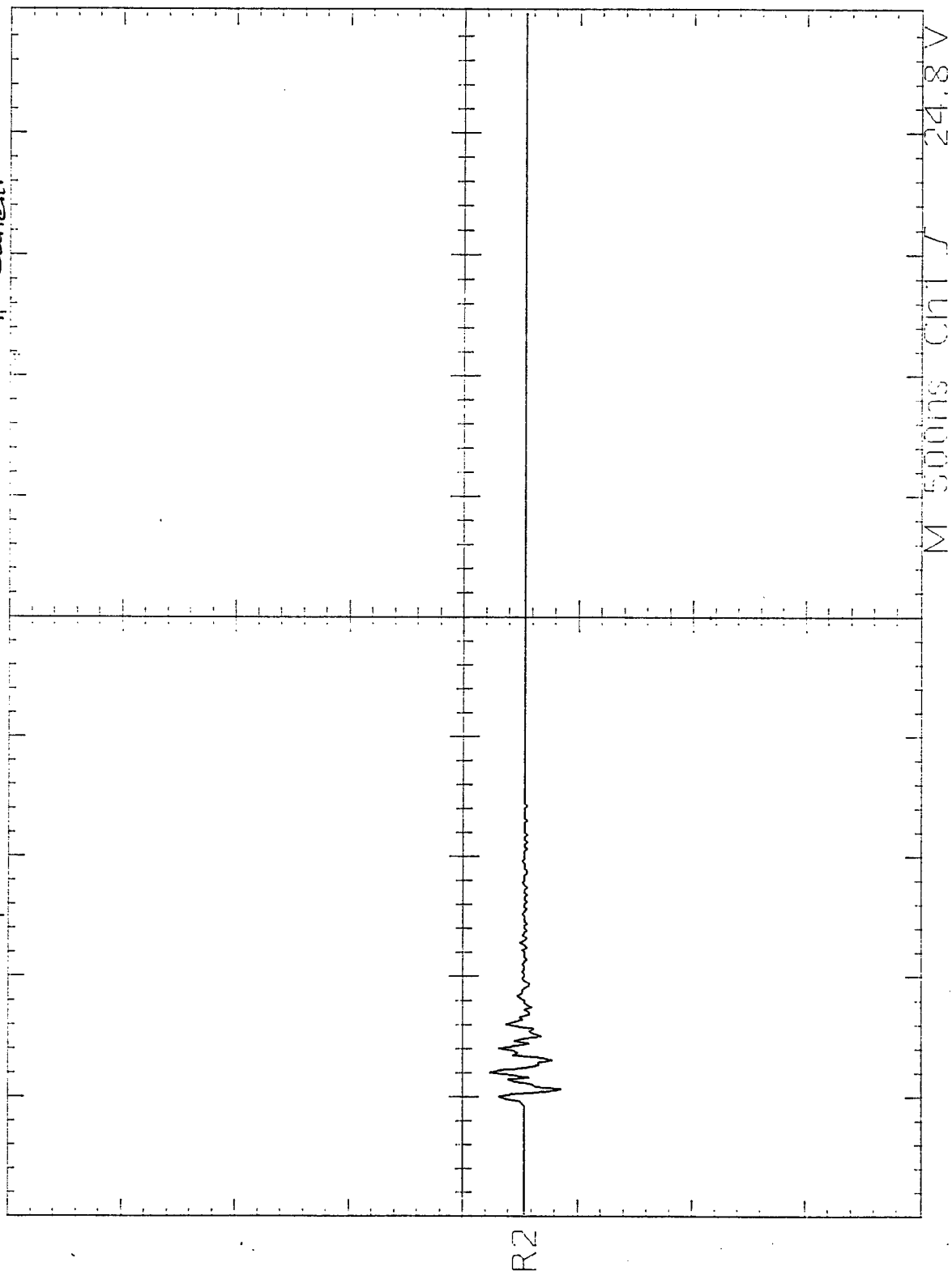
Ref2 Max
3.0 V

R2

M 500ns Ch1 ∫   24.8 V

Ref2   10.0 V   500ns

Tek Run: 100MS/s   Average

DI H₂O @ 72kv w/o T$_{Al}$ resistors / Jun 96
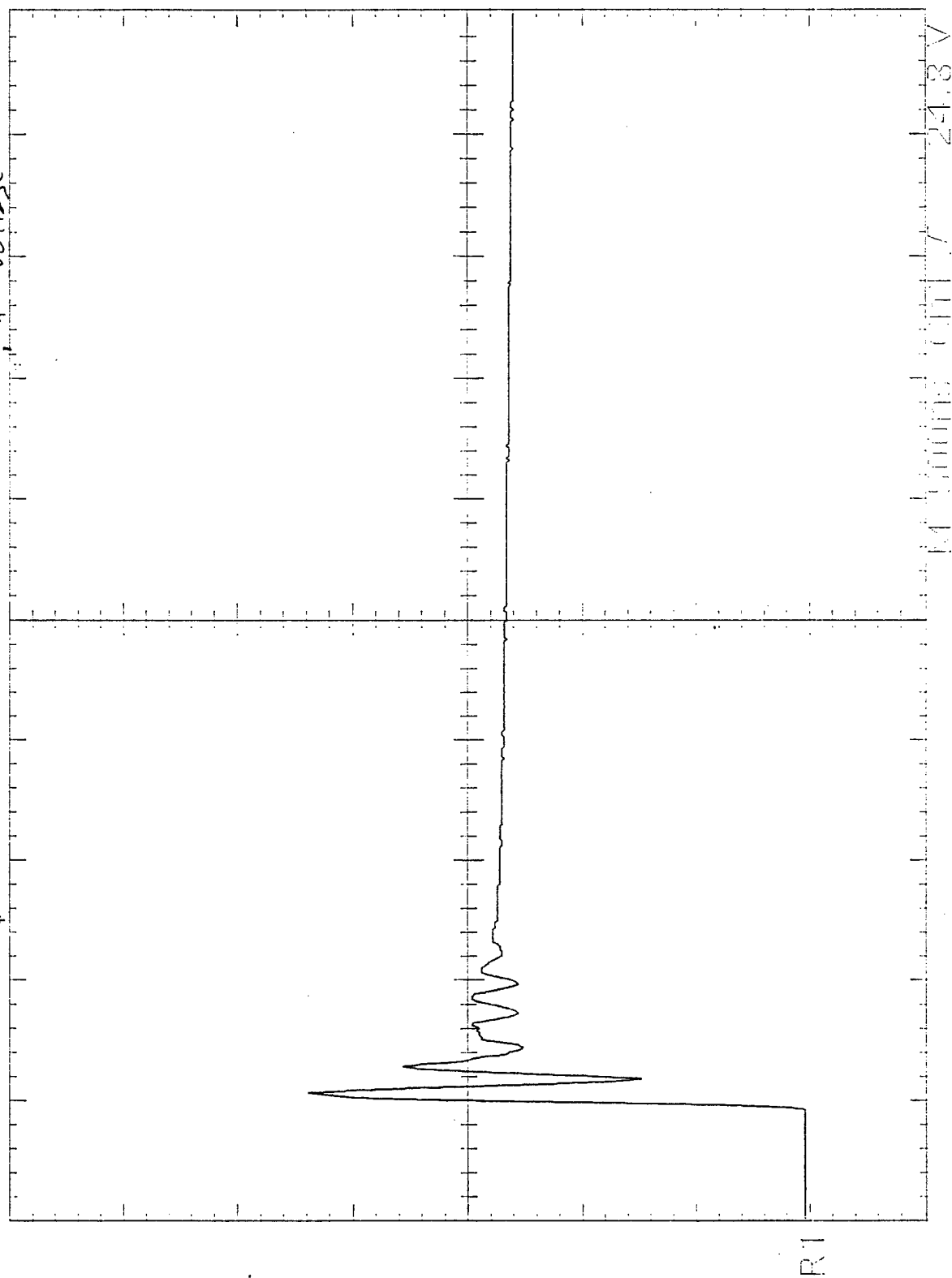
Voltage

Ref1 Max
43.8 V

Ref1 Rise
22ns

Ref1   10.0 V   500ns

R1

24.3

Tek Run: 100MS/s   Average

DI H$_2$O @ 30 kV w/o Tail Resistors Current
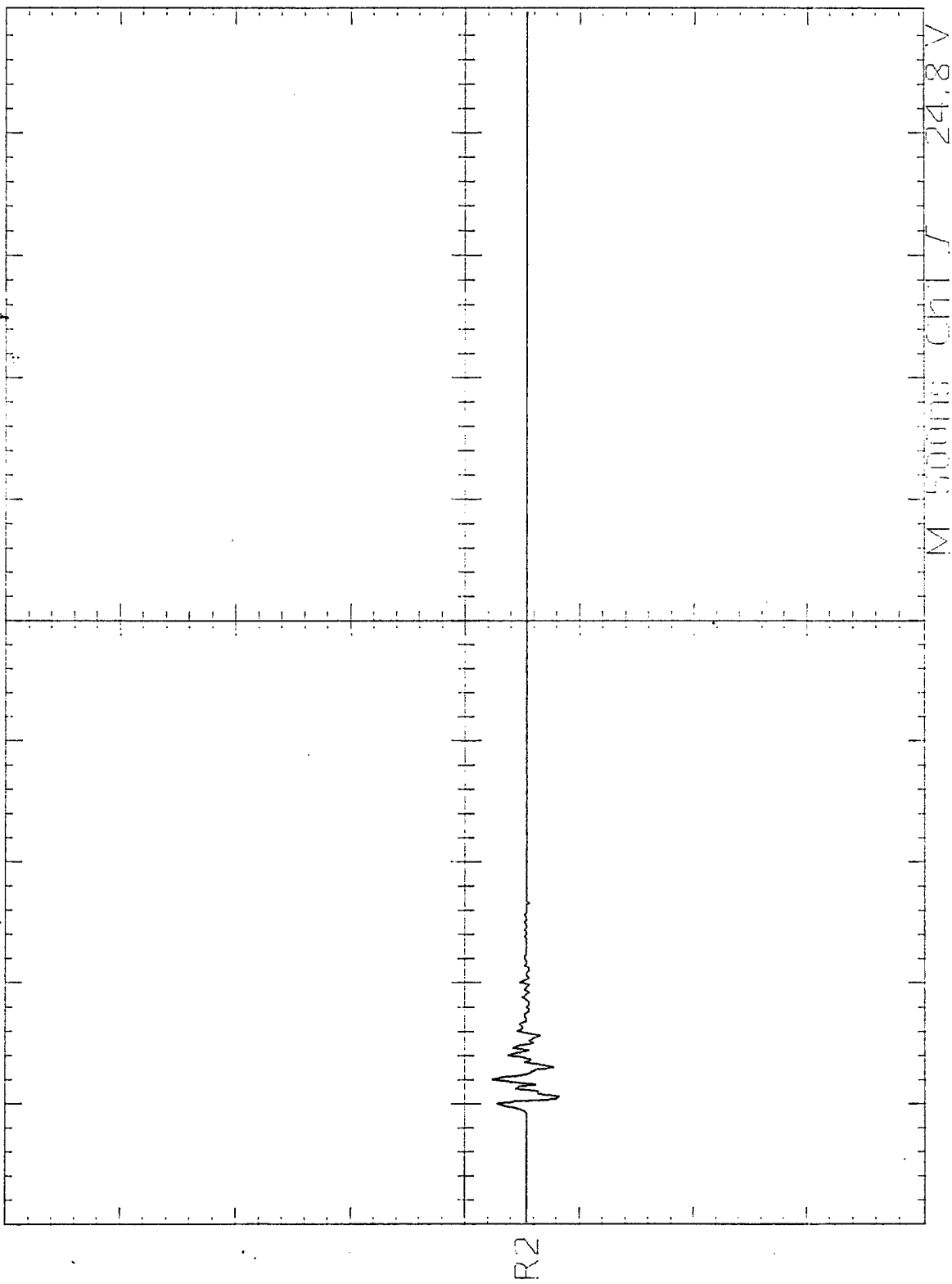
1 Jun 96

Ref2 Max
3.0 V

R2

M 500ns Chl / 24.8 V

Ref2   10.0 V   500ns
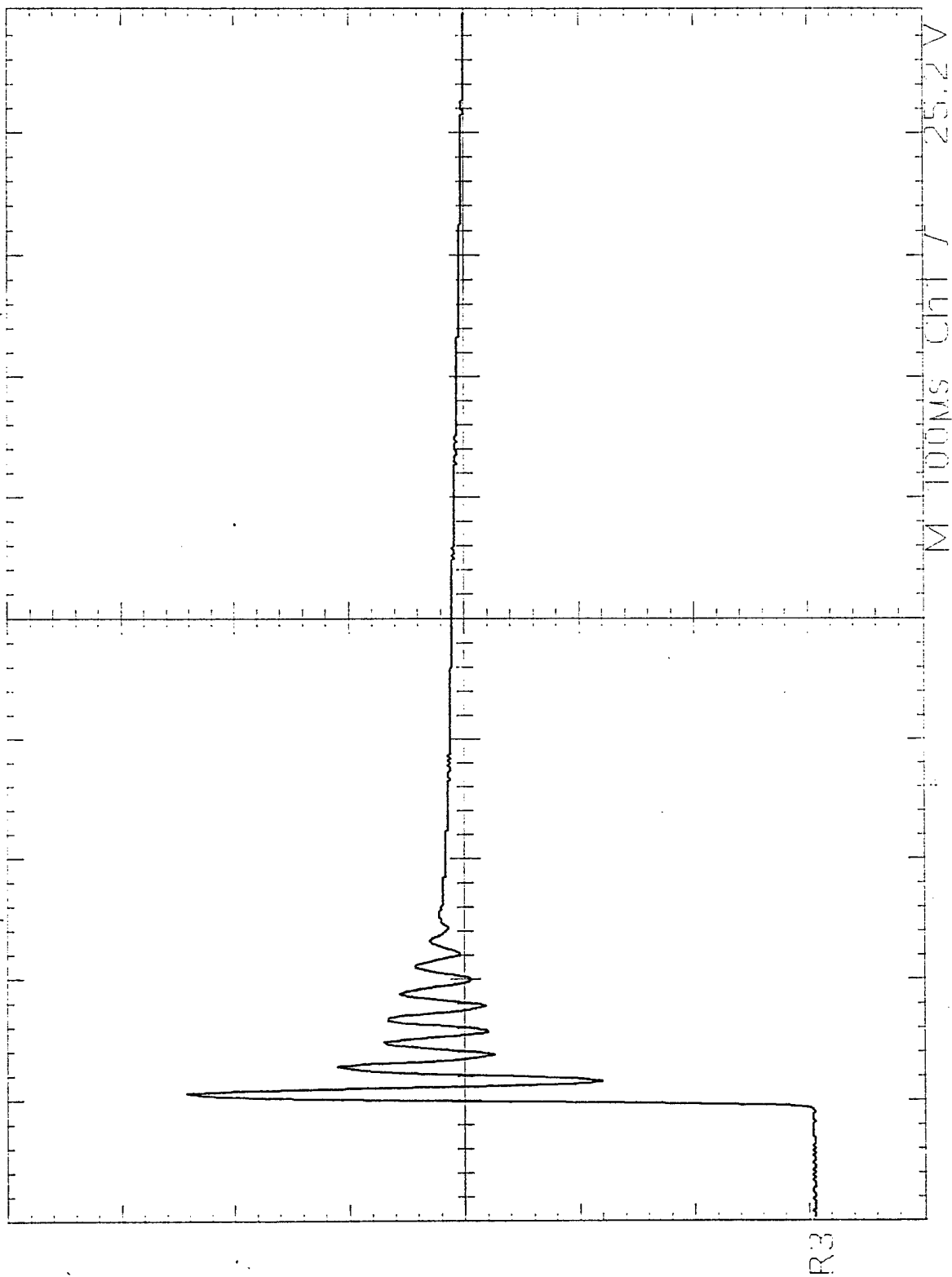
Tek Run: 250kS/s   Average DI H_2O w/o Tail Resistors @ 35 kV w/ Air in Spark Gap
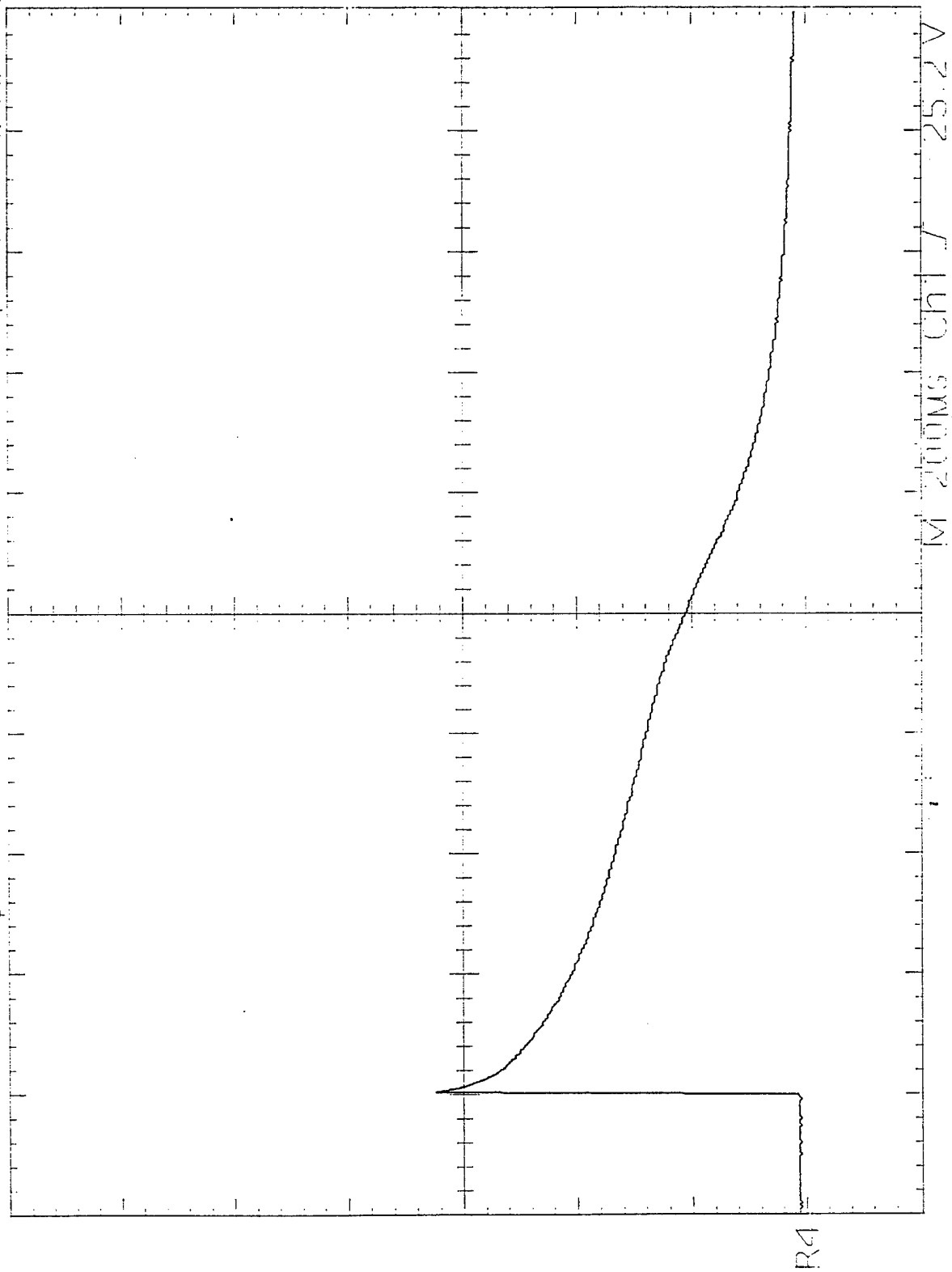
@ Time = 10 min

Ref4.+Width
865.6ms
Low signal
amplitude

Voltage

M 200ms Ch1 / 25.2 V

100ms

Ref4   10.0 V

R4

A-28

Tek Run: 250kS/s   Average

DI H₂O w/o Tail Resistors @ 25 µl w/ Air in Spark Gap

@ Time=10 min Voltage
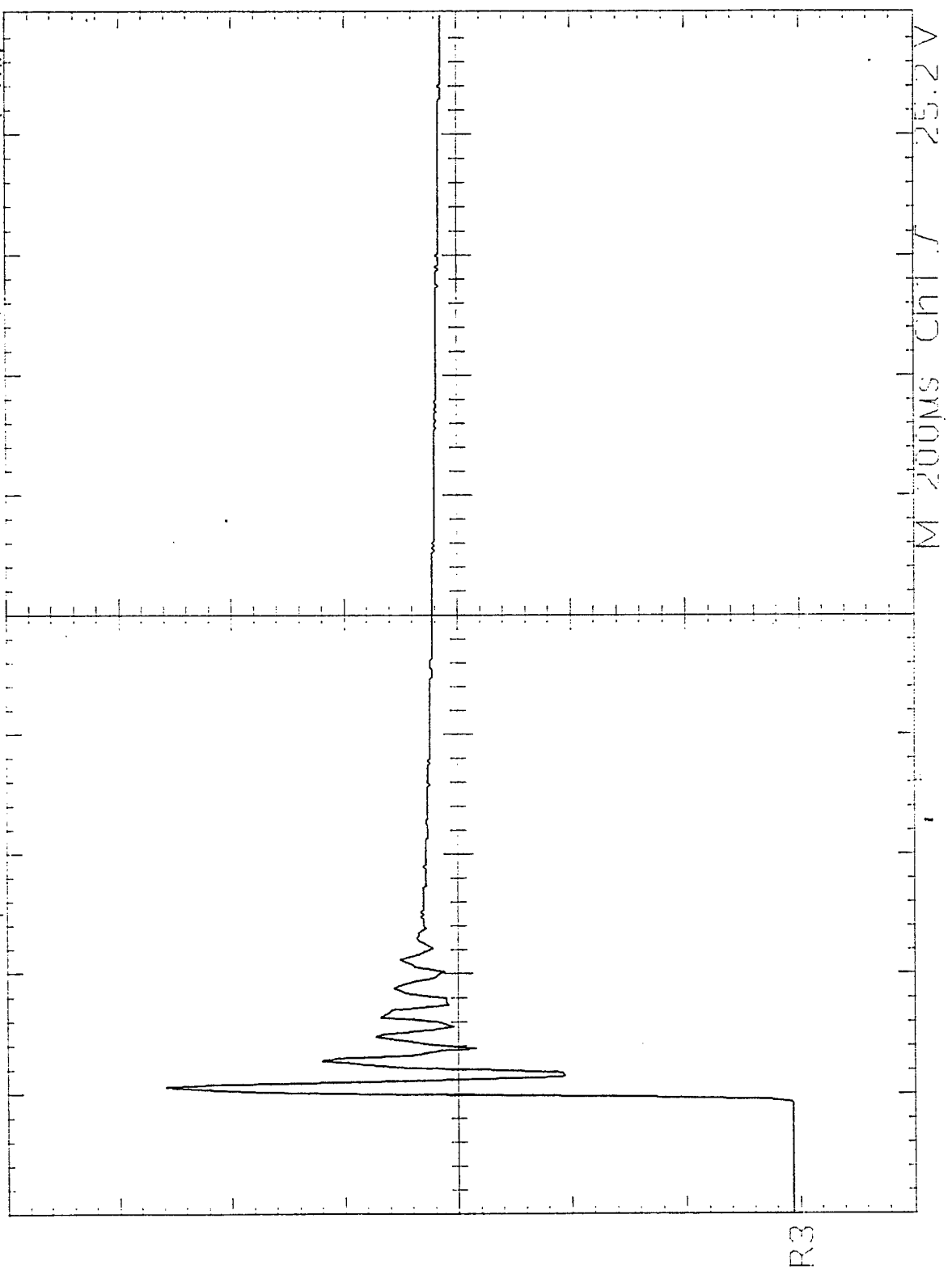
Ref3 Max
55.8 V

Ref3 Rise
16ns
Low
resolution

M 200µs Chi1 ⌐ 25.2 V

Ref3   10.0 V   500µs

R3

Tek Run: 250kS/s   Average

DI H2O w/ Tail Resistors @ 35 kV w/ Air in Spark Gap @ Time=0 Current

Ref2 Max
4.4 V

R2

M 200μs Ch1 / 25.2 V

Ref2   10.0 V   500ns

Tek Run: 250kS/s   Average   DI H2 ⊘ w/o Tail Resistors @ 35kV w/ Air in Spark Gap @ Time=0 Voltage
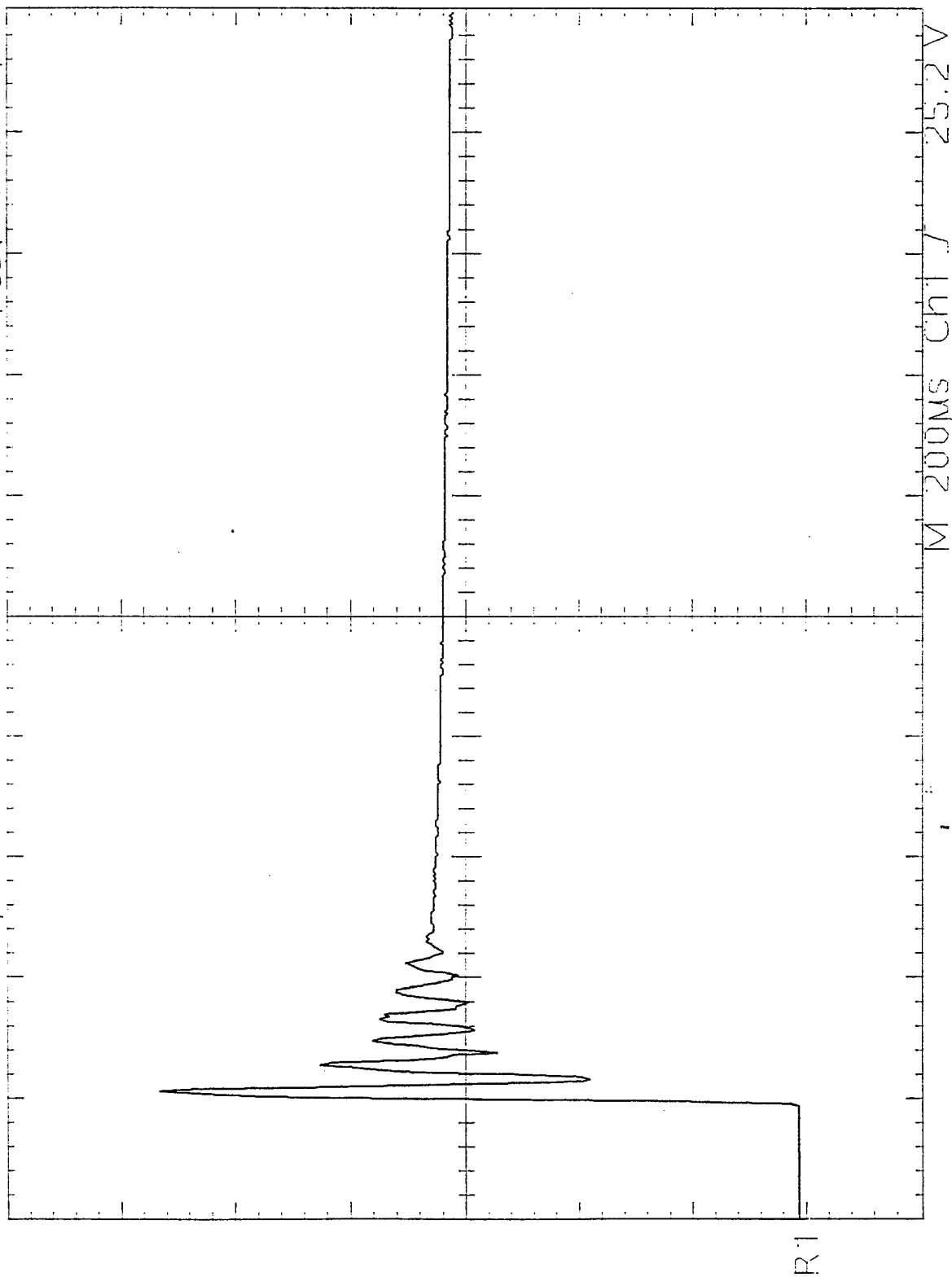
Ref1 Max
56.4 V

Ref1 Rise
16ns
Low
resolution

Ref1

R1

M 200µs Ch1 ⌐ 25.2 V

10.0 V   5.00ns

A-31

Tek Run: 250kS/s   Average   DI H_2O w/o Tail Resistors @ 55 kV w/ Compressed Air in Spark

Convert Time = 10 min

Voltage
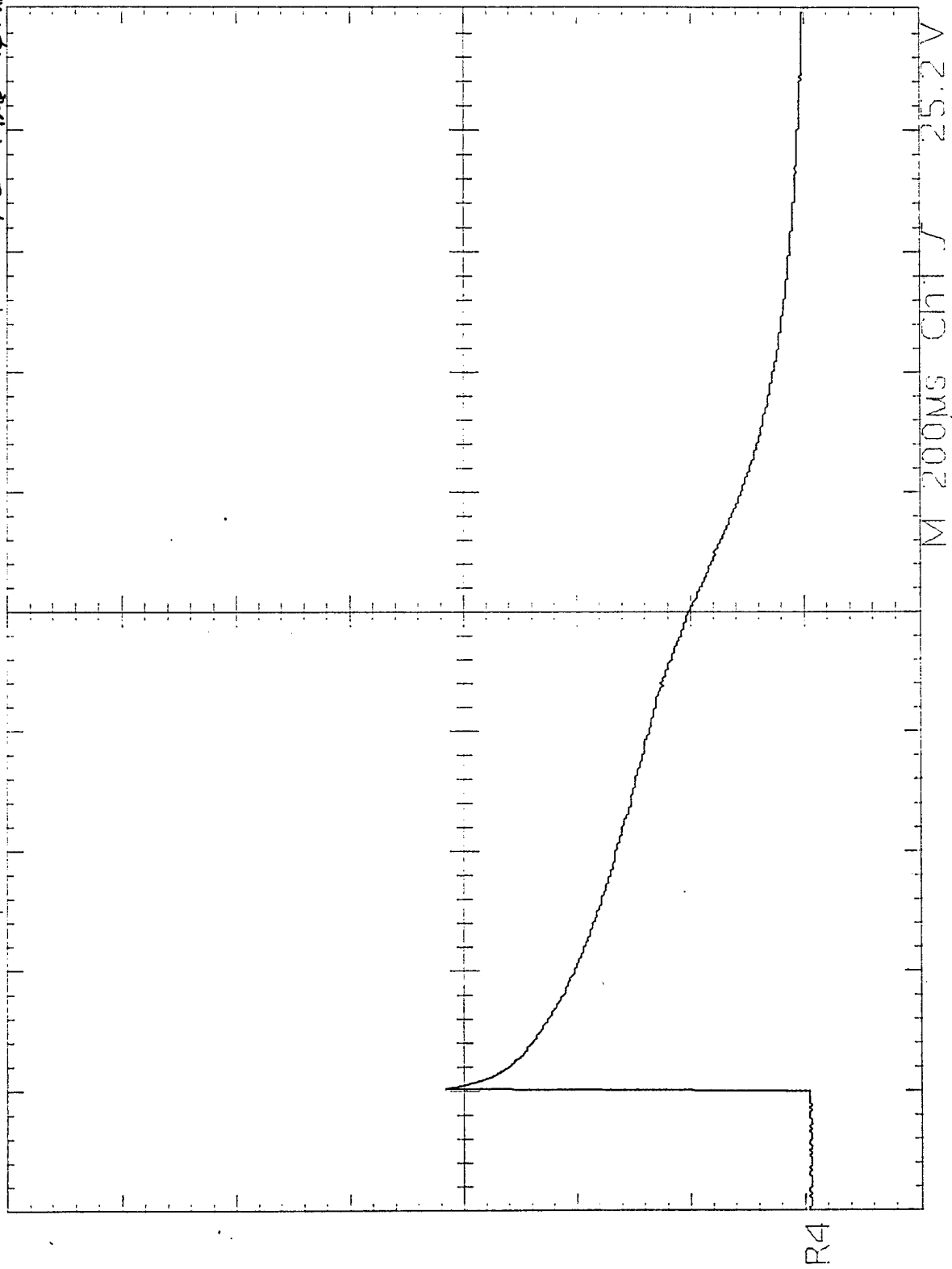
Ref4 +Width
886.4MS
Low signal
amplitude

M 200MS Ch1 / 25.2 V

Ref4   10.0 V   200MS

R4

Tek Run: 250kS/s   Average DE   H₂O w/o Tail Resistors @ 35 kV w/ compressed Air in Spark Voltage

6⊃p ⊅ Time = 10 min

Ref3 Max
54.8 V

Ref3 Rise
16ns
Low
resolution

Ref3   10.0 V   500ns   M 200μs Ch1 ↗ 25.2 V

A–33

Tek Run: 250kS/s   Average DI H_2O w/o Tail Resistors @ 35 kV w/ compressed Air in Spark

Gap at Time = Ø   Current
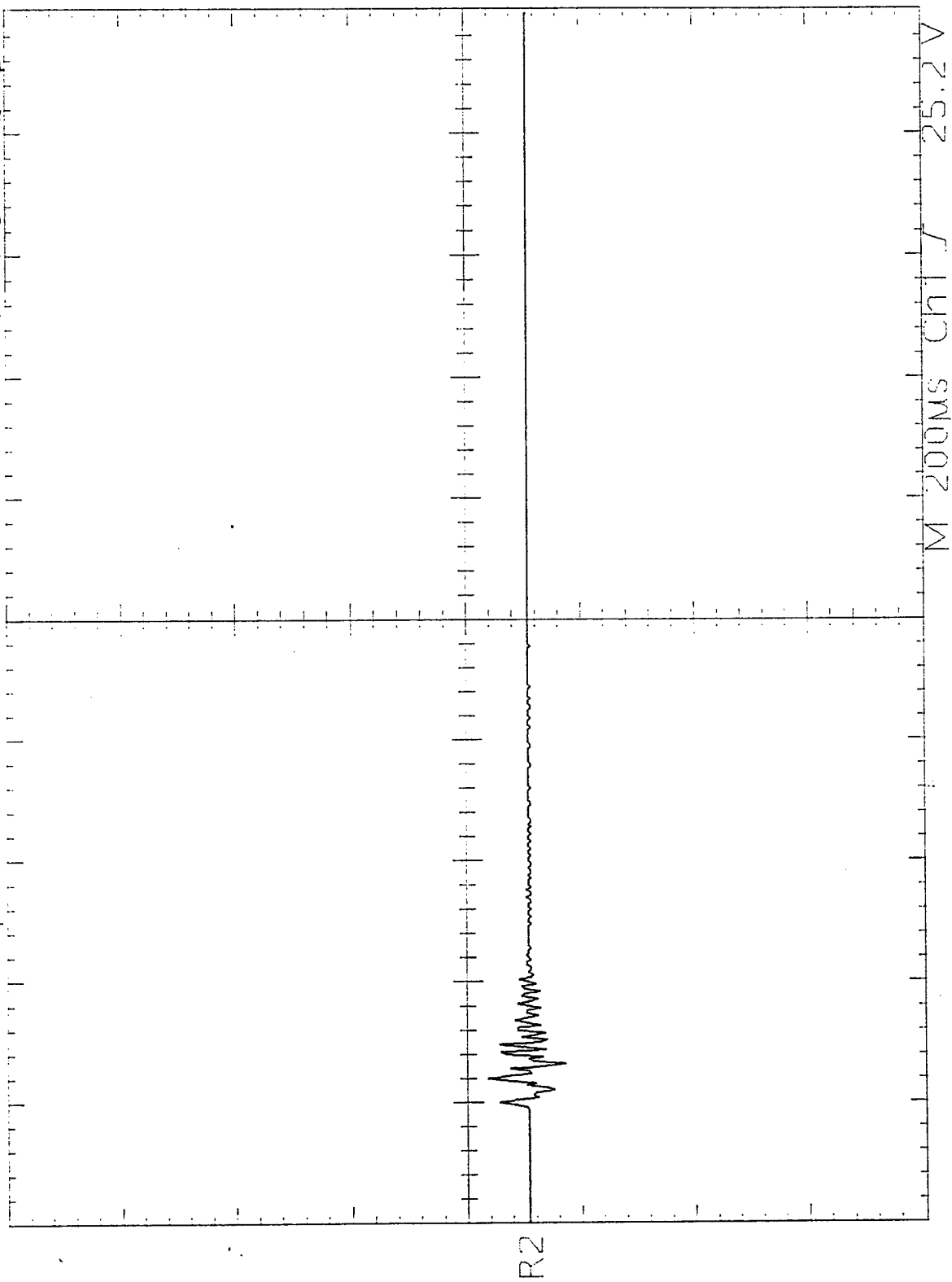
Ref2 Max
3.6 V

R2

M 200μs Ch1 $\int$ 25.2 V

Ref2   10.0 V   500ns

Tek Run: 250kS/s   Average   DI H₂O w/o Tail Resistors @ 35 kV w/ compressed Air in Spark
Gap @ Time=0 Voltage
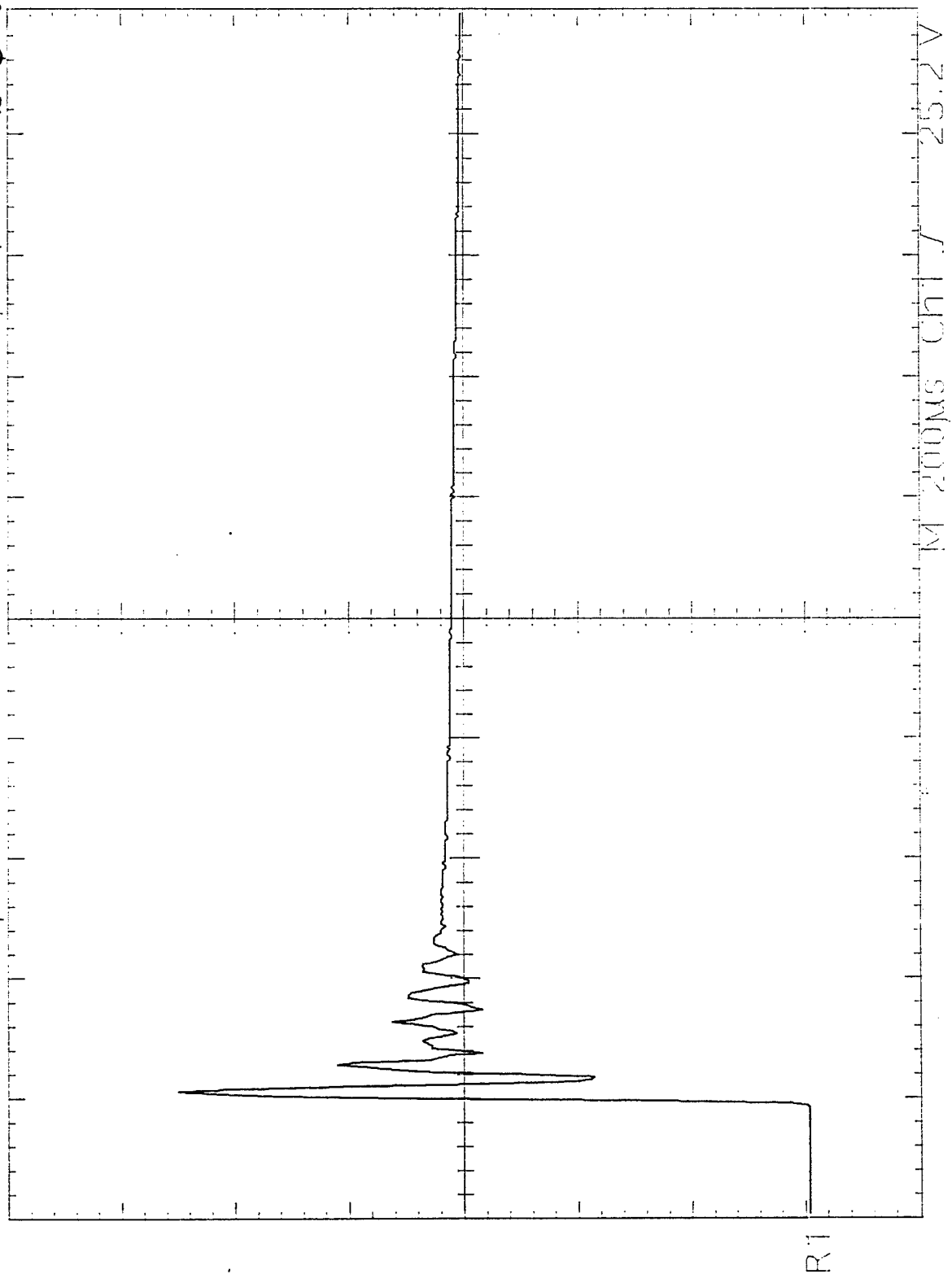
Ref1 Max
55.8 V

Ref1 Rise
16ns
Low
resolution

M 200ns Ch1 / 25.2 V

Ref1   10.0 V   500ns

R1

A-35

Tek Run: 500kS/s   Average DI H2O w/o tail resistors @ 35 kV w/ Nitrogen in Spark
Gap @ Time=10min Voltage

Ref4 +Width
822.8μs
Low signal
amplitude

M 100μs   Ch1 ∫   25.2 V

100μS

Ref4   10.0 V

A-36
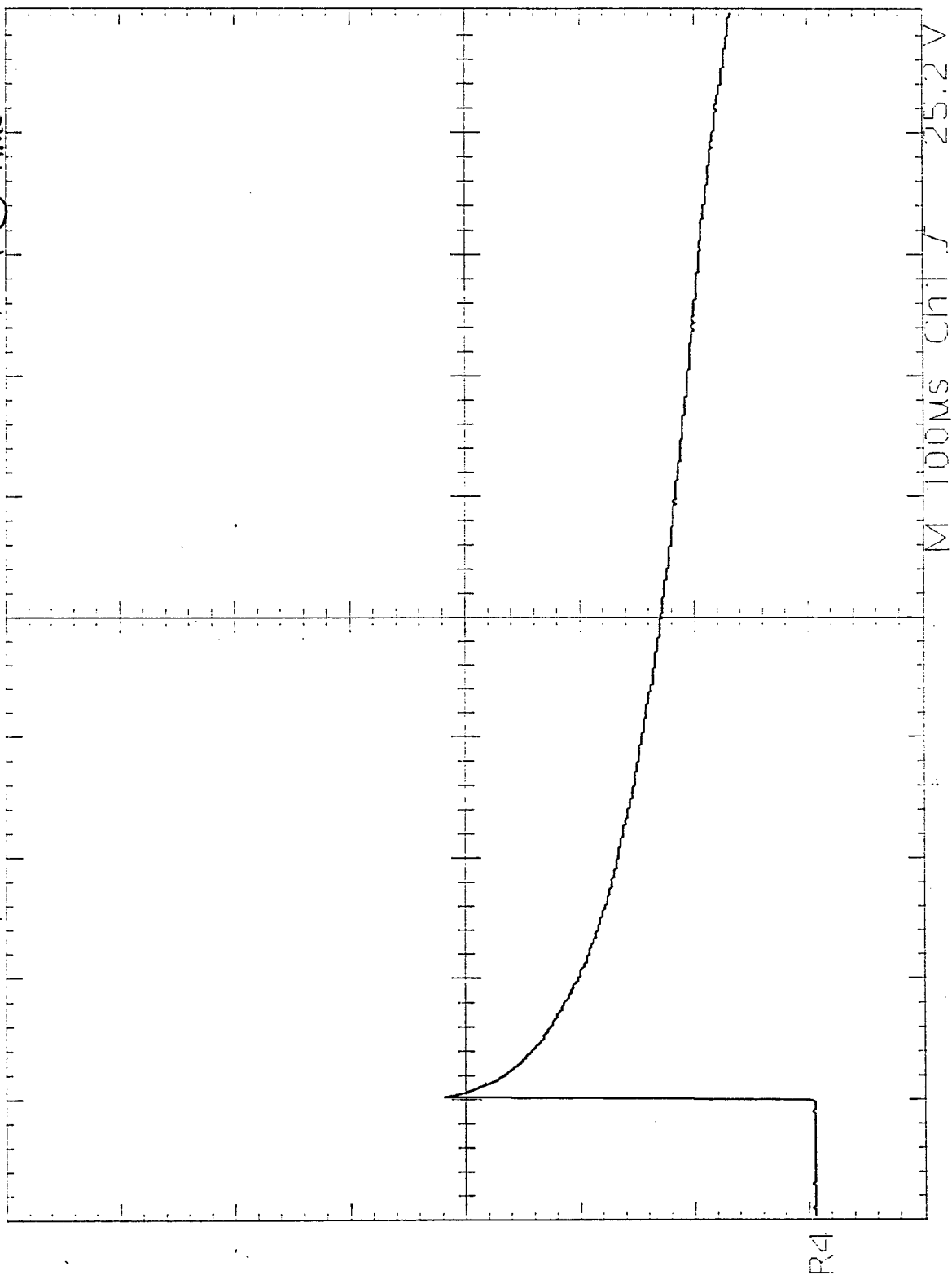
Tek Run: 500kS/s   Average   DI H_2O w/o Tail Resistors @ 35 kV w/ Nitrogen in Spark

Gap @ Time=10min Voltage

Ref3 Rise
16ns
Low
resolution

Ref3 Max
55.2 V

25.2 V

M 100ms Ch1 ⌐

500ns

Ref3   10.0 V

R3

Tek Run: 500kS/s   Average   Trig'd

DI H_2O w/o Tzi; Resistors @ 35kV w/ Nitrogen in Spark

Gap @ Time = Ø   Voltage
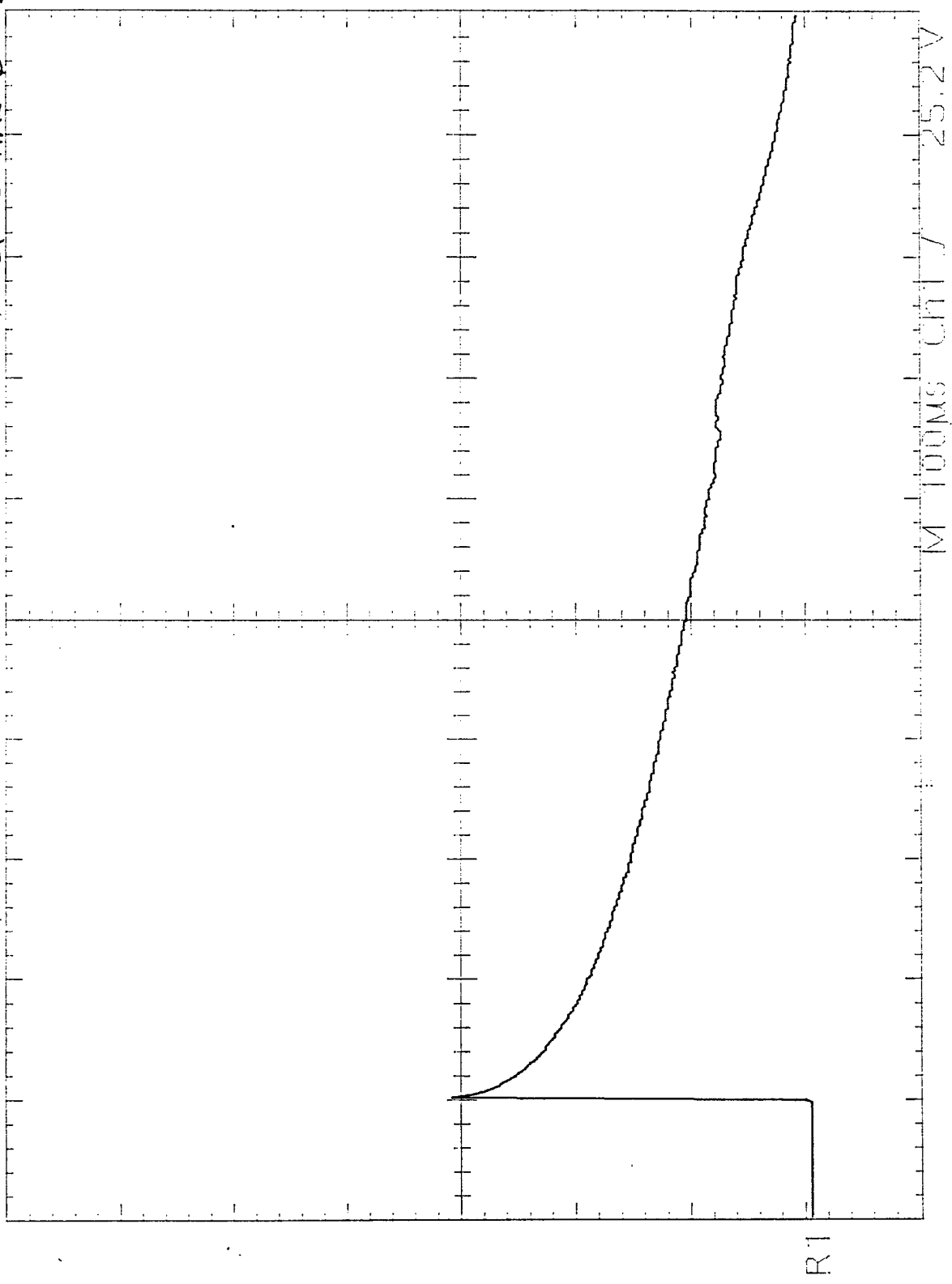
Ref1 Max
31.6 V

Ref1 +Width
1.1920ms
Low signal
amplitude

Ref1 Rise
1.6ms
Low signal
amplitude

R1

Ref1   10.0 V   200ms

M 100ms Ch1 ʃ 25.2 V

A-38

Tek Run: 500kS/s

Average DI H_2O w/o Tail Resistors @ 35 kV w/ Nitrogen in Spark
Gap @ Time=0 Current
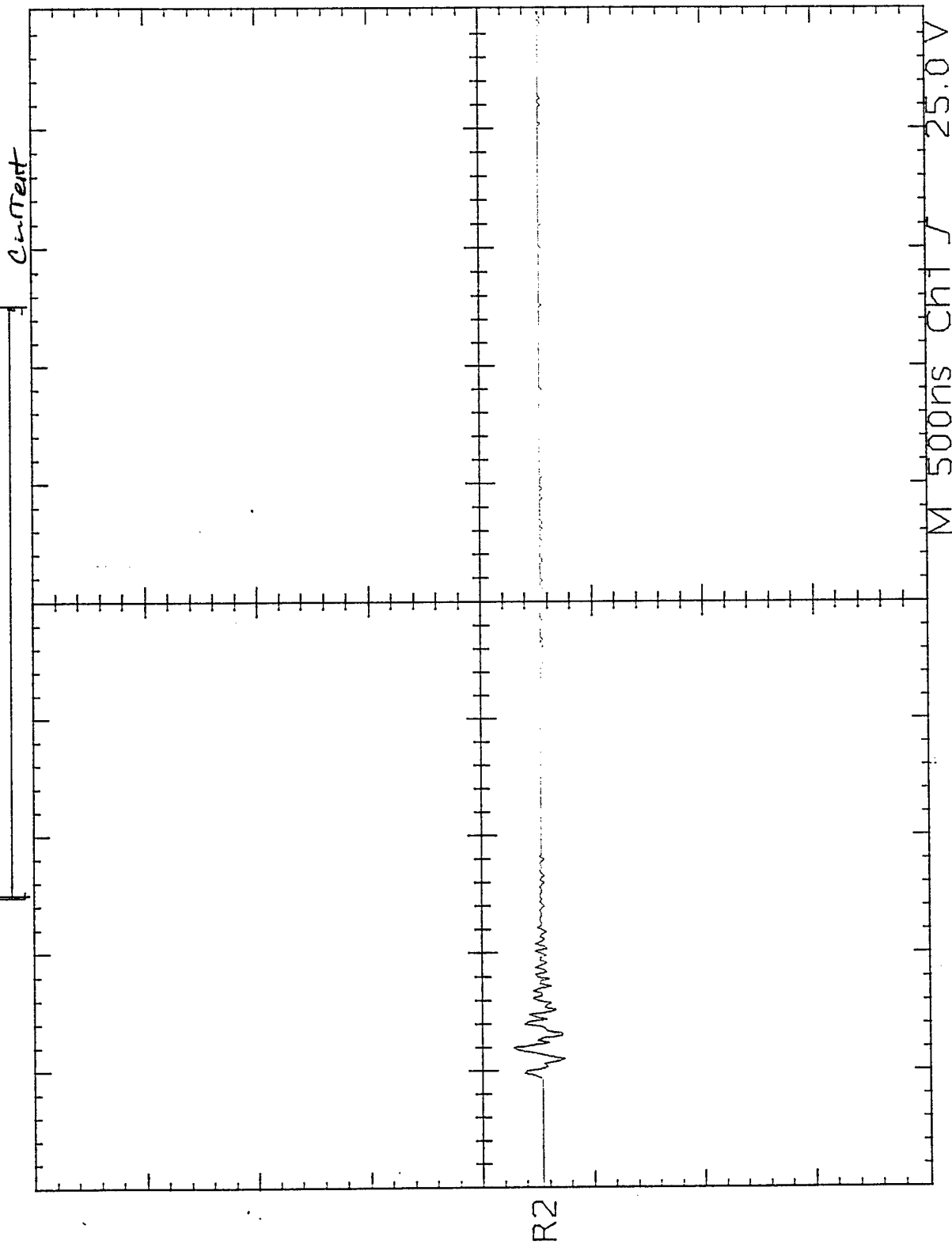
Ref2 Max
1.4 V

R2

Ref2   10.0 V   500ns   M 100ms Ch1 / 25.2 V

A-39
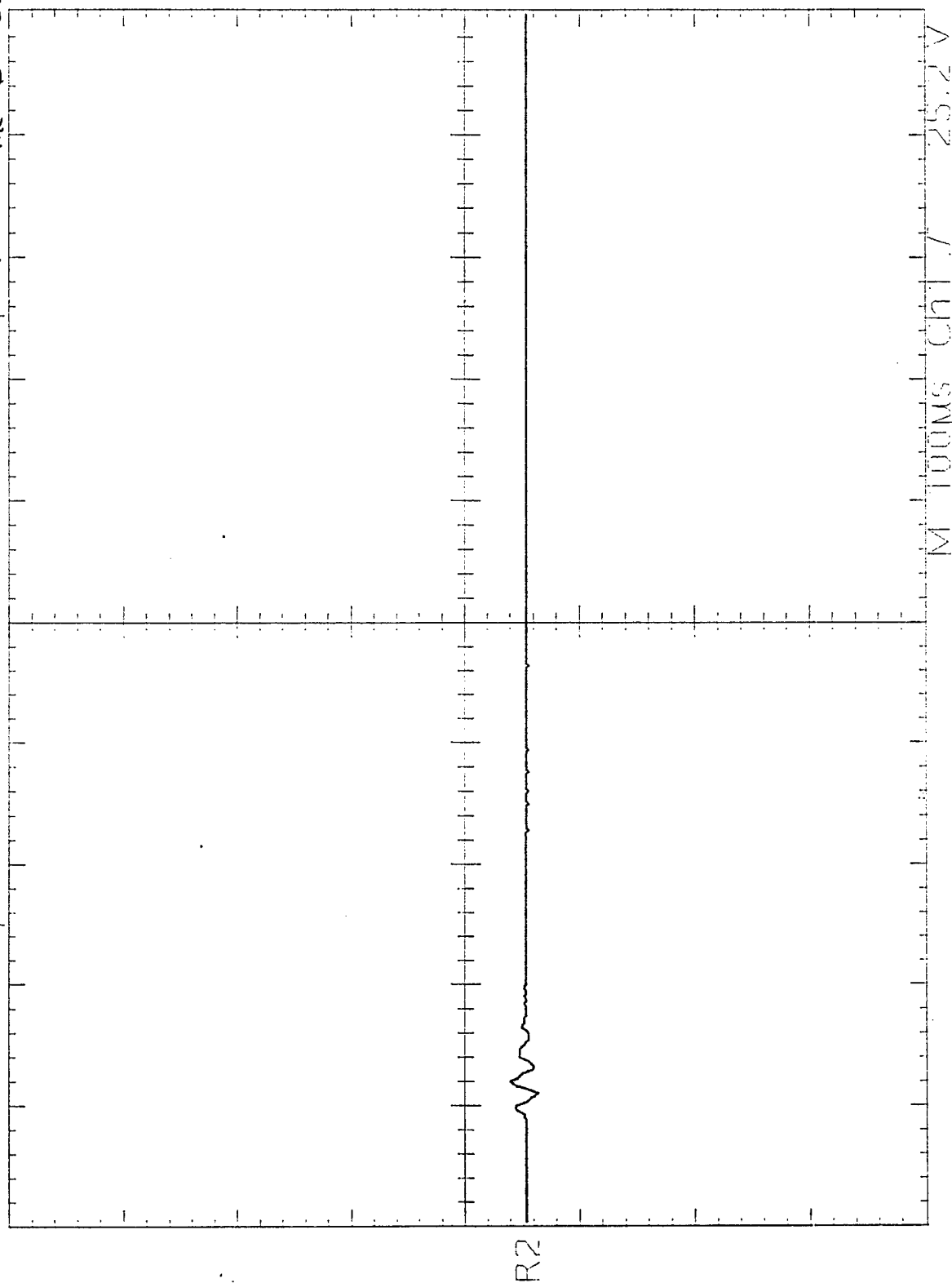
Tek Run: 250kS/s   Average   Trig?

DI H₂O w/o Tail Resistors @ 35 kV w/ Helium in Spark Gap @ Time = 10 min to min to voltage
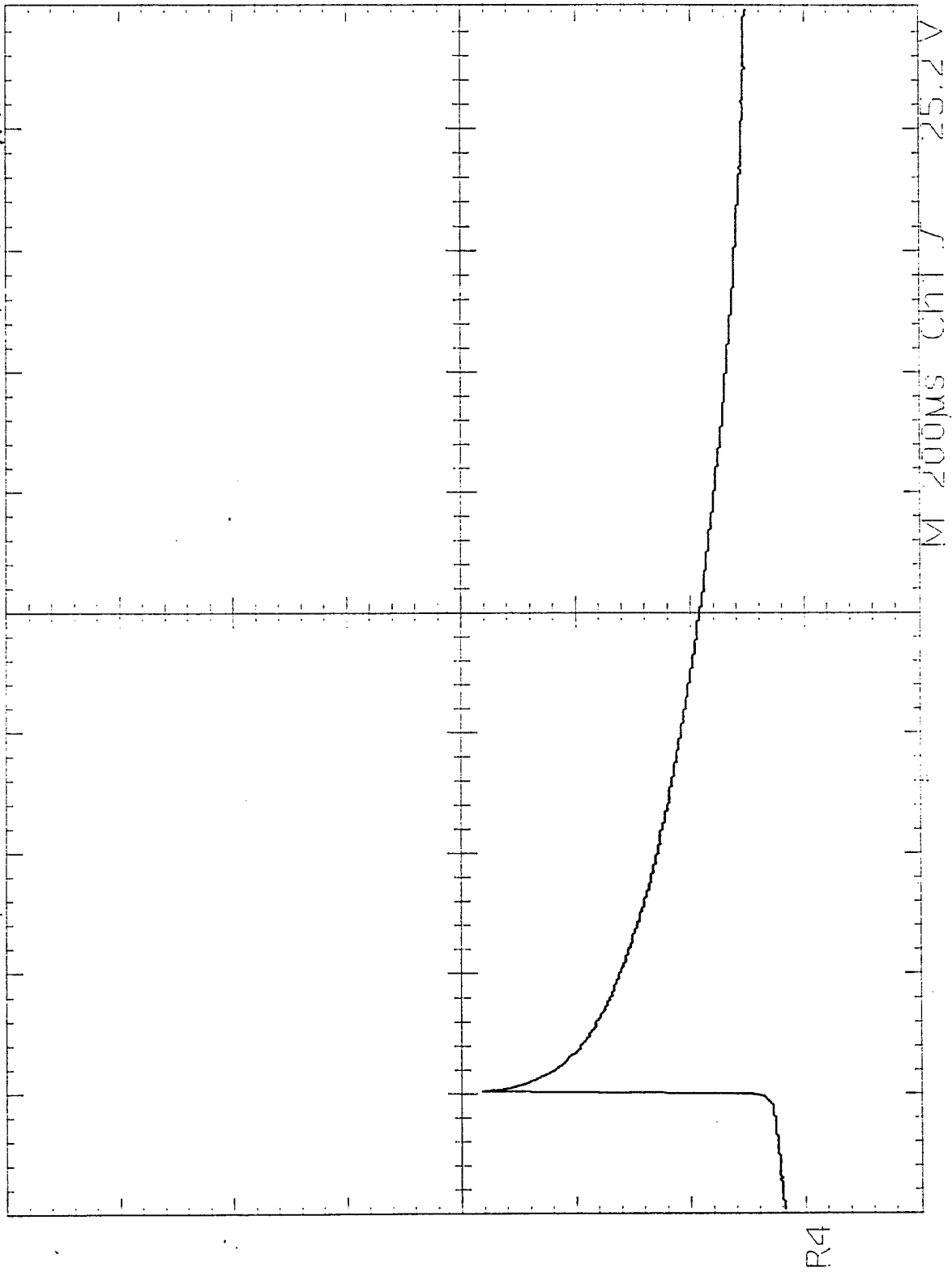
Ref4 +Width
631.2NS
Low signal
amplitude

Δ 25.2

M 200MS Ch1 /

Ref4   10.0 V   200MS

R4

A-40

Tek Run: 250kS/s

Average DI H₂D w/o Tail Resistors @ 33kV w/ Helium in Spark
Gap @ Time = 10 min. Voltage
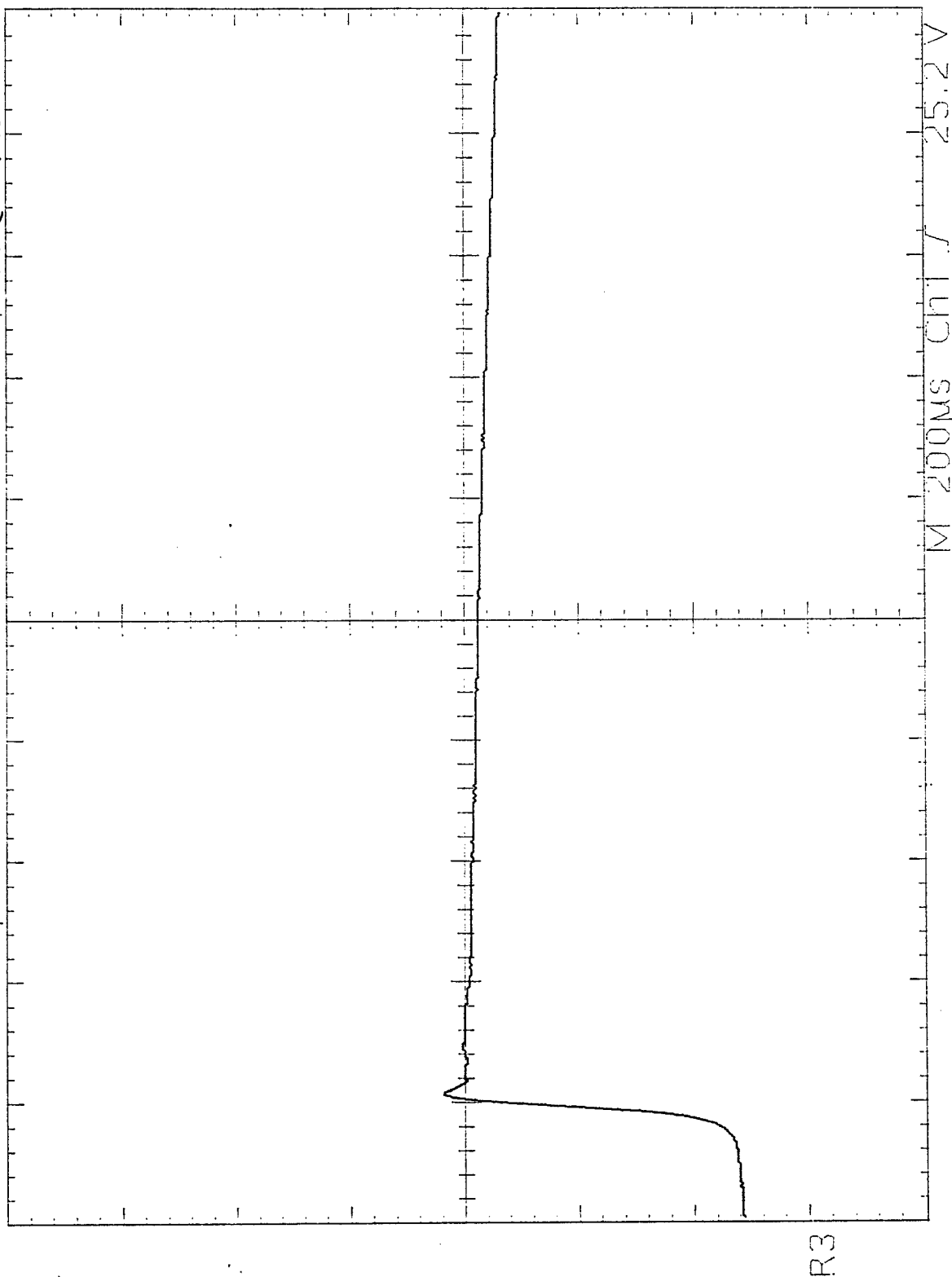
Ref3 Max
32.8 V

Ref3 Rise
92ns

M 200µs Chl / 25.2 V

Ref3   10.0 V   500µs

R3

Average

DI H_2O w/o Tail Resistors @ 35 kV w/ Helium in Spark

Gap @ Time=0

Total Current

Ref2 Max
3.2 V

R2

M 200µs Chn1 ∫ 25.2 V

Ref2   10.0 V   500ns

Tek Run: 250kS/s   Average   DI H_2O w/o Tail Resistors @ 35kV w/ Helium in Spark

6AR @ Time=0   Voltage
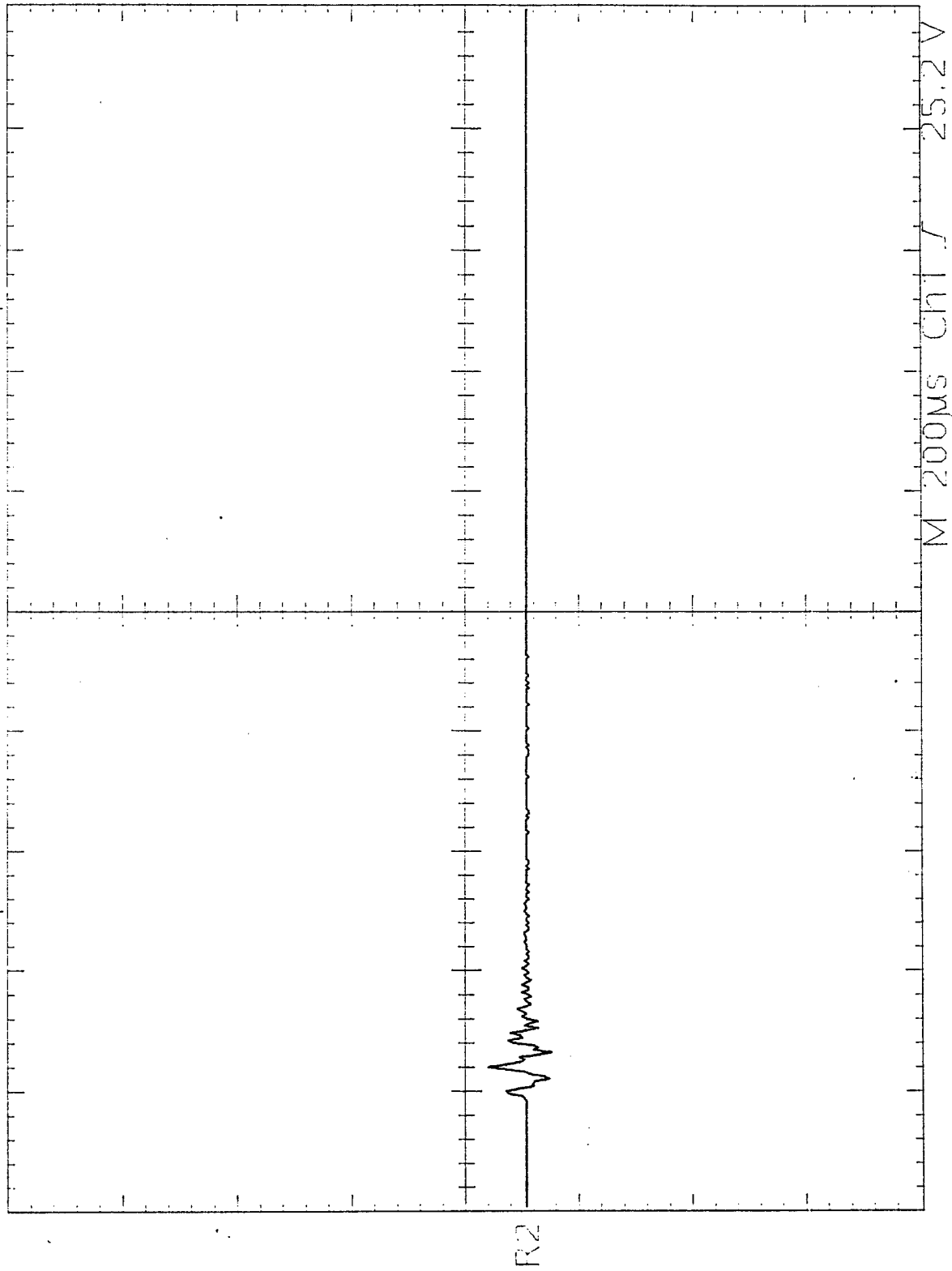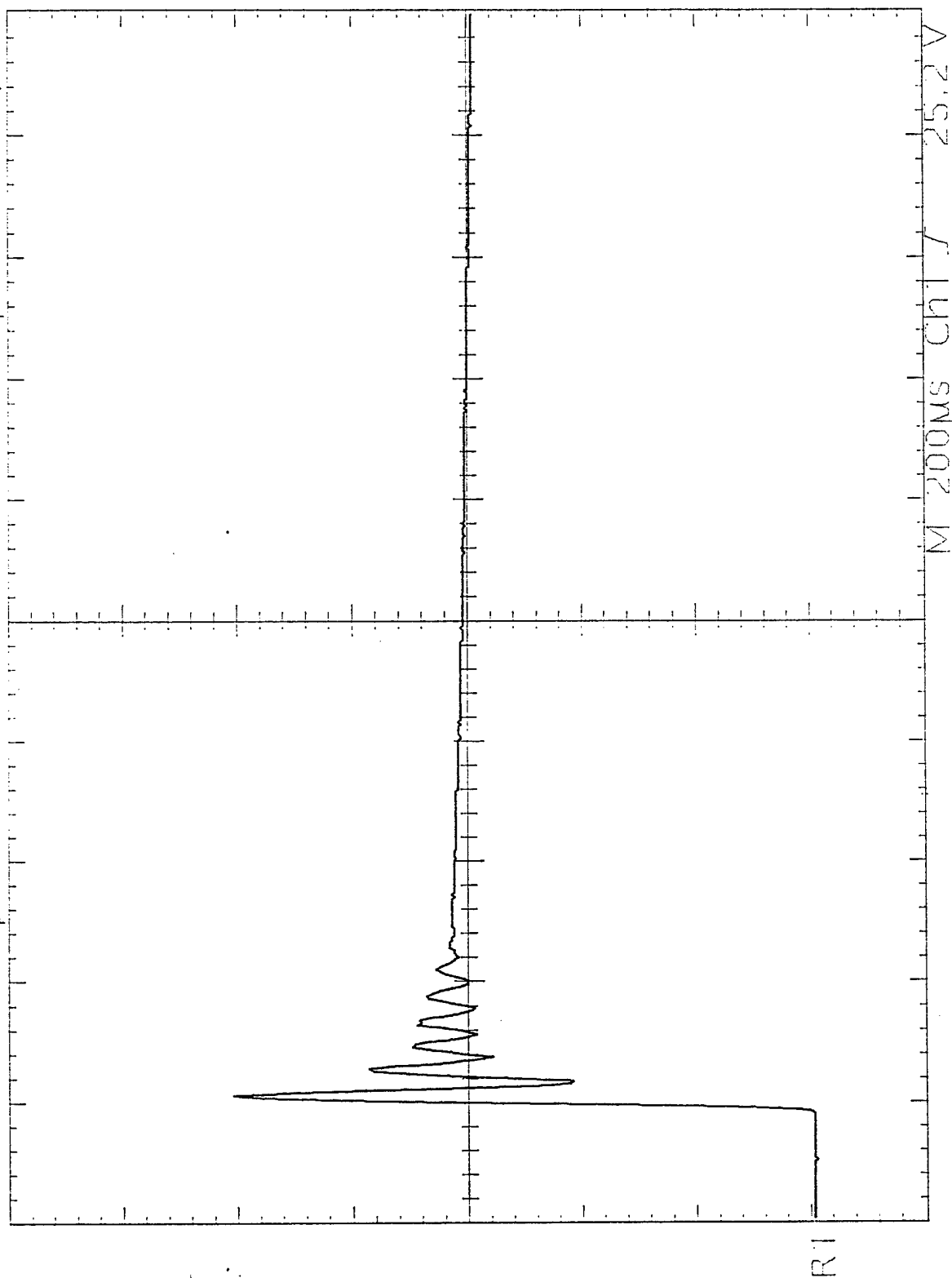
Ref1 Rise
24ns

Ref1 Max
51.4 V

R1

M 200µs Ch1 / 25.2 V

Ref1   10.0 V   500ns

A-43

Tek Run: 100MS/s   Average   Imb/L corr C. @ 30 kV w/o Tail Resistors   3 June 96

Ref2 Max
2.6 V

Current

R2

Ref2   10.0 V   500ns   M 500ns Ch1 ∫   25.0 V

A-44

Tek Run: 100MS/s   Average   w/o Tail Resistors   3 June 94
                                        Int'l Conc. @ 30 kV
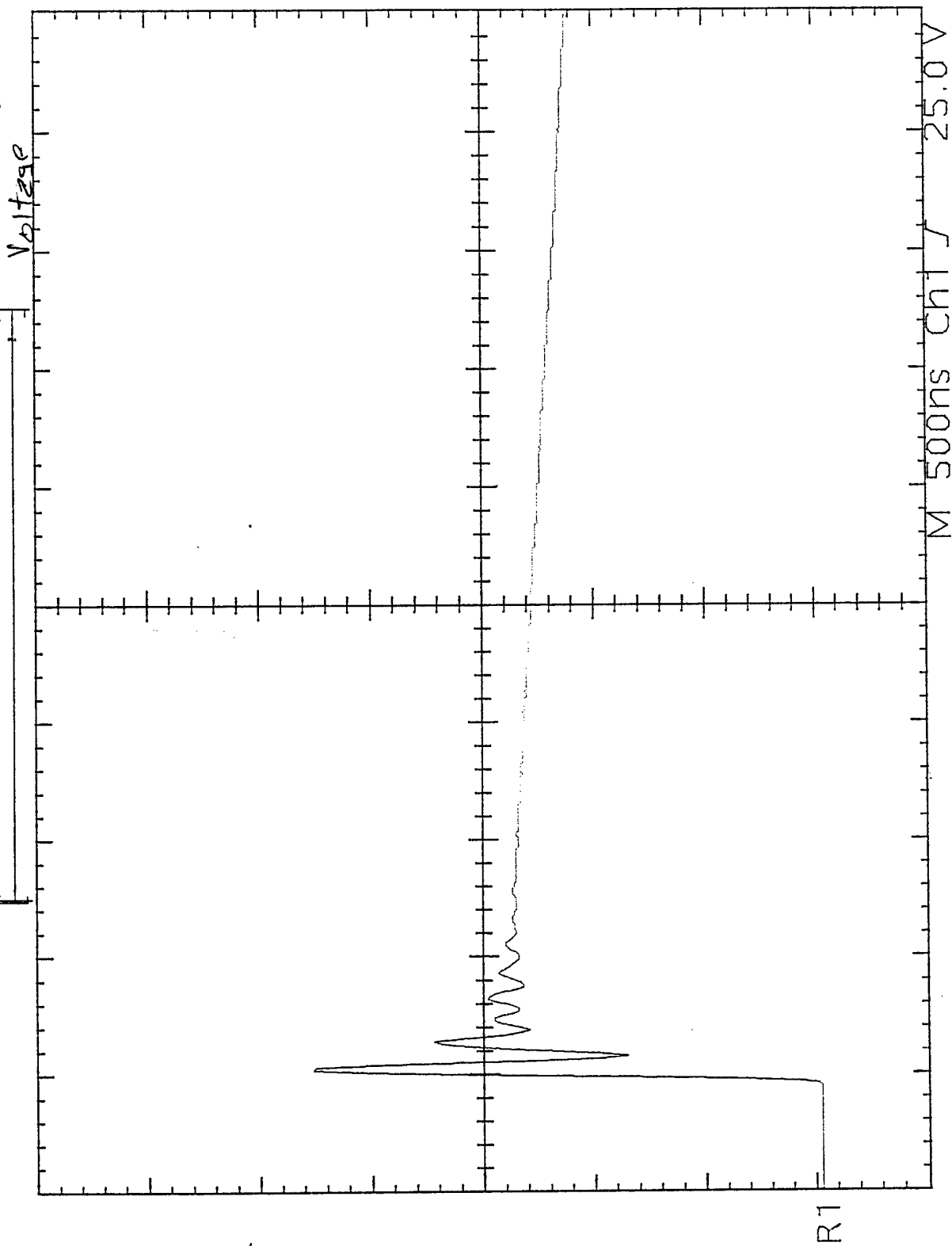
                                        Voltage

Ref1 Rise
23ns

Ref1 Max
46.0 V

R1

Ref1   10.0 V   500ns   M 500ns Ch1 ʃ 25.0 V

A-45

Tek Run: 100MS/s

Average H$_2$O @ 30 kV w/o tail resistors 1 Jun 96 Current

Ref2 Max 1.2 V

R2
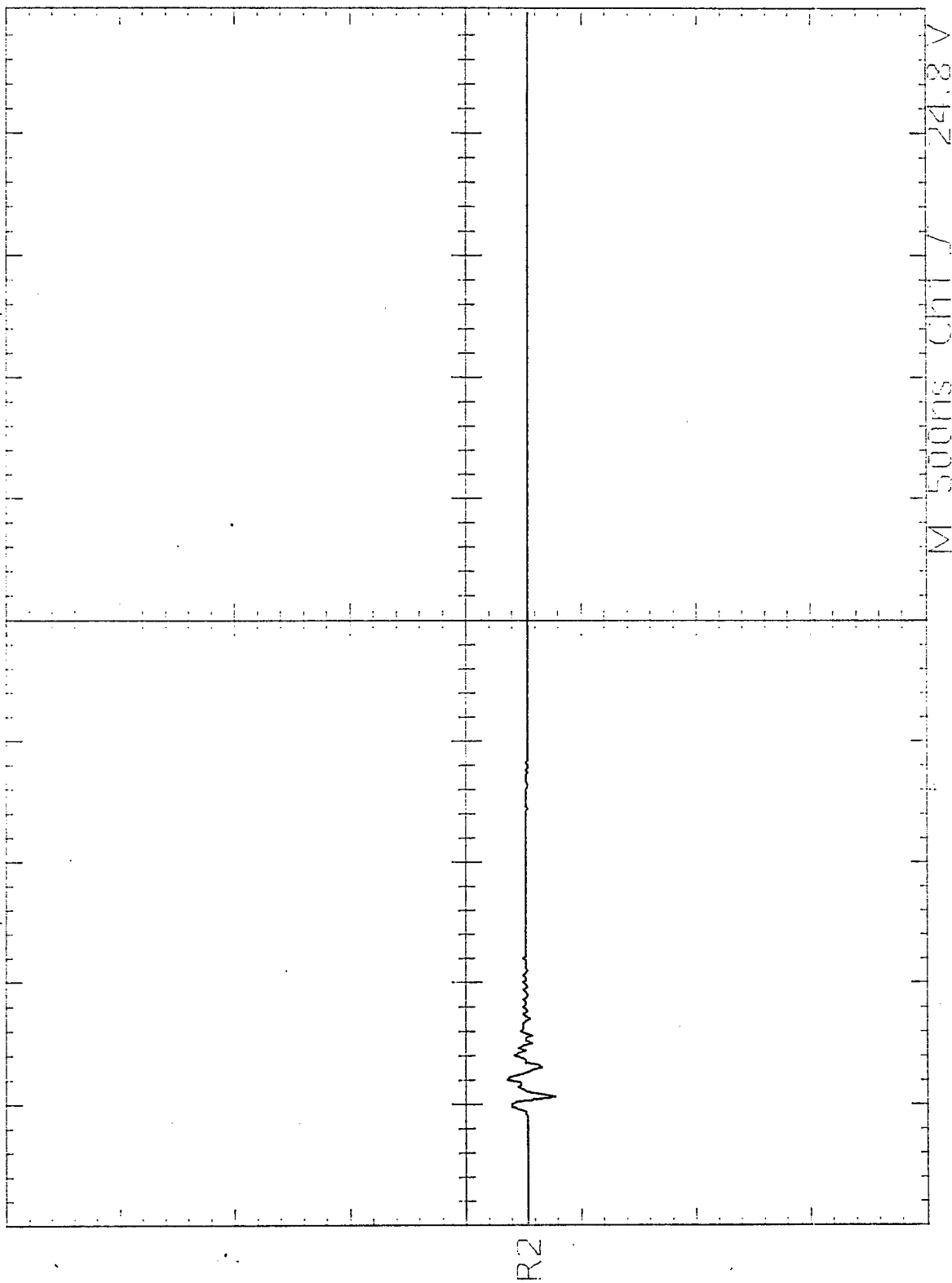
M 500ns Ch1 ∫ 24.8 V

Ref2 10.0 V 500ns

Tek Run: 10.0MS/s   Average   1mΩ/L @ 25kV   w/b Tail Resistors 6 June 96
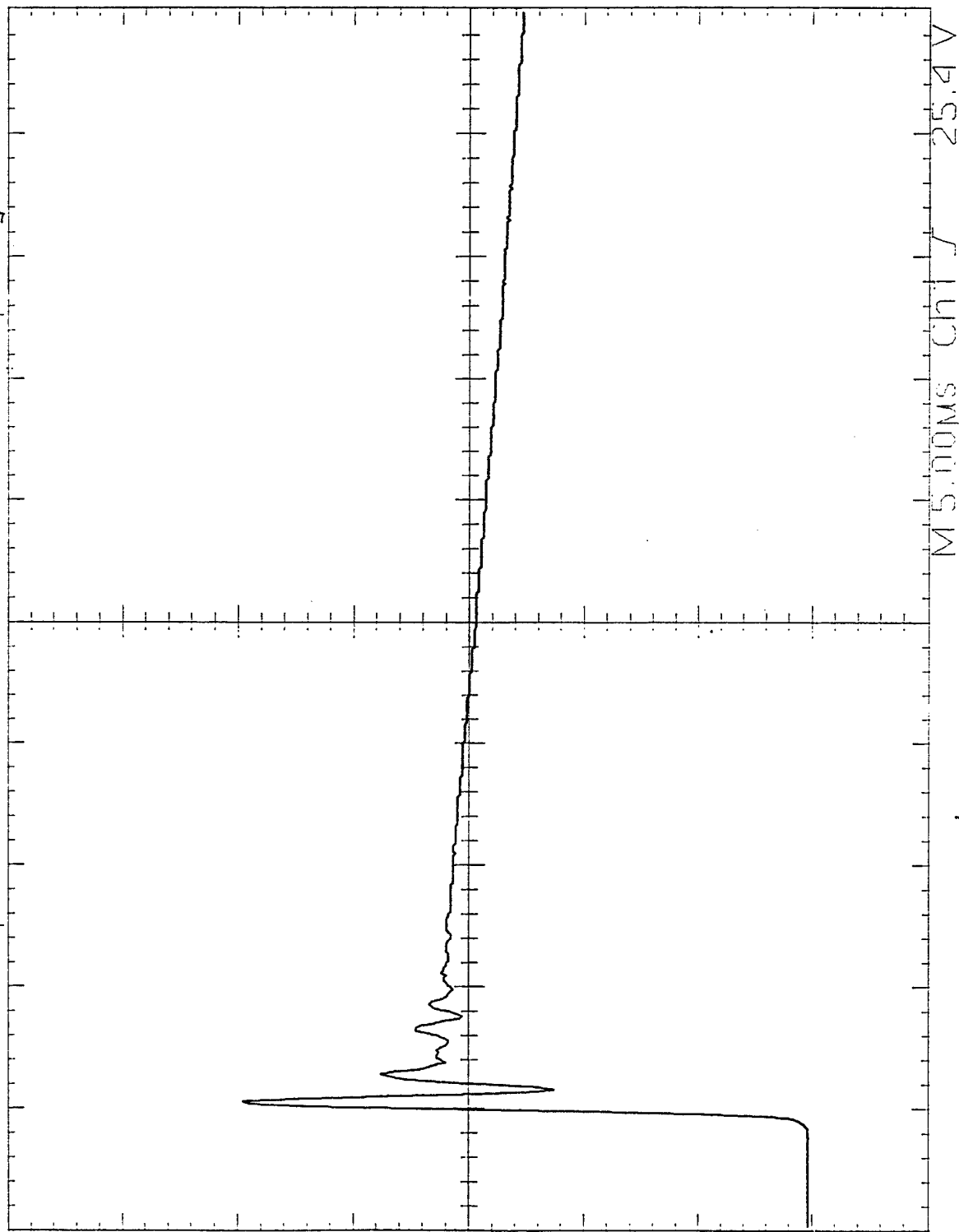
Voltage

Ref1 Max
49.4 V

Ref1 Rise
28ns

M 5.00ms Ch1 ∫ 25.4 V

Ref1   10.0 V   500ns

R1

Tek Run: 100MS/s   Average   Resistors 10 June 96

Average 1mH/L @ 35 kV w/ Tail Resistors 10 June 96

½ foam Voltage

Ref1 Rise
26ns
Unstable
histogram

Ref1 Max
52.0 V
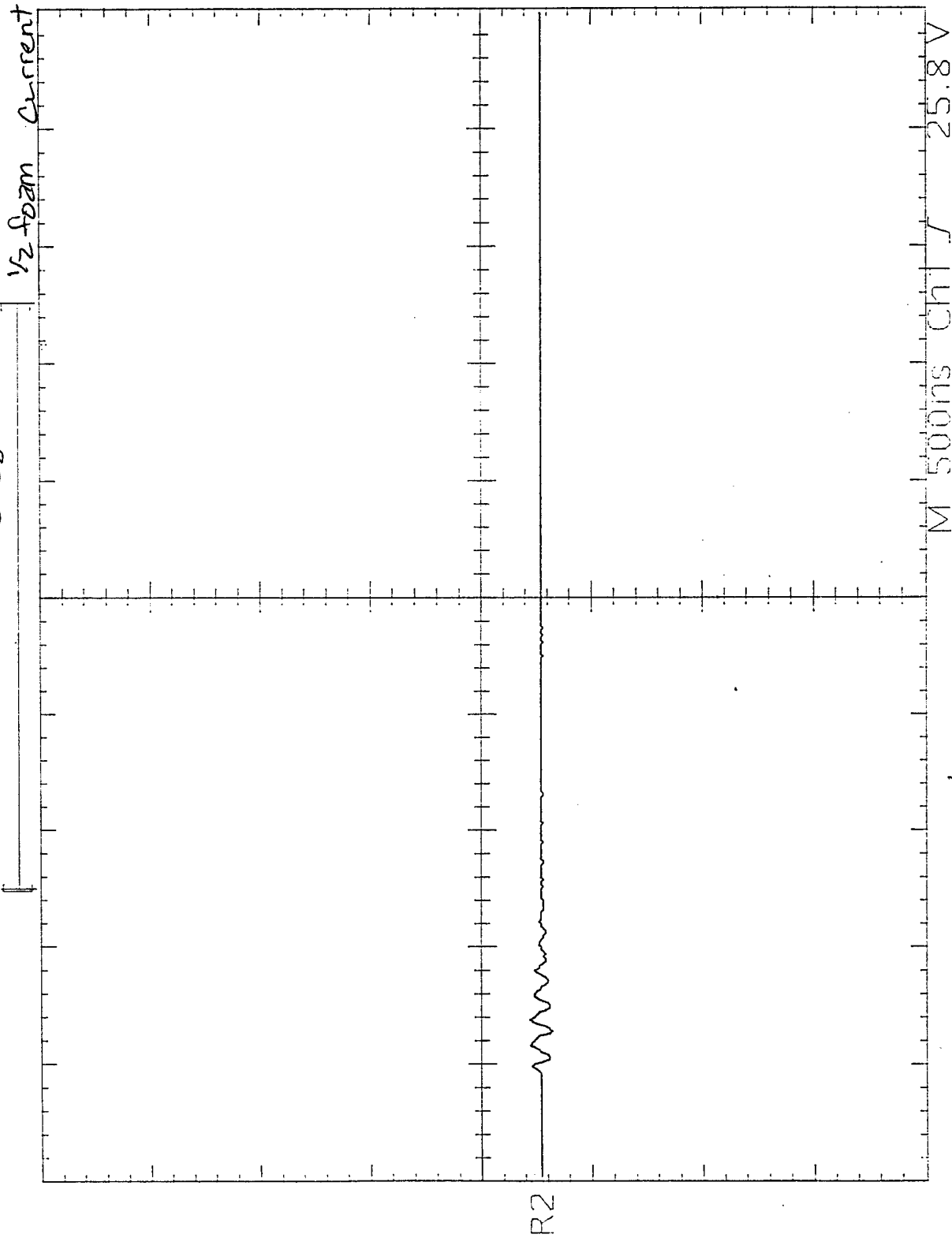
R1

Ref1   10.0 V   500ns

M 500ns Ch1 ƒ 25.8 V

Tek Run: 100MS/s   Average 1mL/L @ 35kV ω)/& Tail Resistors 10 June 96

½ foam Current

Ref2 Max
800mV

R2

M 500ns Ch1 ∫ 25.8 V

Ref2   10.0 V   500ns

Tek Run: 100MS/s   Average

Average | $m^1/_L$ @ 35 kV w/o Tail Resistors 6 June 96

½ 82m Half-Current

Ref2 Max
1.4 V

R2

M 500ns Ch1 ∫ 25.4...

A Ch5...

Ref2   10.0 V   500ns

A-50

Tek Run: 100MS/s   Average   1mH/L @ 35 kV w/o Tail Resistors 6 June 96

½ foam   V=H+zgR
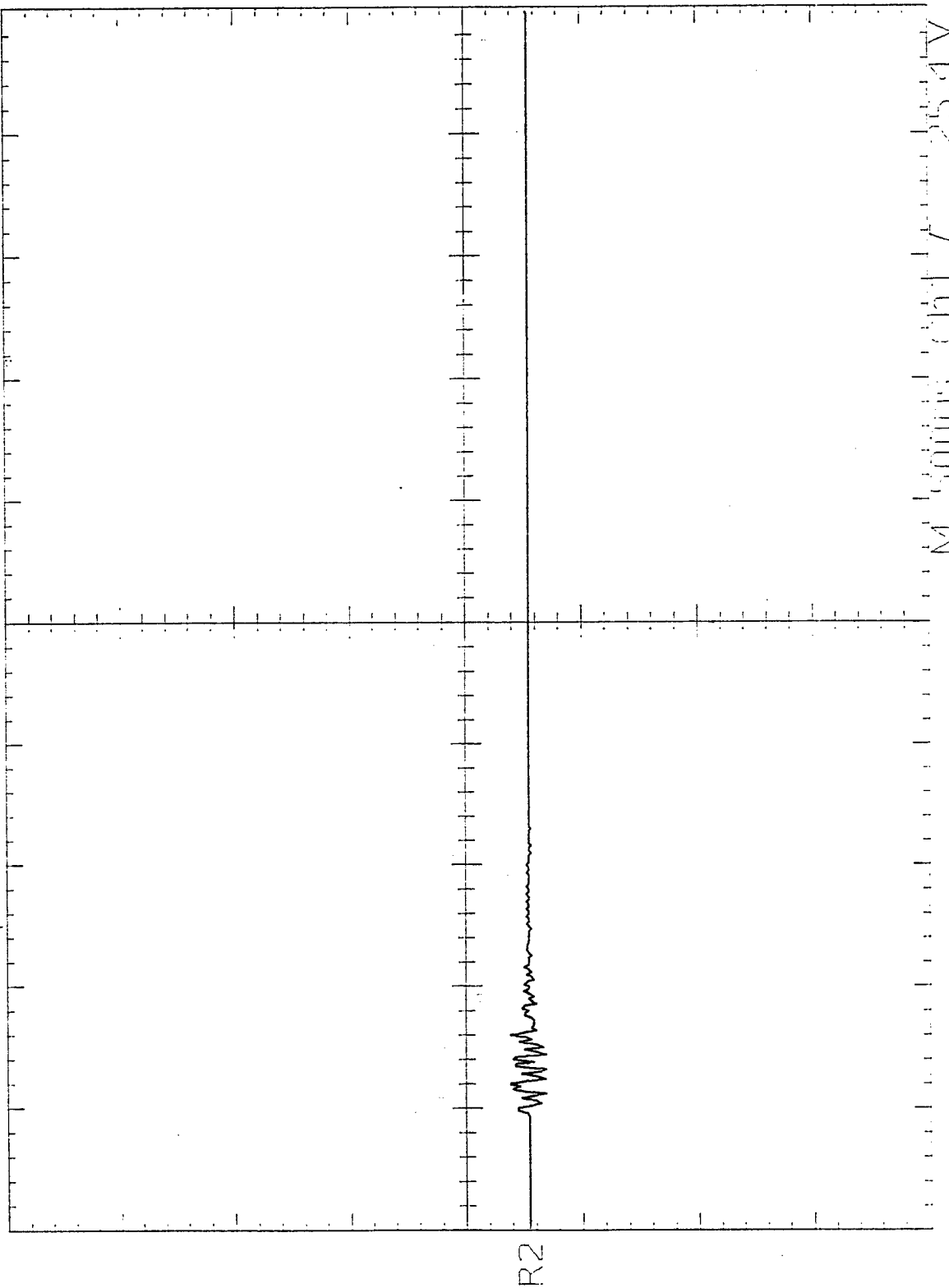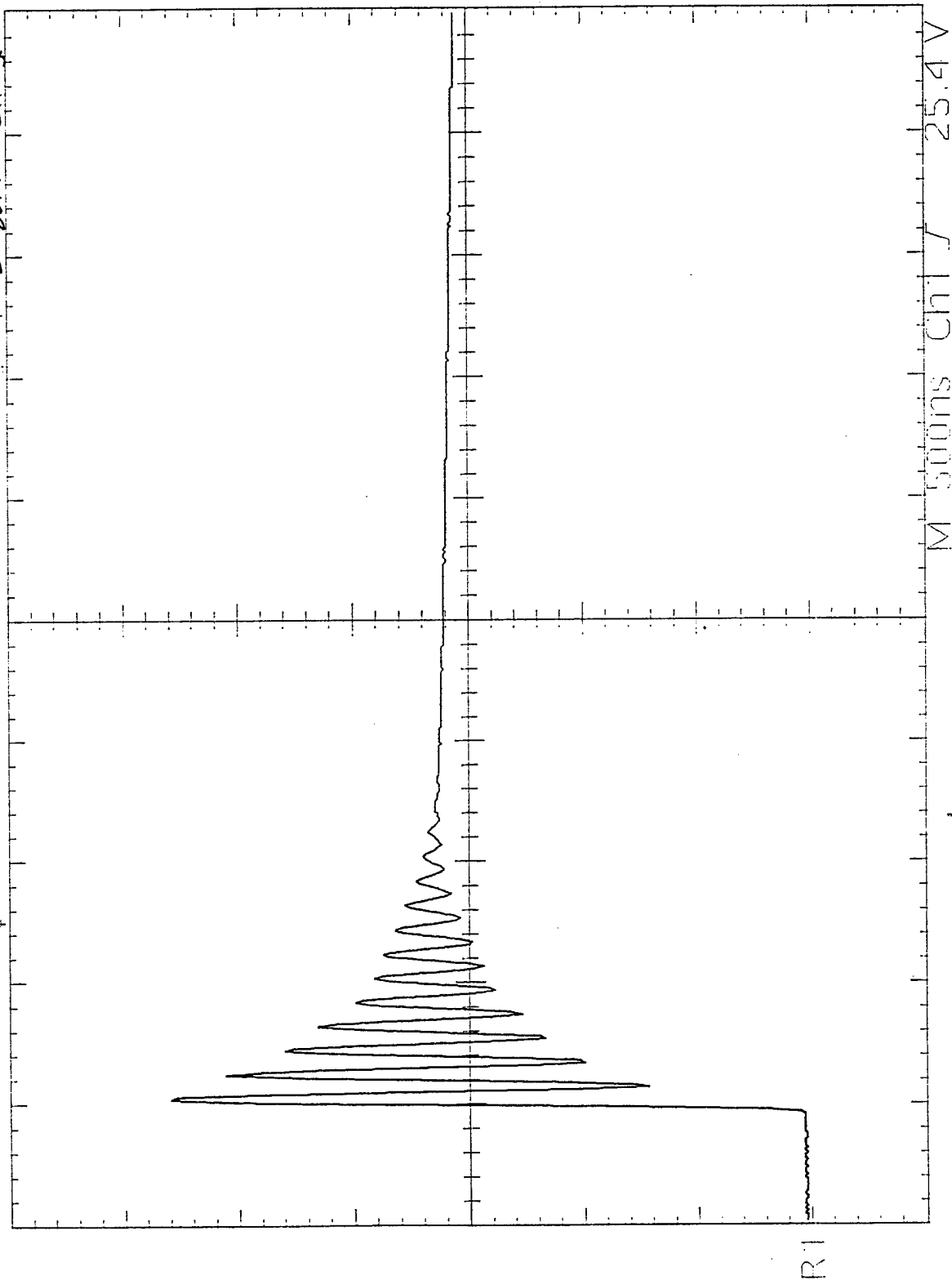
Ref1 Rise
17ns
Low
resolution

Ref1 Max
55.8 V

R1

M 500ns Ch1 ∫   25.4 V

Ref1   10.0 V   500ns

Tek Run: 100MS/s   Average
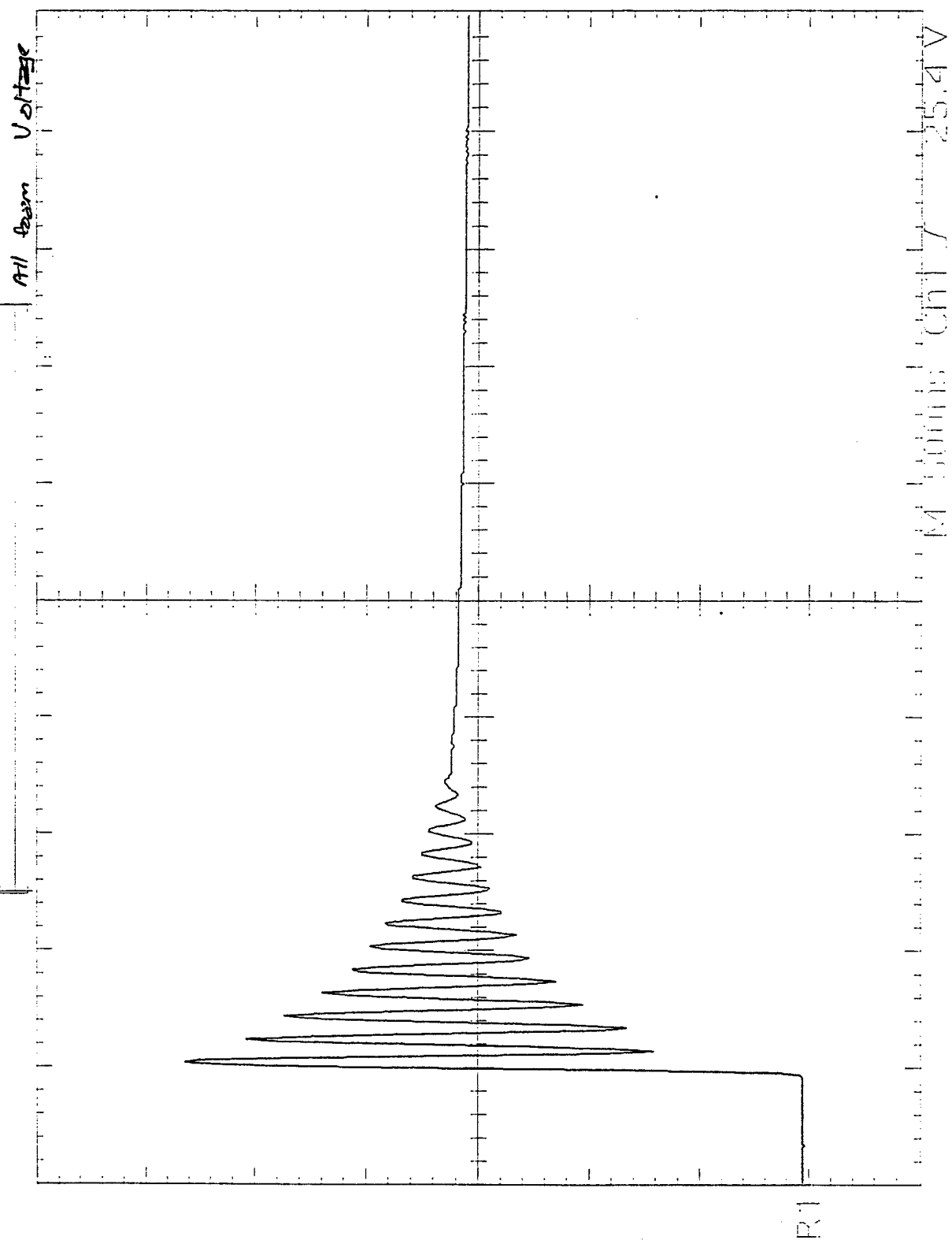
Ref1 Max
56.2 V

Ref1 Rise
15ns
Low
resolution
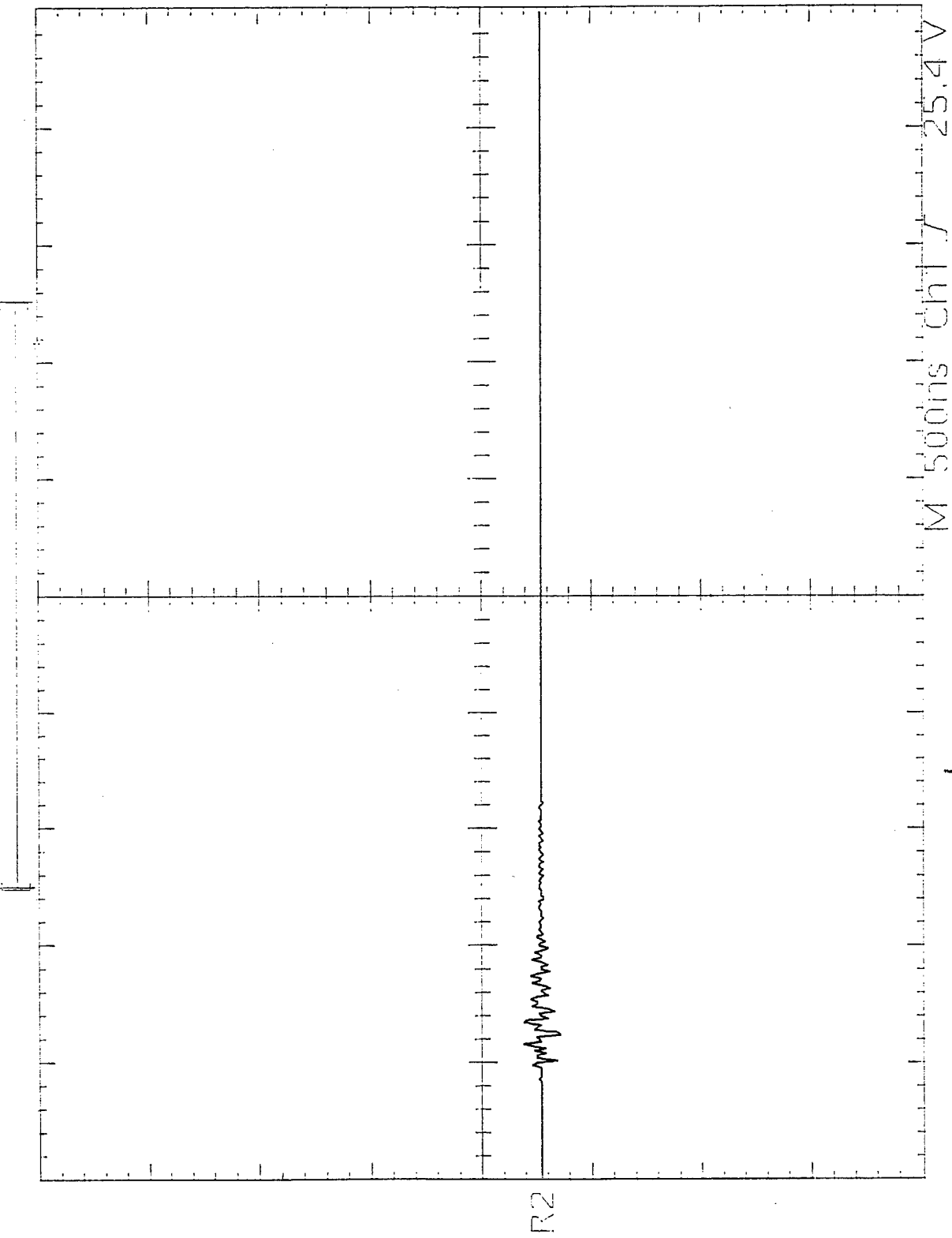
Average 1 nL/L @ 35 kV ab Tail Resistors   6 June 96

All from Voltage

M 500ns Chl / 25.4 V
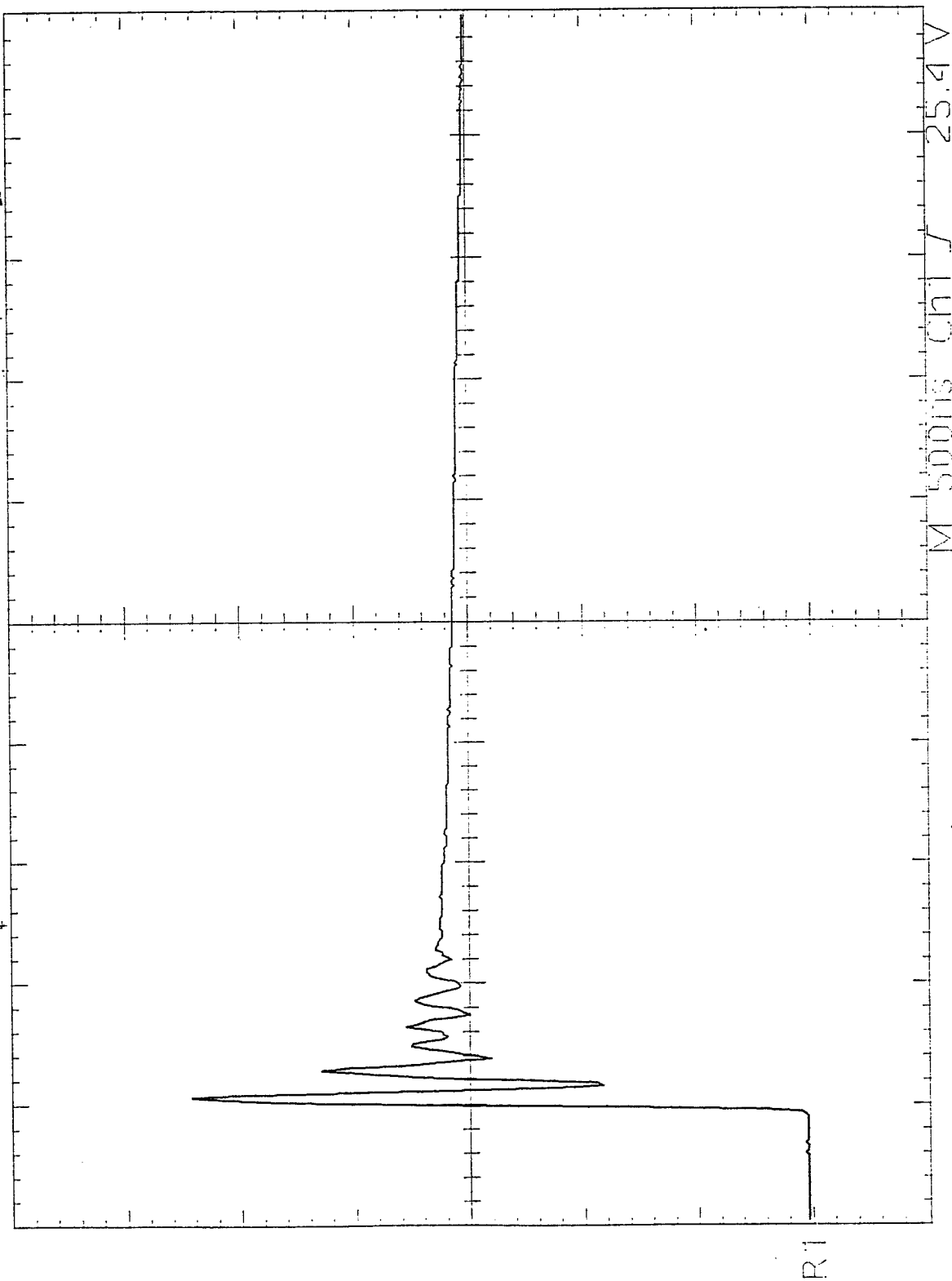
R1

Ref1   10.0 V   500ns

A-52

Tek Run: 100MS/s   Average 1 mH/L @35kV w/o Tzil Resistors 6 June 96

Voltage

Ref1 Rise
19ns
Low
resolution

Ref1 Max
54.2 V

R1

Ref1   10.0 V   500ns   M 500ns Ch1 ƒ   25.4 V

Tek Run: 10.0MS/s   Average

Ref2 Max
2.2 V

Average 1 mL/L @ 35 kV w/o Tail Resistors   6 June 96

Current
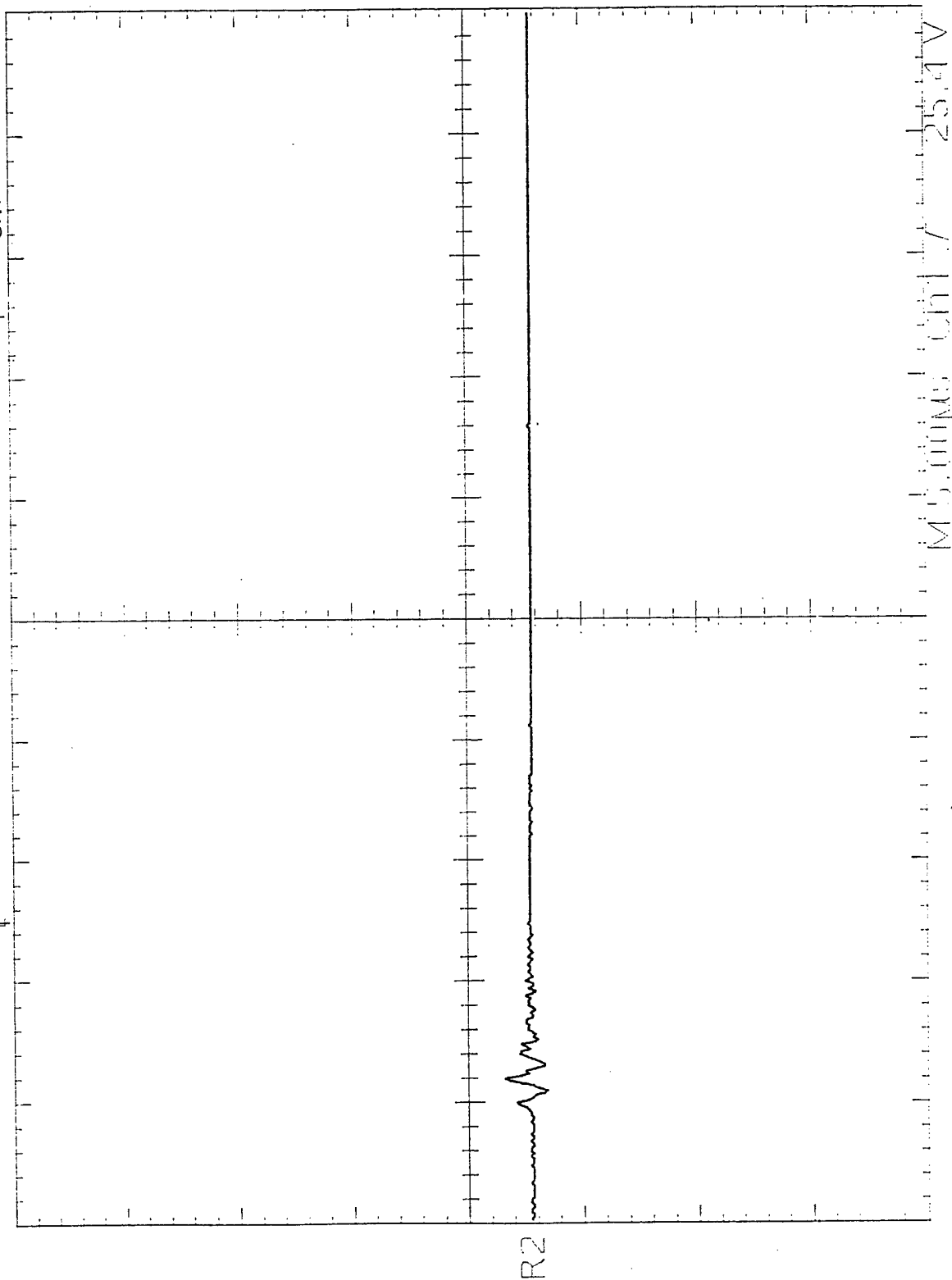
R2

M 5.00ms Ch1 ⌐ 25.4 V

Ref2   10.0 V   500ns

Tek Run: 100MS/s   Average
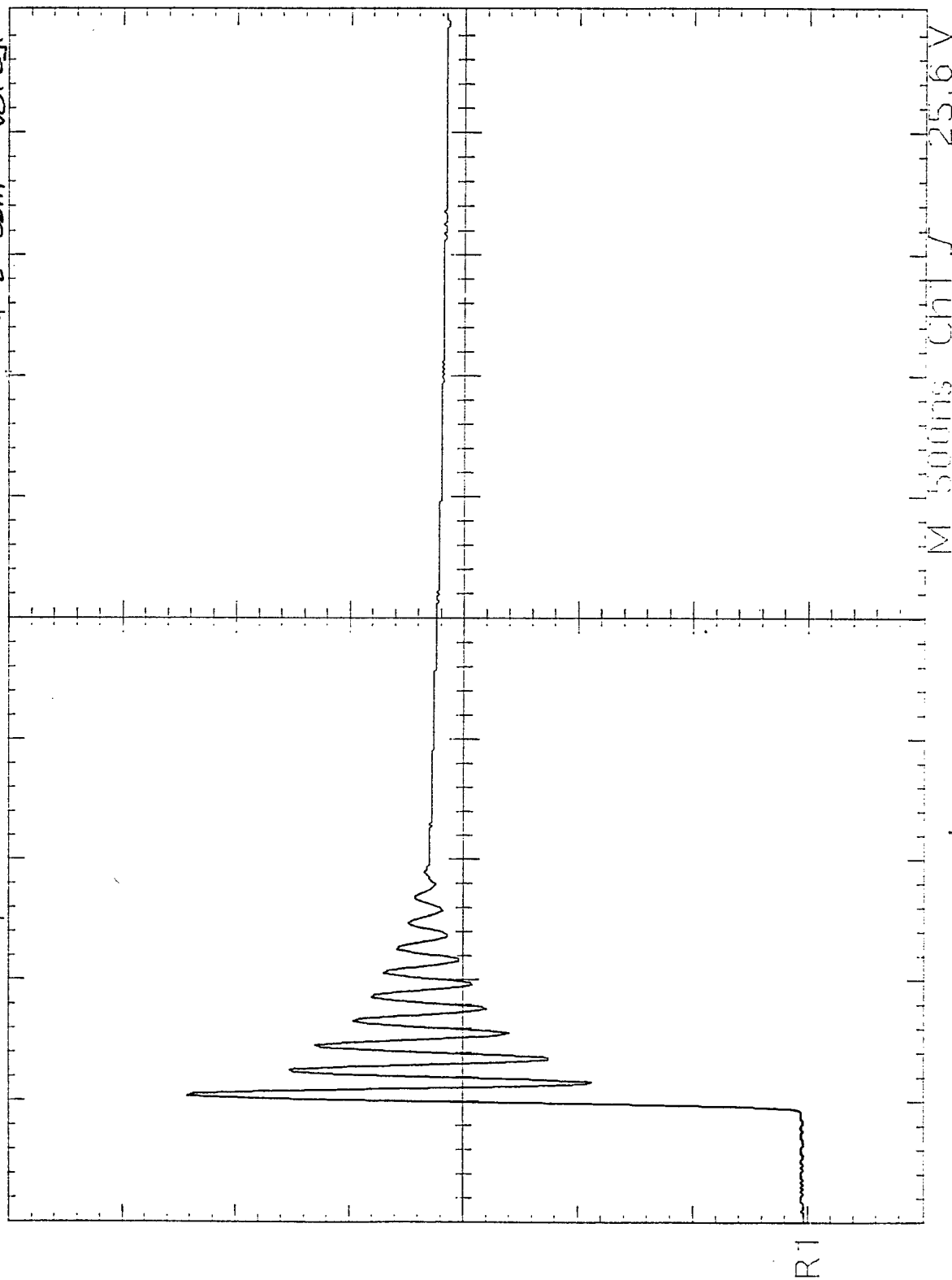
Ref1 Max
54.0 V

Ref1 Rise
21ns

Average , 1 mL/L w/o tail Resistors @ 35kV 7 June 96
½ foam Voltage

M 500ns Ch1 ∫ 25.6 V

Ref1   10.0 V   500ns

R1

A-56

Tek Run: 100MS/s   Average .1 mL/L w/o Tail Resistors @ 35 kV 7 June 96

½ foam Current

Ref2 Max
1.8 V

R2

M 500 μs Ch1 ⌐ 25.6 V

Ref2   10.0 V   500 μs